Dissertation

submitted to the combined faculties for the Natural Sciences and for

Mathematics of the Ruperto-Carola University of Heidelberg, Germany,

for the degree of

Doctor of Natural Sciences

presented by

M. Sc. **Julia Maria Jäger**

born in Oberhausen, Germany

Heidelberg 2013

The Role of Hepatic Transforming Growth Factor Beta1-stimulated Clone 22 D1 (TSC22D1) in the Regulation of Systemic Cholesterol Metabolism

Referees:

Prof. Dr. Frauke Melchior

Prof. Dr. Stephan Herzig

"If you knew what you were doing it wouldn't be called research"

Albert Einstein

Acknowledgements

A PhD thesis is never the work of one person alone. A lot of people contributed also to this work the one or the other way. So, I would like to take the opportunity to thank you.

First of all, I would like to thank Stephan Herzig for his constant support and very valuable advices throughout all my time in the A170 group. What helped me a lot was that whenever I looked at the black side of things, which was basically all of the time, he kept looking at the bright side.

I also would like to thank our collaborators in Mannheim, Munich, Marburg and Amsterdam, Maria Muciek, Carsten Sticht, Marc Martignoni, Sigrid Stöhr and Geesje M. Dallinga-Thie who contributed to this work.

I am very grateful to my TAC members Frauke Melchior and Thomas Hofmann for good discussions and valuable advice, which helped my project to progress. Next to Frauke Melchior, I also thank Karin Müller-Decker and Rüdiger Hell for being part of my examining board.

Lab work would have been much tougher and also quite boring without my colleagues. I appreciate all the help I got from present and former members of the A170 group from my first day on. I would like to thank Allan for setting the grounds for my final project. Big thanks to Oksana who greatly helped me and made work a lot of fun. Thanks also to Kilian for keeping me company at the Western blot place. Thanks to Vera, even though we did not work in the same lab we were connected through a special protein. Thanks also to Mauricio, Tjeerd, Adam and Dan for technical support and helpful scientific discussions. Dany, thank you so much for always giving me a helping hand when needed and making a lot of things possible which I would not have managed myself. And of course I need to thank the "Bitchy Box" (mainly Dany, Maria, Michaela, Anke, Anja and Yvonne) which were always willing to help me the one or the other way and really coped well with all my swearing. Also, I would really like to know how much chocolate I consumed throughout the years either from delicious cakes or out of the "Frustlade". And, Maria, Michaela and Dany I had a lot of fun with you, especially in very non-scientific discussions….

Thanks also to Hanna and Claudi for our after-work dates, which helped me to see all the good sides of my work and the lab.

Away from the lab I want to thank my friends (Verena, Vivi, Judith and Saskia) who are there for me since school and who helped me in different ways to get through my PhD.

Finally, I would like to thank my family. These are first of all you Mama and Papa, who supported me for as long as I can remember and helped me more than I can tell. Thank you! Also, thanks to you Poki, for being my sister! Thanks to Wo-An-Ka-Ja who kept asking about me. And I also want to mention my "Schweinchen" Ernie who kept me entertained even from far. And last but not least, I want to thank you Kshitij. I cannot tell how grateful I am for always encouraging me, enduring my bad moods and for all your efforts in cheering me up when needed: "all is well".

Index

1   Abstract

Energy storage and consumption of the healthy human body are well geared to the needs under physiological conditions. Any disturbances in this balance can result in metabolic diseases such as obesity. A key feature of metabolic disorders is an abnormal lipid profile, as characterized by elevated serum triglycerides, elevated low density lipoprotein (LDL) cholesterol and reduced high density lipoprotein (HDL) cholesterol. These alterations can increase the risk for the development of type 2 diabetes or atherosclerotic cardiovascular diseases.

In this study, the transcriptional co-factor transforming growth factor beta1-stimulated clone 22 D1 (TSC22D1) was identified as novel regulator of systemic cholesterol metabolism. Acute or chronic knockdown of TSC22D1 in livers of wild-type mice resulted in a significant decrease of serum HDL cholesterol and mildly elevated liver cholesterol. These changes are caused by a reduced expression of key genes involved in cholesterol efflux such as Apolipoprotein A1 (ApoA1), or transporters as ATP binding cassette protein A1 (ABCA1), ABCG5 and ABCG8. Interestingly, serum HDL cholesterol could be elevated by overexpression of hepatic TSC22D1 in wild type mice.

Moreover, TSC22D1 expression was found to be differentially regulated in mouse models of opposing energy supply. Whereas levels of TSC22D1 transcripts were significantly reduced in states of energy wasting as in cancer cachexia, they were increased by energy surplus as under obese conditions.

Along these lines, hepatic TSC22D1 expression was increased in ob/ob mice, which are highly resistant to the development of atherosclerosis due to their elevated HDL levels. Again, TSC22D1 knockdown significantly lowered serum HDL cholesterol and reduced expression of ApoA1, ABCA1, ABCG5 and ABCG8.

Intriguingly, plasma concentrations of HDL/ApoA1 inversely correlate with the risk for atherosclerotic cardiovascular disease in humans. Thus, hepatic TSC22D1 transcription factor complex may represent an interesting new target for beneficial manipulation of HDL cholesterol levels.

2   Zusammenfassung

Energieaufnahme und -verbrauch sind im gesunden menschlichen Körper unter physiologischen Bedingungen genau aufeinander abgestimmt. Jegliche Abweichungen von dieser Balance können in metabolischen Funktionsstörungen wie Fettleibigkeit resultieren. Ein klinisches Hauptmerkmal von metabolischen Erkrankungen sind Störungen im Serumlipidprofil, gekennzeichnet durch einen erhöhten Triglyzeridspiegel, erhöhte LDL-(low density lipoprotein) und reduzierte HDL-(high density liporotein) Cholesterinwerte. Diese Veränderungen sind Risikofaktoren für Typ 2 Diabetes oder atherosklerotische Herz-Kreislauf-Erkrankungen.

In dieser Studie wird gezeigt, dass der transkriptionelle Co-Faktor "transforming growth factor beta1-stimulated clone 22 D1" (TSC22D1) die Konzentration von zirkulierendem HDL-Cholesterin reguliert. Akute oder chronische „Knockdown"-Studien mit TSC22D1 in Lebern von Wildtypmäusen führten zu einer deutlichen Verringerung des HDL-Cholesterins im Blut. Eine Erklärung hierfür bietet die signifikante Reduktion in der Genexpression von Schlüsselgenen im Cholesterintransport, wie Apolipoprotein A1 (ApoA1), „ATP binding cassette" Protein A1 (ABCA1), ABCG5 und ABCG8. Im Gegensatz zum „Knockdown"-Effekt konnte die hepatische Überexpression von TSC22D1 den HDL-Cholesterinspiegel erhöhen.

Weiterhin wurde gefunden, dass hepatisches TSC22D1 in Mausmodellen mit gegensätzlichem Energiestatus auch konträr exprimiert wird. Während die Expression bei Energieverlust, wie bei Krebskachexie, massiv reduziert ist, wird sie bei Energieüberschuss, wie bei Übergewicht, verstärkt.

In diesem Zusammenhang wurde auch eine erhöhte Expression von TSC22D1 in ob/ob Mäusen beobachtet, die durch ihre erhöhten HDL-Cholesterinspiegel sehr resistent gegenüber Atherosklerose sind. Der leberspezifische „Knockdown" von TSC22D1 konnte auch hier zirkulierendes HDL-Cholesterin verringern und die Expression von ApoA1, ABCA1, ABCG5 und ABCG8 reduzieren.

Interessanterweise korrelieren in humanen Studien die HDL/ApoA1 Serumlevel negativ mit dem Risiko für atherosklerotische Herz-Kreislauf-Erkrankungen. Dieser Befund legt den Schluss nahe, dass TSC221 ein neues und attraktives therapeutisches Ziel zur Verbesserung des HDL-Cholesterinspiegels darstellt.

3   Introduction

3.1   Metabolic homeostasis

Under normal physiological conditions energy uptake and utilization are well geared to the body's energy needs. This is referred to as metabolic homeostasis. Excessive uptake and storage of energy substrates or increased energy wasting can result in metabolic disorders. In order to maintain metabolic homeostasis it is crucial to understand the tight regulation of underlying molecular mechanisms and know the players which are in involved in keeping a healthy balance.

3.2   Metabolic disorders

3.2.1   Obesity

In recent years obesity has become a new major health threat in developed as well as in developing countries. The World Health Organization (WHO) states that worldwide obesity has nearly doubled since 1980 (Fig 1) and the numbers are on the rise (WHO fact sheet No 311, 2013).
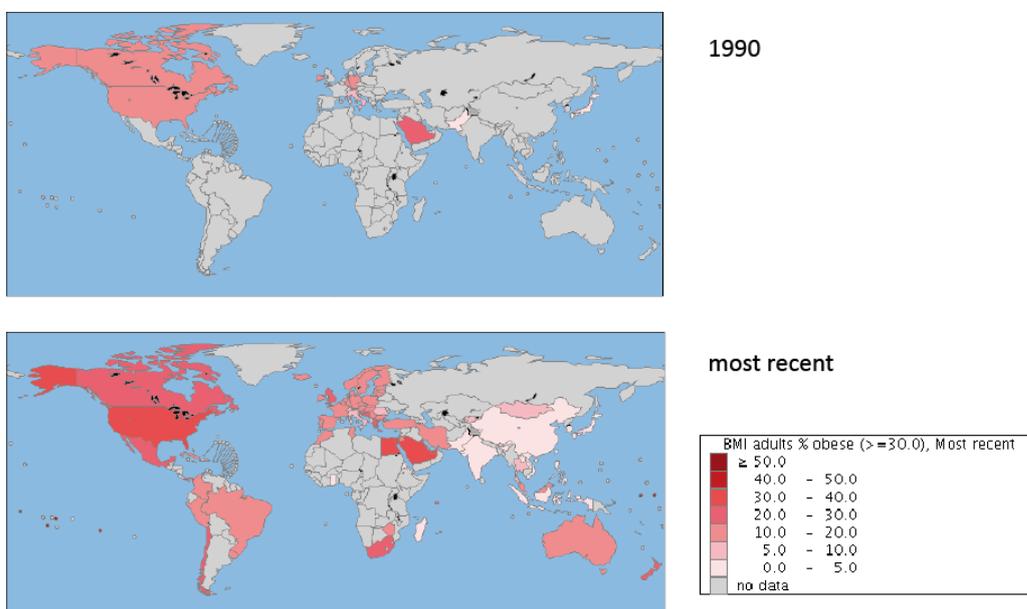
Fig 1: Emerging obesity. *Incidence of obesity defined by a body mass index ≥ 30 in 1990 and most recent (2012).*
(Generated from global database on body mass index WHO.)

The underlying causes for the emerging prevalence of obesity are diverse. Factors that can affect obesity are genetic predisposition, sedentary lifestyle and high energy intake (P.G.

Kopelman, 2000). Recent research also links the composition of the gut microbiota to obesity (V. Tremaroli and F. Backhed, 2012).

Overweight and obesity are defined by a body mass index (BMI) of ≥25 or ≥30, respectively. Obesity is the fifth leading cause of death worldwide (WHO fact sheet No 311, 2013). This is due to the close relationship between BMI and increasing risks for several non-communicable medical conditions such as type 2 diabetes, hypertension, coronary heart diseases and cholelithiasis (P.G. Kopelman, 2000). Furthermore, the risk for certain types of cancer as breast (R.E. Patterson *et al.*, 2013), endometrial, cervical (W. Gu *et. al.*, 2013) and colon cancer (M. Bardou *et al.*, 2013) is increased in obese patients.

In 2011 already more than 40 million children under the age of five were overweight (WHO fact sheet No 311, 2013), demonstrating the emerging need to discover new approaches for prevention or treatment of obesity.

3.2.2 Metabolic syndrome

The term "metabolic syndrome" describes a complex combination of metabolic disorders rather than a specific disease. The exact definition of this term is debated by experts worldwide as are the criteria which have to be met for the diagnosis of a metabolic (R.G. Thaman and G.P. Arora, 2013). In 1988, G.M. Reaven was the first who defined a constellation of metabolic derangements then known as syndrome X (G.M. Reaven, 1988). However, despite these controversies it is generally accepted that central obesity, insulin resistance or impaired glucose tolerance, dyslipidemia, a low-grade proinflammatory state and hypertension are key features of the metabolic syndrome (K.G. Alberti *et al.*, 2009) (Fig 2).

Taken together, these factors are associated with an increased risk for the development of cardiovascular diseases (CVD) and type 2 diabetes (K.G. Alberti *et al.*, 2009) or further comorbidities such as nonalcoholic fatty liver disease.
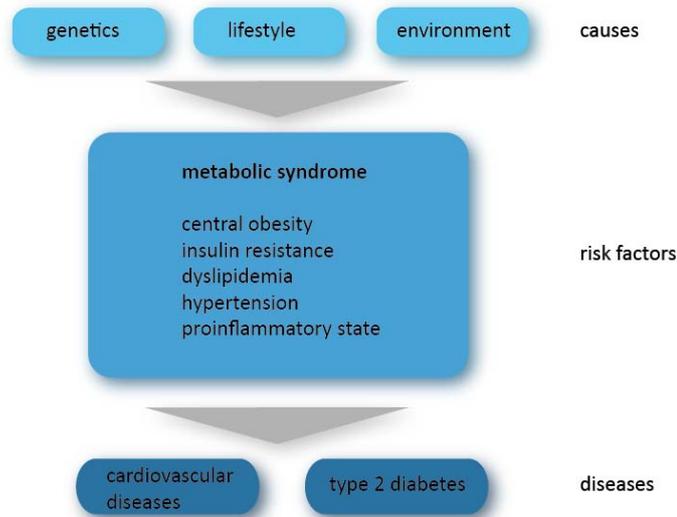
Fig 2: The metabolic syndrome. *Schematic representation of possible causes, risk factors and consequences of the metabolic syndrome**.** The metabolic syndrome is a clustering of risk factors which can increase the development of type 2 diabetes and cardiovascular diseases. There is no fixed pathogenesis, all factors interact dynamically.*

Due to the complex nature of the metabolic syndrome, therapeutic intervention is difficult. Pharmacological treatment mostly targets individual components, mainly aiming to reduce the risk for CVD and type 2 diabetes. In addition, so-called life-style therapies including dietary changes and increased physical exercise are approaches to reduce obesity (H. Bays *et al.*, 2006).

Considering that in the US approximately 34% of all adults meet the criteria for the metabolic syndrome (R.B. Ervin, 2009), there is an ongoing search for new treatment strategies.

3.2.3   Cachexia

Whereas obesity is a disorder of energy surplus conditions, the energy balance can also be disturbed energy deprivation conditions such as cachexia. This multifactorial wasting disease is associated with either chronic or end-stage diseases as chronic obstructive pulmonary disease, chronic heart failure, infections, rheumatoid arthritis, tuberculosis, AIDS or cancer. Cachexia is associated especially with cancers of the gastrointestinal tract and the lung, and it accounts for up to 20% of all cancer related deaths (K. Fearon *et al.*, 2012). Even though there are no specified clinical criteria for diagnosis, cachectic patients are commonly recognized by severe weight loss, early satiety, weakness, impaired immune

function and reduced physical performance (M. Puccio and L. Nathason, 1997). Moreover, there are multiple metabolic alterations accompanying cachexia (Table 1).

Up to now, cachexia cannot be cured; current treatments mainly focus on improving patients' quality of life (S. Lucia *et al.*, 2012). The only approved drugs available in Europe as progesterone, improve appetite and body weight but show no improvement of in muscle mass or survival (E. Tazi and H. Errihani, 2010). In order to find new approaches for treating cachexia, most studies have focused so far on the role of adipose tissue and skeletal muscle. However, recent studies indicate, that the liver, as an organ being crucial for overall energy homeostasis, needs to be taken into consideration as well (A. Jones *et al.*, 2013, M.E. Martignoni *at al.*, 2009).

Table 1: Alterations in carbohydrate, lipid and protein metabolism in cancer cachexia

Carbohydrate	Lipid	Protein
↑ Hepatic gluconeogenesis	↑ Adipose tissue lipolysis	↑ Muscle protein breakdown
↑ Cori cycle activity	↓ Lipogenesis	↑ Hepatic protein synthesis
↓ Uptake of glucose into skeletal muscle	↓ Whole-body lipid storage	↓ Protein synthesis
	Altered lipoprotein metabolism	
	Hyperlipidemia	

(summarized from M. J. Tisdale 2002, S. Lucis and D. H. Esper, 2005)

↑: increase, ↓: decrease in the respective process

3.3   The liver as a metabolic organ

The liver is an organ with diverse functions. It integrates nutritional, neural and endocrine signals and it can thereby participate in carbohydrate, lipid and amino acid metabolism. It is the largest internal organ, with an average weight of roughly 1.5 kg in a healthy adult. As a heterogeneous organ the liver consists of different cell types with hepatocytes as the largest population, which make up 80% of the liver volume; the remaining cells are endothelial cells, hepatic stellate cells, immune reactive Kupffer cells, natural killer cells and other cells (W. Liu *et al.*, 2011). The liver is supplied with blood and hence with nutrients, hormones or drugs by the portal vein.

3.3.1   Hepatic lipid metabolism

One major task of the liver is to balance the body's blood sugar levels. But, other than contributing to glucose homeostasis, the liver is a key organ in regulating systemic lipid

metabolism. To maintain lipid homeostasis it can clear lipids from dietary sources, break down lipids for energy production or store lipids. Four sources supply the liver with fatty acids, namely a) hydrolysis of adipose tissue generating plasma non-esterified fatty acids, b) chylomicron remnants, c) cytoplasmic triglyceride stores and d) *de novo* lipogenesis (S. Tiwari and S. A. Siddiqi, 2012; J. Huang *et al,.* 2010). Uptake of fatty acids into the liver is mediated by transporters as CD36 or diffusion. Within the hepatocyte they bind to fatty acid binding proteins (FABP) and are either oxidized or processed to form neutral lipids. Oxidation takes place in mitochondria or in peroxisomes. During this process called β-oxidation, fatty acids are broken down to acetyl-CoA, which is then fed into the TCA cycle to generate NADH. At high concentrations acetyl-CoA cannot completely be metabolized *via* the TCA cycle and is then utilized by incomplete β-oxidation, and can serve as an alternative energy source. Moreover, acetyl-CoA is a precursor in the synthesis of cholesterol (P. Nguyen *et al.*, 2008).

Acetyl-CoA, which can also be generated by breakdown of glucose is the precursor molecule for triglyceride (TG) synthesis as well. To this end, several chemical reactions form long chain fatty acids in the cytoplasm which can subsequently, be esterified with glycerol forming TGs. These are either stored in the liver or released into the circulation as part of very low density lipoprotein particles (VLDL) (J. Huang *et al*., 2010).

3.3.2 Lipoproteins

Triglycerides as well as cholesterol are water insoluble, thus, they are packed into lipoprotein particles to be transported through the blood stream. Lipoproteins are macromolecular complexes which vary in composition, size, density and function (Table 2). The hydrophobic core of the lipoprotein comprises TGs and cholesterol-esters (CE). The surface is covered by amphipathic phospholipids, free cholesterol and apolipoproteins. Apolipoproteins help to solubilize the core lipids and they are crucial scaffolds for interaction with lipid processing enzymes or transporters (H. N. Ginsberg *et al.*, 2005) (Fig 3).

Table 2: Physico-chemical characteristics of the major lipoprotein classes

Lipoprotein	Density (g/ml)	Diameter (nm)	Apolipoprotein component	Lipid content (%)		
				TG	C	PL
Chylomicron	0.95	75-1200	ApoB48, ApoE, ApoAI, ApoAII, ApoAIV, ApoCII, ApoCIII	80-95	2-7	3-9
VLDL	0.95-1.006	30-80	ApoB100, ApoE, ApoCII, ApoCIII	55-80	5-15	10-20
IDL	1.006-1.019	25-35	ApoB100, ApoE	20-50	20-40	15-25
LDL	1.019-1.063	18-25	ApoB100	5-15	40-50	20-25
HDL	1.063-1.21	5-12	ApoAI, ApoAII, ApoAV	5-10	15-25	20-30

adapted from: H.N. Ginsberg 2005

VLDL: very low density lipoprotein, IDL: intermediate density lipoprotein, LDL: low density lipoprotein, HDL: high density lipoprotein, % lipid content indicates percentages of triglycerides (TG), cholesterol (C) and phospholipids (PL) within the respective lipoprotein class, the remaning part consists of apolipoproteins
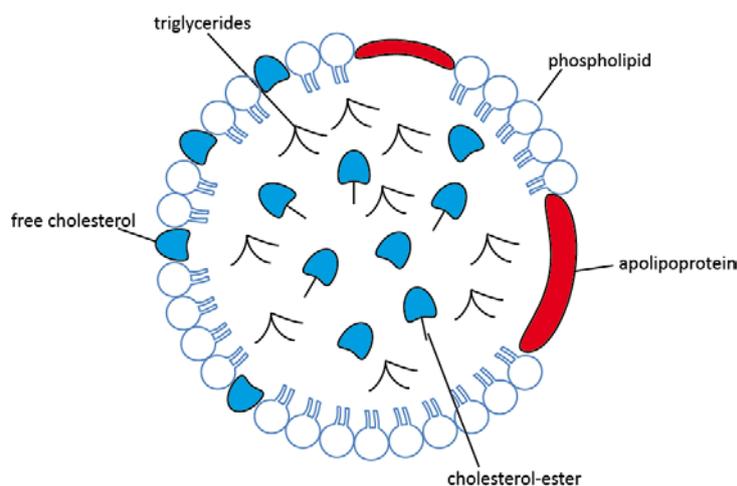
Fig 3: Schematic representation of the general structure of a lipoprotein.
The surface of a lipoprotein is consisting of phospholipids, free cholesterol and apolipoproteins. Free cholesterol, cholesterol-ester and triglycerides are packed into the core.

3.3.3   Exogenous lipid metabolism

Dietary lipids mostly consist of TGs, additionally phospholipids, free fatty acids, cholesterol (in the form of cholesterol-esters) and fat soluble vitamins are present. In the stomach and the duodenum fats are broken down to fatty acids and free cholesterol by gastric and pancreatic lipase and are then solubilized by bile acids micelles. In this way they are transported into the enterocyte where they are re-esterified to TGs and cholesterol-ester and packed onto ApoB48. On their way through the plasma they recruit additional apoliproteins, e.g. ApoCII and ApoE from high density lipoprotein (HDL), forming now a

mature chylomicron. In the capillaries of adipose tissue and muscle, ApoCII activates lipoprotein lipase (LPL), which hydrolyzes the TG core to free fatty acids and glycerol. These can be taken up by fat cells and re-incorporated into TG for storage or used by muscle for energy generation. The cholesterol ester rich chylomicron remnants circulate back to the liver where ApoE enables removal by the liver. Uptake of remnants includes binding to LDL receptor, LDL receptor related protein (LRP), hepatic lipase (HL) and cell surface proteoglycans (Fig 4).

3.3.4 Endogenous lipid metabolism

The endogenous pathway refers to the hepatic secretion and metabolism of TGs and cholesterol-esters by very low density lipoproteins (VLDL), low density lipoproteins (LDL) and intermediate density lipoproteins (IDL) (Fig 4).

One obligatory component of VLDL is apolipoprotein B (ApoB). ApoB occurs in two forms, ApoB100 and ApoB48, which consist of the N-terminal 48% of full length ApoB100 derived from editing ApoB100 mRNA. In humans, ApoB100 is secreted by the liver and ApoB48 from the intestine; the mouse liver, however, secrets both Apo forms (M. Liu *et al.*, 2011). VLDL assembly requires the action of microsomal transfer protein (MTP), which transfers triglycerides to the growing ApoB peptide. Regulation of VLDL-TG secretion is multifactorial. Factors that influence VLDL production are lipid availability, MTP levels, apolipoprotein availability or secretory vesicle trafficking. Once in the circulation VLDL acquires ApoE, ApoCII and ApoCIII. ApoCII activates LPL on the surface of peripheral tissues, which hydrolyzes TG into free fatty acid and glycerol for uptake in the cell. IDLs result from VLDL breakdown and are cleared by the liver via LDL receptors. The predominant remaining proteins are ApoB and ApoE. Further hydrolysis of TGs by hepatic lipase results in the formation of low density lipoproteins, where ApoB is the only apolipoprotein component and cholesterol-esters are the main lipid part. LDL can be cleared by the liver in a process mediated by ApoB and LDL receptors. LDL is often referred to as "bad cholesterol", because it is considered to be atherogenic. LDL particles that are not cleared by the liver can accumulate in the subendothelial space. They can be oxidized and taken up by macrophages leading to the formation of so called lipid filled foam cells. Foam cells can aggregate within the arterial wall and subsequently form atherosclerotic plaques. If they

rupture a thrombus can form, consequently, blood flow is reduced, increasing the risk of infarctions in the heart, brain or other vital organs (H.N. Ginsberg, 2000).
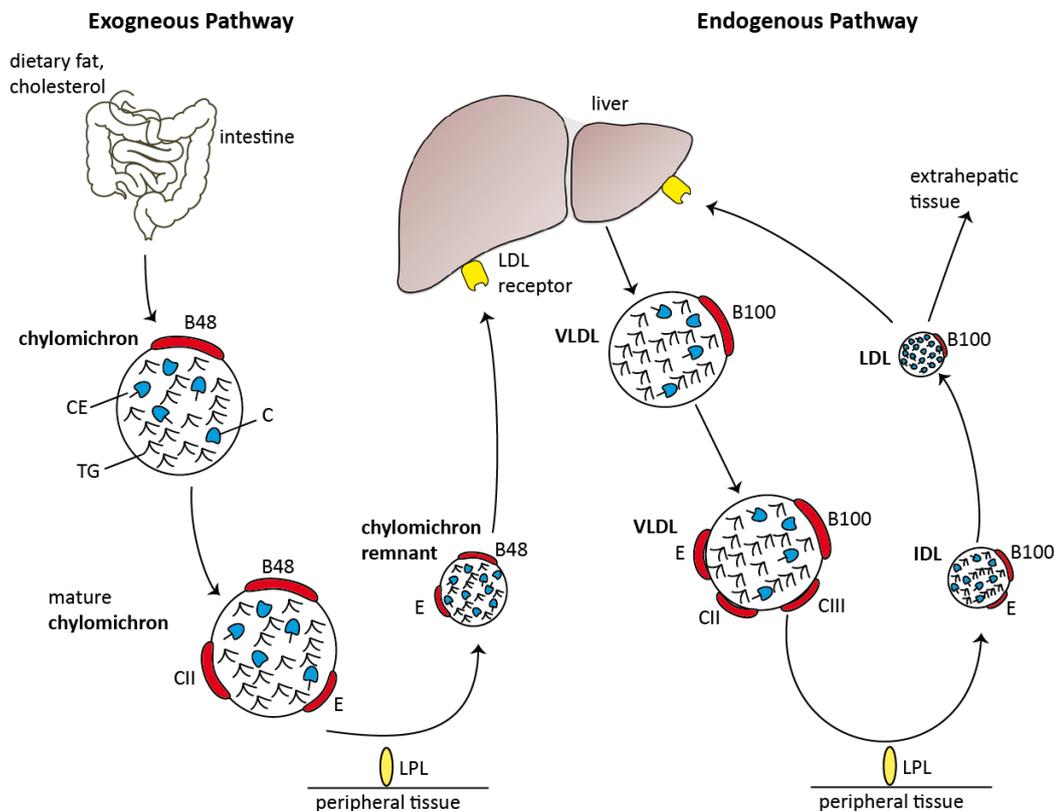
Fig 4: Schematic representation of exogenous and endogenous lipid metabolism.
In the exogenous pathway dietary fat and cholesterol is packed into chylomicrons containing ApolipoproteinB48 (ApoB) in form of free cholesterol (C) und triglycerides (TG). During transport through the bloodstream chylomicrons mature, obtaining ApoCII (CII) and ApoE (E) from high density lipoproteins (HDL). In peripheral tissues, lipoprotein lipase (LPL) hydrolyses TGs and the remnants are taken up into the liver by LDL receptors. In the endogenous pathway TGs are secreted by the liver in form of ApoB containing very low density lipoprotein (VLDL). On the way through the plasma, VLDL obtains ApoE, ApoCII and ApoCIII (CIII). Hydrolysis by LPL leads to the formation of intermediate density lipoprotein (IDL) containing ApoB100 and ApoE. IDL is further hydrolyzed to low density lipoprotein (LDL) with ApoE as the sole lipoprotein. The cholesterol rich particle is taken up by the liver or extrahepatic tissues.
B48/100: ApolipoproteinB48/100; C: cholesterol; CE: cholesterol-ester, TG: triglycerides; CII/III: ApolipoproteinCII/III; E: ApolipoproteinE; HDL: high density lipoprotein; VLDL: very low density lipoproteins; ILD: intermediate density lipoproteins; LDL: low density lipoproteins; LPL: lipoprotein lipase

3.3.5   HDL metabolism and reverse cholesterol transport

The cholesterol in our diet comes exclusively from animal sources. It is important to maintain membrane fluidity; it is a precursor for bile acids, steroid hormones and vitamin D. All nucleated cells can synthesize cholesterol, but only hepatocytes can metabolize cholesterol and enable its secretion from the body. In a process called reverse cholesterol transport (RCT) cholesterol is transported from the periphery to the liver by HDL particles, taken up by the liver, secreted in the bile and finally via feces (R. Ross and J. A. Glomset, 1973) (Fig 5). HDL levels in the serum are inversely associated with the risk of developing atherosclerosis (T. Gordon *et al.*, 1977; S. Lewington *et al.*, 2007) and hence HDL is also referred to as the "good cholesterol".

Formation of HDL particles begins with synthesis of ApoAI in the liver or the intestine. ApoAI proteins are the most abundant apolipoproteins in the HDL particle followed by ApoAII. The lipid poor nascent HDL acquires cholesterol and phospholipids from the liver, intestine or macrophages forming mature HDL. Transport is mediated by the membrane protein ATP-binding cassette protein A1 (ABCA1). Humans affected with Tangier disease, caused by a homozygous mutation in the ABCA1 gene, exhibit severe HDL deficiency (M. Marcil, 1999). Further important factors for reverse cholesterol transport are ABCG1, which also effluxes cholesterol to HDL, lecithin-cholesterol acetyltransferase (LCAT), which esterifies free cholesterol and cholesterol-ester transfer protein (CETP), which enables the transfer of cholesterol-esters from HDL to TG rich lipoproteins as VLDL. Mice naturally lack cholesterol-ester transfer protein (CETP) (Y.C. Ha and P. J. Barter, 1982), which can explain their high levels of plasma HDL as compared to humans. After conversion of VLDL to LDL, cholesteryl esters are finally removed from the circulation by LDL receptor mediated endocytosis. Scavenger receptor B1 (SR-B1) plays a major role in the uptake of HDL into the liver. Finally, ABCG5/8 heterodimers facilitate hepatobilary cholesterol transport for final excretion.
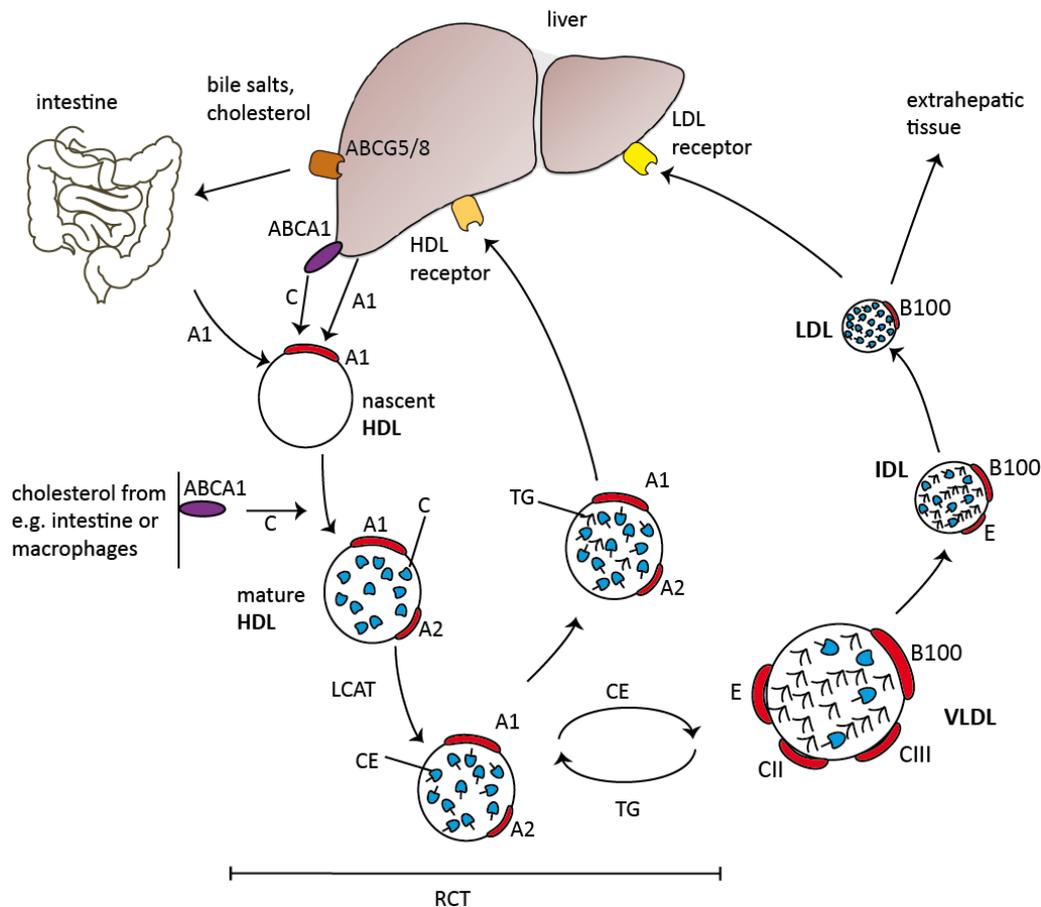
Fig 5: Schematic representation of HDL metabolism and reverse cholesterol transport in humans

The liver or the intestine synthesize ApoA1 (A1), via transporters as ATP-binding cassette protein A1 (ABCA1) nascent HDL acquires cholesterol (C), which is subsequently esterified by lecithin-cholesterol acetyltransferase (LCAT). Mature high density lipoprotein (HDL) is taken up by liver cholesterol is either converted to bile or directly excreted via transporters as such ABCG5/8. This process of cholesterol removal from the body is called reverse cholesterol transport (RCT). In HDL some cholesterol-esters (CE) are transferred from mature HDL to very low density lipoproteins (VLDL) in exchange for triglycerides (TG). VLDL particles are hydrolyzed to intermediate density lipoproteins (IDL) and low density lipoproteins (LDL) and taken up by receptors in the liver or further transported through the body for uptake by other tissues.

A1/2: ApolipoproteinA1/2; C: cholesterol; LCAT: lecithin-cholesterol acetyltransferase; CE: cholesterol-ester, HDL: high density lipoprotein; ABC A1/G5/G8: ATP-binding cassette protein A1, G5, G8; VLDL: very low density lipoproteins; TG: triglycerides; ILD: intermediate density lipoproteins ; LDL: low density lipoproteins

3.3.6   Dyslipidemia

The metabolic syndrome is associated with an increased risk for CVD, which in turn is linked to lipid and lipoprotein abnormalities of insulin resistance (T. J. Chahil and H. N. Ginsberg, 2006). Dyslipidemia describes a disorder that is marked by deregulated blood lipid content, as elevated serum TGs, low HDL cholesterol levels and normal or slightly elevated LDL cholesterol levels. In a state of insulin resistance there is an increased flux of free fatty acids

to the liver, resulting in the accumulation of TGs in the liver. This leads increased production and secretion of VLDL, leading to hypertriglyceridemia. If too much TGs accumulate steatosis (fatty liver) develops. Once in the serum, cholesterol-ester transfer protein (CETP) transfers TGs and cholesterol between VLDL and HDL or LDL. In the end this results in lower levels of HDL cholesterol and higher levels of small dense LDL particles. Furthermore, in state of insulin resistance clearance of VLDL and intestinal derived chylomicrons is impaired. This leads to prolonged plasma retention of VLDL and chylomicron remnants, which are in combination with low HDL levels particularly atherogenic (B. Klop *et al.*, 2013).

There are different strategies to treat dyslipidemia. One arm is lifestyle interventions, such as diet or physical activity (A.M. Haffner, 2003), the other arm is pharmacological treatment, such as statins or fibrates (H. E. Bays *et al.*, 2013), which can help to reduce risk for developing atherosclerosis. CVDs are a major health burden; therefore, a thorough understanding of the molecular mechanisms of lipid metabolism is important to find novel approaches for prevention or treatment of dyslipidemia and its associated disorders.

3.4 Transcriptional regulation by nuclear receptors

3.4.1 Nuclear receptors

Metabolic homeostasis happens on different levels. One level is the long-term overall metabolic homeostasis from birth during time of growth and development to adulthood, which includes adapting the energy intake to the body's needs. The second level is the daily rhythm of fasting and feeding cycles, where one of the major aims is to keep the blood sugar balanced. Overall, these processes require a tight regulation, also to prevent metabolic disorders. One key aspect in this context is transcriptional regulation.

The key concepts of regulating gene expression have been established in a bacterial system (F. Jacob and J. Monod, 1961). Their seminal work and many following studies found DNA binding transcription factors to occupy specific DNA sequences at control elements (cis-elements) and to recruit and regulate the transcription apparatus.

One well described class of transcription factors comprises nuclear receptors (NR), which are crucial for integrating signals from dietary, metabolic and endocrine pathways to control target gene expression. NRs are a superfamily of structurally-related ligand-

dependent transcription factors. There are 48 known family members in humans and 49 family members in rodents, out of which 37 are expressed in the liver (M. Downes and C. Liddle, 2008).

All NR receptors exhibit common structural features (Fig 6), namely the highly variable N-terminal activation domain (AF1), a central much conserved DNA binding domain (DBD), containing two zinc fingers and the C-terminal ligand binding domain (LBD). The LBD harbors a further activation domain (AF2), which is important for binding of ligands, such as steroid hormones, cholesterol or fatty acids, and for co-regulator recruitment (R.M. Evans, 1988).

Based on their ligand and DNA binding properties nuclear receptors can be subdivided into three different classes (D.J. Mangelsdorf *et al.,* 1995). The first class of NR comprises the classical steroid receptors such as the estrogen (ER) or glucocorticoid receptors (GRs), which act as receptors for fat-soluble hormones and vitamins. A second class of NR comprises the so called adopted orphan receptors including the peroxisome proliferator-activated receptors (PPARs) or liver X receptor (LXR), which are central regulators of lipid and glucose homeostasis and therefore, interesting molecular targets for drugs to treat hyperlipidaemia and type 2 diabetes (M. Downes and C. Liddle, 2008). The last class are the orphan receptors where no physiological or synthetic ligand have been discovered yet (D.J. Mangelsdorf *et al.*, 1995).

Fig 6: Schematic representation of nuclear receptor structure
The primary and tertiary common domain structure of a nuclear receptor is depicted. It consist of the N-terminal ligand independent activation domain (AF-1), a central DNA binding domain (DBD), with 2 zinc finger motifs (ZN), a hinge region and the C-terminal ligand binding domain (LBD) with a further activation domain (AF-2).
N: N-terminus; AF-1/2: activation domains; DBD: DNA binding domain; ZF: zinc fingers; C: C-terminus; LBD: ligand binding domain.

3.4.2 The role of transcriptional co-regulators

Nuclear receptors or transcription factors do not regulate transcription by themselves; they require co-regulators to modify and remodel chromatin structure and to recruit the

transcriptional machinery (J. N. Feige and J. Auwerx, 2007). Co-regulator complexes function either as co-activators or co-repressors, depending on their composition (Fig 7). As they cannot bind to DNA directly, they influence gene transcription by either recruiting further regulatory units, the reservoir for interacting partners comprises more than 200 proteins (J. N. Feige and J. Auwerx, 2007), or they exert themselves post-translational modifications as phosphorylation, acetylation, ubiquitination and SUMOylation (M. Anbalagan *et al.*, 2011).

Two of the best described co-repressors are nuclear receptor co-repressor (NCoR) and silencing mediator of retinoic and thyroid hormone receptor (SMRT) (A.J. Horlein *et al.*, 1995; J.D. Chen and R. M. Evans, 1995), which interact with unliganded nuclear receptors. A further part of the NCoR/SMRT complexes are histone deacetylase (HDACs). Removal of acetyl residues from histone tails results in a condensed DNA structure, transcription is inhibited.

Transcriptional activators either bind to histone acetyl transferases (HAT) or have intrinsic HAT activity (X. Liu *et al.*, 2008). Acetylation of histones opens the DNA structure and makes it accessible for the transcriptional machinery (C. A. Johnson, 2000).

One way to mediate the change between repression and activation of gene transcription is the exchange of co-activator and co-repressor complexes. One cofactor that has been described to be a so-called nuclear exchange factor is transducing beta like 1 (TBL1) (V. Perissi *et al.*, 2004). Together with transducing beta like related 1 (TBL1) it has been established to be part of the NCoR/SMART, HDAC3, G-protein pathway suppressor-2 (GPS2) complex (M. G. Guenther, 2000; J. Li, 2000; J. Zhang, 2000). TBL1 and TBLR1 were described to recruit ubiquitin/19S proteasome units to the transcriptional complex, resulting in dismissal of SMRT-NCoR-HDAC3 complex and consecutive binding of co-activators (V. Perissi *et al.*, 2004). Furthermore, TBL1 and TBLR1 have been shown to actively recruit co-activators as RIP140 (V. Perissi *et al*., 2004).

Our group described TBL1/TBLR1 as regulators of hepatic lipid metabolism (P. Kulozik *et al.*, 2011). In mice liver specific knockdown of TBL1 resulted in hepatic steatosis and hypertriglyceridemia. The increase in liver and serum TGs could be explained by reduced mitochondrial and peroxisomal fatty acid oxidation pathways and increased lipogenesis. Consistent with these findings, it was shown that TBL1 interacts with and activates PPARα.

This was the first implication that the TBL1/TBLR1 co-factor complex plays a critical role in liver metabolism.

Altogether, transcriptional co-factors add another level of complexity to the regulation of metabolic balance. However, the discovery of so far unappreciated co-regulators may present new targets for the treatment of metabolic disorder.
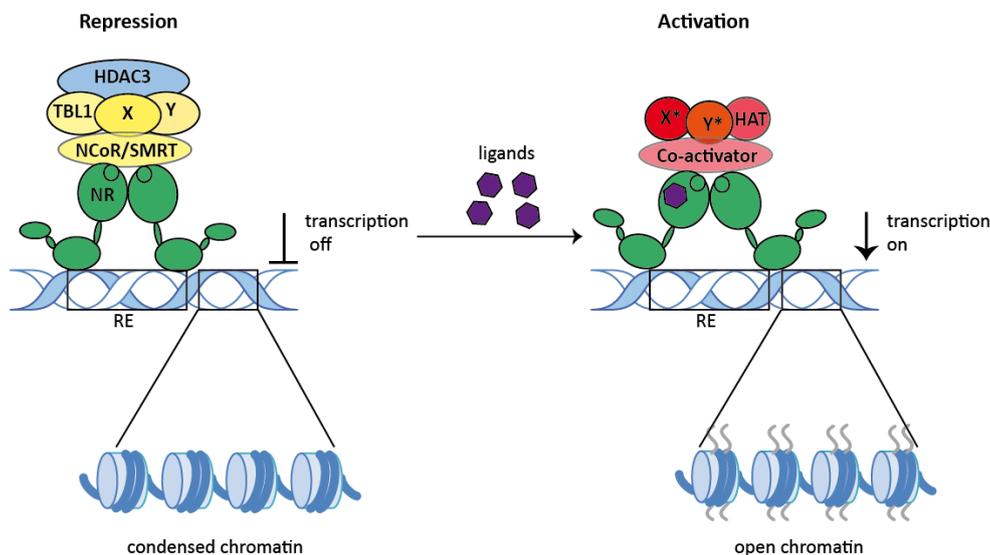
Fig 7: Schematic diagram of transcriptional repression or activation by nuclear receptors and co-regulators.

In case of repression nuclear receptor (NR) dimers are bound to response elements (RE) on the DNA. Well described co-repressor complexes contain nuclear receptor co-repressor (NCoR) and silencing mediator of retinoic and thyroid hormone receptor (SMRT), transducing beta like 1 (TBL1) and histone deacetylase 3 (HDAC3) and other factors (X, Y). These mediate histone deacetylation so that target gene transcription is switched off. Ligand binding leads to conformational changes in the NR dimer. Co-activator complexes containing histone acetylase (HAT) can bind. Chromatin is opened and target gene transcription is switched on.

NCoR: nuclear receptor co-repressor; SMRT: silencing mediator of retinoic and thyroid hormone receptor; TBL1: transducing beta like 1; HDAC3: histone deacetylase 3; HAT: histone acetylase; X/Y: co-repressors; X*/Y*: co-activators

3.4.3 Transforming growth factor beta stimulated clone 22D 1 as a novel co-regulator

Transforming growth factor beta stimulated clone 22D 1 (TSC22D1) was first isolated from mouse osteoblastic cells in 1992 (M. Shibanuma *et al.,* 1992). Prior to this study, TSC22D1 has been identified in a screen to directly bind to transcriptional co-regulator TBL1 (PhD thesis, Allan Jones, Herzig Lab). It is a member of a family of 4 structurally related proteins named TSC22D1-TSC22D4 (H.A. Kester *et al.*, 1999) conserved from *Caenorhabditis elegans* to humans (S. Gluderer *et al.*, 2010.).

TSC22D1 expression *in vitro* is strongly but transiently induced by TGF-β stimulation (M. Shibanuma *et al.,* 1992; T. Kawa-Uchi *et al.,* 1995; R.A. Gupta *et al.,* 2003) and it has been speculated that this is due to post-transcriptional regulations like an increase in mRNA stability (D. Uchida *et al.,* 2003) or an enhanced TSC22D1 translation (M. Kato *et al.,* 2010). Several studies describe TSC22D1 in the context of transcriptional regulation. TSC22D1 contains a leucine zipper structure in mice (M. Shibanuma *et al.,* 1992) and humans (P. Jay *et al.,* 1996). However, it has no DNA binding domain as it lacks the basic region at the N-terminus of the zipper. One study has shown that it can directly bind to the promoter of human C-type natriuretic peptide (CNP) and can as well enhance CNP promoter activity in a rat pituitary derived cell line (GH3) (S. Ohta *et al.,* 1996). Most studies concerning the function of TSC22D1 in regulation of gene transcription indicate, however, that it is a transcriptional co-factor rather than a transcription factor. Fused to a heterologous-DNA binding domain it was described to activate transcription in a mammalian cell system (S. Hino *et al.,* 2000). In this study activation only worked in CHO cells but not in two other cell lines. Another study with TSC22D1 fused to a heterologous-DNA binding domain reported repression of transcription (H.A. Kester, 1999). Interestingly, this repressive function was dependent on dimerization with TSC22D4. Moreover, TSC22D1 can directly interact with transcription factor Smad4 and increase its transcriptional activity in vitro (S.J. Choi *et al.,* 2005). Along these lines, TSC22D1 was to shown to interact with the transcription factor Tfe3 in co-immunoprecipitation studies (M. Kato *et al.,* 2010) and enhance transcription. ChIP experiments displayed an increased occupancy of TSC22D1 at enhancer E-boxes of collagen type I alph-2 (Col1a2) through TGFbeta1 stimulation in primary mouse MC, strengthening the idea of TSC22D1 as a transcriptional co-factor.

Regarding its function, some work on TSC22D1 indicates that it acts as a tumor suppressor. Downregulation of TSC22D1 enhanced growth of a human salivary gland cancer cell line (K. Nakashiro, 1998). Moreover, it has shown to be downregulated in human salivary gland tumors (K. Nakashiro, 1998) in a set of human brain tumors (K.O. Shostak *et al.,* 2003) and in aggressive forms of astrocystic tumors (K.O. Shostak *et al.,* 2003). Furthermore, several publications demonstrate that in cell culture models overexpression of TSC22D1 induces apoptosis (S. Ohta *et al.,* 1997; S. Hino *et al.,* 2000), presumably by a caspase 3 dependent pathway (J.H. Lee *et al.,* 2008) or inhibits tumor cell growth by preventing proteosomal degradation of p53 (Y. Lu *et al.,* 2007, C.H. Yoon *et al.,* 2012). In the only *in vivo* study

published so far, TSC22D1-deficient mice were susceptible to tumorigenesis in a mouse model of chemically-induced liver tumors bearing active mutations of Ras/Raf (M. Nakamura *et al.*, 2011), emphasizing the tumor suppressive function of TSC22D1.

Up to date, there are no publications about a role of TSC22D1 in metabolism in general. Interestingly, its family member TSC22D4 has proven to be a critical molecular determinant of systemic lipid homeostasis and lipoprotein metabolism (A. Jones *et al.*, 2013 and A. Jones unpublished work). Liver-specific ablation of TSC22D4 triggered hypertriglyceridemia through the induction of hepatic VLDL secretion. The fact that TSC22D1 and TSC22D4 can heterodimerize (H.A. Kester *et al.*, 1999) and the observation that TSC22D1 interacts with another crucial regulator of hepatic lipid metabolism TBL1 (P. Kulozik *et al.*, 2011 and PhD thesis Allan Jones, Herzig Lab), prompted us to hypothesize that hepatic TSC22D1 is a further novel regulator of liver metabolism.

3.5 Aim of the study

Given the previous work from this lab, the aim of this study was to elucidate the role of transcriptional co-factor TSC22D1 in liver metabolism. To this end, the regulation of hepatic TSC22D1 expression was to be analyzed in various mouse models of metabolic imbalance. Further, TSC22D1 knockdown and overexpression tools were to be generated. Subsequently, studies in relevant mouse models were to be performed to investigate TSC22D1 function *in vivo*.

4 Results

4.1 TSC22D1 is a candidate transcriptional co-regulator

4.1.1 TSC22D1 interacts with transcriptional co-factor TBL1

Transcriptional co-factors play an important role in the regulation of metabolic processes, as previously demonstrated by studies from this lab (M. Berriel-Diaz *et al.*, 2008; P. Kulozik *et al.* 2011; A. Jones *et al.,* 2013; M. Rohm *et al.,* 2013). One example is the transcriptional co-factor TSC22D4 (A. Jones *et al.,* 2013), which was shown to be important for liver lipid handling. TSC22D4 was discovered in a luminescence-based mammalian interactome mapping (LUMIER) screen (PhD thesis Allan Jones, Herzig Lab) aiming to detect novel interaction partners of the transcriptional co-factor TBL1 (P. Kulozik *et al.,* 2011) or TBLR1 (M. Rohm *et al.,* 2013), which are both regulators of lipid metabolism in liver as well as in fat. In this screen, also TSC22D1, which is known to dimerize with TSC22D4 (H.A. Kester *et al.*, 1999), showed a strong interaction with TBL1 and TBLR1 (PhD thesis Allan Jones, Herzig Lab). Thus, we hypothesized that TSC22D1 might play a role in liver metabolism as well. As a first step, the interaction between TBL1 was verified by Flag-co-immuoprecipitation studies (Fig 8), whereas, the interaction with TBLR1 could not be verified. These results indicated that TSC22D4 and TSC22D1 have distinct interaction partners and therefore also distinct functions. The previously published interaction between TSC22D1 and TSC22D4 (H.A. Kester *et al.*, 1999) could be recapitulated as well. However, it was impossible to map the interaction between TBL1 and TSC22D1 by Glutathione-S-Transferase (GST)-pulldowns (data not shown).
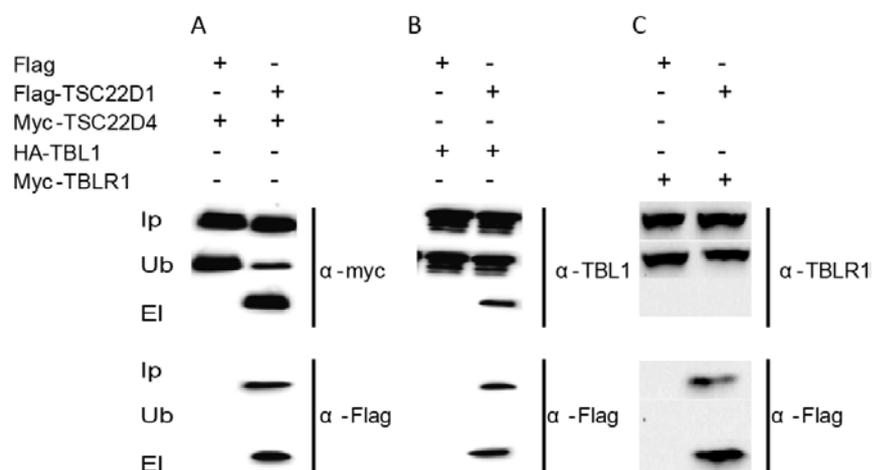
Fig 8: TSC22D1 co-precipitates with TBL1 in Flag co-immunoprecipitation studies. *Co-immunoprecipitation studies, in HEK293 cells transfected with Flag-TSC22D1 and a vector encoding either the control Flag peptide, (A) Myc-TSC22D1 (B) HA-TBL1 or (C) HA-TBLR1. Affinity purification was performed with an anti-Flag antibody. Bound proteins were resolved by SDS-PAGE and subsequently detected by Western blotting with Myc, Flag, TBL1 and TBLR1 antibodies. Ip: Input; Ub: unbound; El: elution*

4.2   Hepatic TSC22D1 expression is altered by energy status

4.2.1   Analysis of hepatic TSC22D1 expression in mouse disease models

The mouse can serve as a good model system to study human diseases. Mice and men both have 3 million base pairs of DNA, which share about 85% similarity. The whole mouse genome has been sequenced in 2002 (R.H. Waterston *et al.*, 2002). Metabolic, physiological and behavioral stresses can be tested in mouse models and the results can be compared directly with human clinical information (N. Rosenthal and S. Brown, 2007). Given the importance of TBL1 and TSC22D4 for hepatic lipid metabolism (P. Kulozik *et al.*, 2011 and A. Jones *et al.*, 2013) combined with the results from the co-immuniprecipitation study (Fig 8) we chose the liver as a target organ for this study. Prior work from this lab (P. Kulozik *et al.,* 2011 and A. Jones *et al.,* 2013) has shown that TBL1 and TSC22D4 expression as such are altered in mouse disease models; therefore, we analyzed the expression of TSC22D1 in livers of mice challenged with different metabolic conditions.

4.2.2   TSC22D1 expression is strongly downregulated by fasting

Prolonged fasting results in a state of nutrient deprivation and energy wasting. As a result of falling blood sugar levels glucagon is secreted from the pancreas which signals to a variety of organs. In the liver, fasting signals cause glycogenolysis and gluconeogenesis, followed by the release of glucose. Additionally, fatty acids (FA) and glycerol are released from adipose tissue and taken up by the liver. In prolonged fasting, when glycerol stores are empty, free fatty acids are broken down for the generation of ketone bodies.
In the postprandial state, blood sugar rises and subsequently, insulin signaling results in the uptake of glucose and lipids into the liver, adipose tissue or muscle. The FAs are packaged into lipoproteins for further transport throughout the body. Altogether, these processes underlie a tight regulation.

In order to see if hepatic TSC22D1 expression is altered by fasting signals, male and female C57BL/6 mice were fasted for 16 hours. After starvation, one group of mice was sacrificed immediately and the other mice were refed for 6 hours. Hepatic TSC22D1 mRNA expression was determined by quantitative PCR (qPCR) (Fig 9A). Levels of TSC22D1 expression were not gender dependent. Interestingly however, in the fasting state TSC22D1 mRNA levels were decreased by approximately 80%. In a further approach, male C57BL/6 mice were fasted for 24 hours one group of mice was sacrificed immediately and the other mice were fed for either 1, 6 or 24 hours (Fig 9B). Taking 24 hours of reseeding as the baseline value for TSC22D1 expression, TSC22D1 expression was 80-90% decreased after 24h fasting and returned to its baseline level 6 hours after refeeding. These results indicate that fasting signals might control TSC22D1 expression.

A **B**
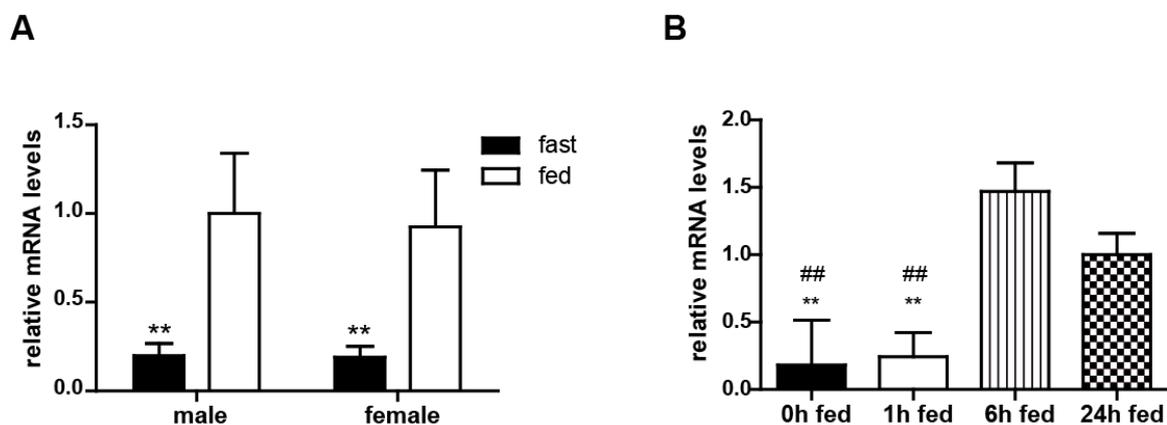
Fig 9: TSC22D1 expression is strongly downregulated by fasting. A) TSC22D1 expression in male or female mice fasted for 16h and either directly sacrificed or refed for 6h. B) TSC22D1 expression in mice fasted for 8h or 24h hours and either directly sacrificed or refed for 1h, 6h or 24h. Liver mRNA levels were analyzed by qPCR. (n=5-7), (means ± SEM). (A-B) (**) indicates significance p≤0.01 to 6h fed, (B) (\#\#) indicates significance p≤0.01 to 24h fed

4.2.3 TSC22D1 expression is reduced in mice on a methionine and choline deficient diet

Mice fed with a diet lacking methionine and choline (MCD) encounter dramatic weight loss, develop severe hepatic steatosis and have low serum TG levels (M.E. Rinella *et al.*, 2008). To determine if TSC22D1 expression is altered in this model of energy wasting, hepatic RNA was isolated from mice fed either control diet or an MCD diet for 4 weeks. Subsequently, TSC22D1 mRNA expression was analyzed by qPCR (Fig 10). TSC22D1 mRNA levels were significantly reduced in mice on MCD diet compared to mice on the control diet. This suggests that the energy status can influence TSC22D1 expression.
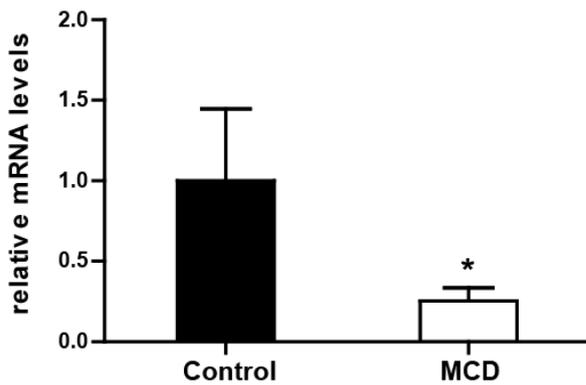
Fig 10: TSC22D1 expression is reduced in mice on methionine choline deficient diet. TSC22D1 expression in mice fed a methionine choline deficient diet (MCD) or a control diet. Liver mRNA levels were analyzed by qPCR. (n=4), (means ± SEM). (*) indicates significance p≤0.05

4.2.4 TSC22D1 levels negatively correlate with weight loss in cachectic patients

Cachexia is a multi-factorial disease characterized by massive wasting of adipose tissue and skeletal muscle mass (M.J. Tisdale, 2002). Further, cachexia causes hepatic dysfunction in the form of reduced VLDL secretion and hypoapolipoproteinemia (A. Jones *et al.*, 2013). For this study we analyzed mRNA expression of TSC22D1 in liver biopsies from 10 patients with pancreatic cancer with or without cachecxia. Interestingly, body weight loss negatively correlated with TSC22D1 expression levels (Fig 11A and B).

The C26 colon carcinoma model is a mouse model for tumor-induced cachexia. Tumor bearing mice suffer from severe weight loss mainly by adipose tissue and muscle wasting, they develop hyperglycemia (Y. Tanaka *et al.*, 1990) and they exhibit reduced serum TG levels (A. Jones *et al.*, 2013). To induce cancer cachexia, Balb/C mice were injected subcutaneously with 1.5 x 10^6 Colon26 adenocarcinoma cells. Mice were sacrificed approximately three weeks after tumor-cell injection with the on-set of cachexia, determined by body weight loss. Hepatic TSC22D1 mRNA levels were significantly reduced in the cachectic mice compared to healthy control mice (Fig 11C). As seen in the patient data (Fig 11B), TSC22D1 expression correlated with the degree of weight loss (Fig 11D). These results are in line with the observations that TSC22D1 expression is reduced in conditions of energy deprivation (Fig 9 and 10).
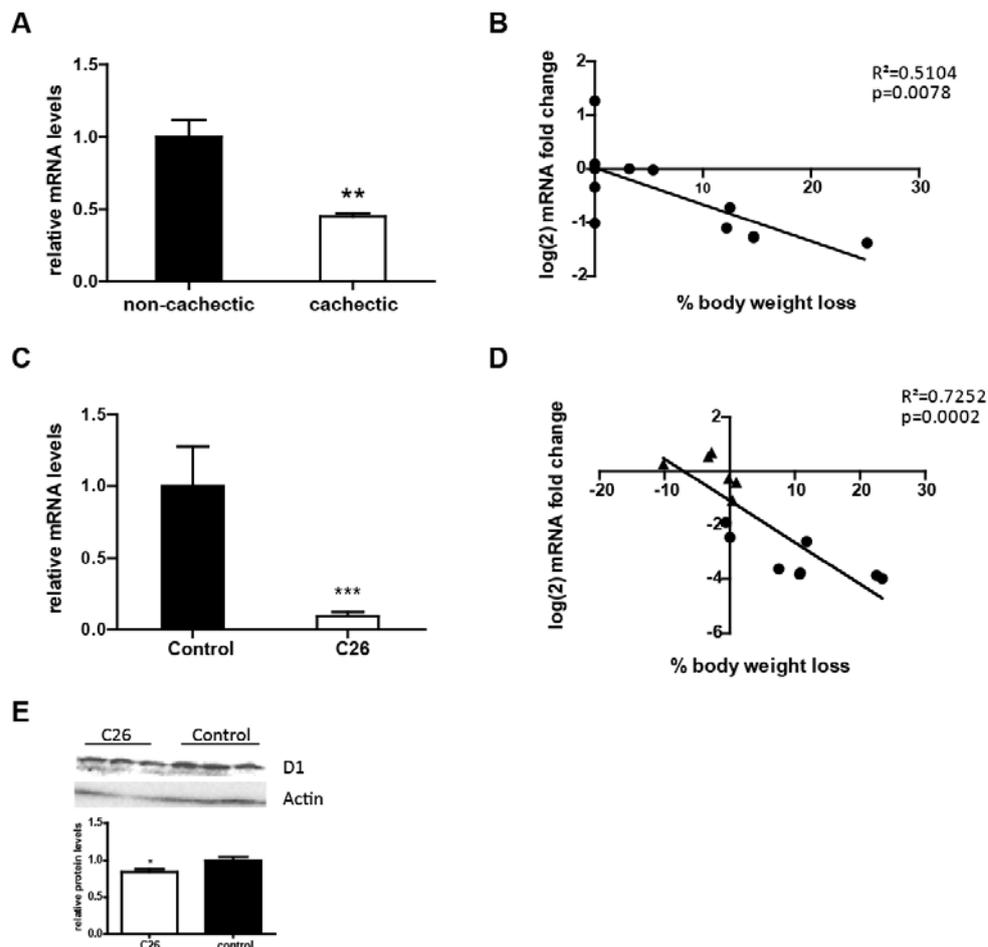
Fig 11: TSC22D1 expression correlates with the degree of cachexia in patients and mice.

A) TSC22D1 expression in livers of pancreatic cancer patients with or without cachexia. Liver mRNA levels were analyzed by qPCR (n=5). (**) indicates significance≤0.01 B) Pearson's correlation of log(2) of TSC22D1 expression and body weight loss as % of initial weight in livers of pancreatic cancer patients. (n=10) C) TSC22D1 expression in male Balb C mice, injected with 1.5x 10^{6} C26 mouse tumor cells and sacrificed with the onset of cachexia. Liver mRNA levels were analyzed by qPCR (n ≥ 6) (means ± SEM) (***) indicates significance p≤0.001 D) Pearson's correlation of log(2) of TSC22D1 expression and body weight loss as % of initial weight at time of sacrifice. ▲ = control mice, ● = C26 (E) Representative Western blot and quantification of liver extracts from same mice as in C. Protein was detected by TSC22D1 and β-actin (loading control) antibodies.

4.2.5 TSC22D1 expression is increased in mice on a high fat diet

Feeding mice a high fat diet over the course of several weeks results in weight gain, development of hyperglycemia, hyperinsulinemia, hypertension and an increased TG content in adipose tissue, serum and liver (R. Buettner *et al.*, 2007). To address if high fat diet feeding influences TSC22D1 expression, livers of mice were analyzed, that were fed either a high fat diet containing 60% energy from fat or a control low fat diet containing 10% energy from fat over a 9 week period. Mice on HFD gained significantly more weight

than mice on a LFD (data not shown). Hepatic TSC22D1 mRNA levels were analyzed by qPCR (Fig 12). TSC22D1 expression was 3 fold increased in mice on a HFD compared to control mice, indicating that TSC22D1 might be involved in the onset of obesity.
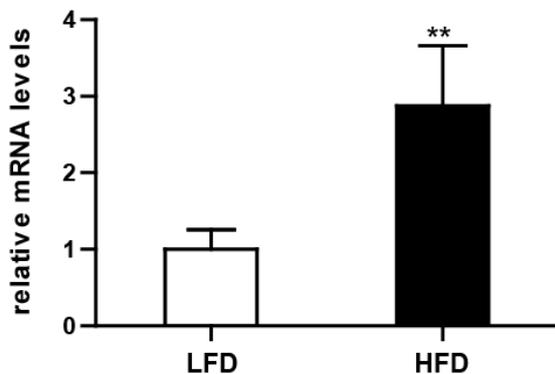
Fig 12: TSC22D1 expression is increased in mice on a high fat diet. Mice were fed a control low fat diet (LFD) or a high fat diet (HFD). Liver TSC22D1 mRNA levels were analyzed by qPCR. (n=4), (means ± SEM). (**) indicates significance; p < 0.01.

4.2.6   TSC22D1 expression is increased in obese mice

There are various monogenetic mouse models available to study obesity. Two of the most widely used mouse models are ob/ob or db/db mice, which harbor homozygous loss of function mutations in the genes for the satiety hormone leptin (ob) or its receptor (db). These mice suffer from obesity and its associated complications as hyperglycaemia, hyperinsulinemia and subsequently pre-diabetes (K. Kobayashi *et al.*, 2000 and P. Lindstrom, 2007). In random fed db/db TSC22D1 expression levels were 3-fold increased as compared to control wild type mice (Fig 13A). Also, TSC22D1 gene expression was analyzed in 5, 9 and 13 week old ob/ob mice and age-matched control wildtype C57BL/6 mice (wt). Whereas TSC22D1 expression did not significantly change with age in the wt mice, from week nine on levels of TSC22D1 were about 3-fold increased in ob/ob mice compared to wt control mice (Fig 13B). These data indicate that TSC22D1 expression might be regulated by changes in signaling due to obesity.

A

B
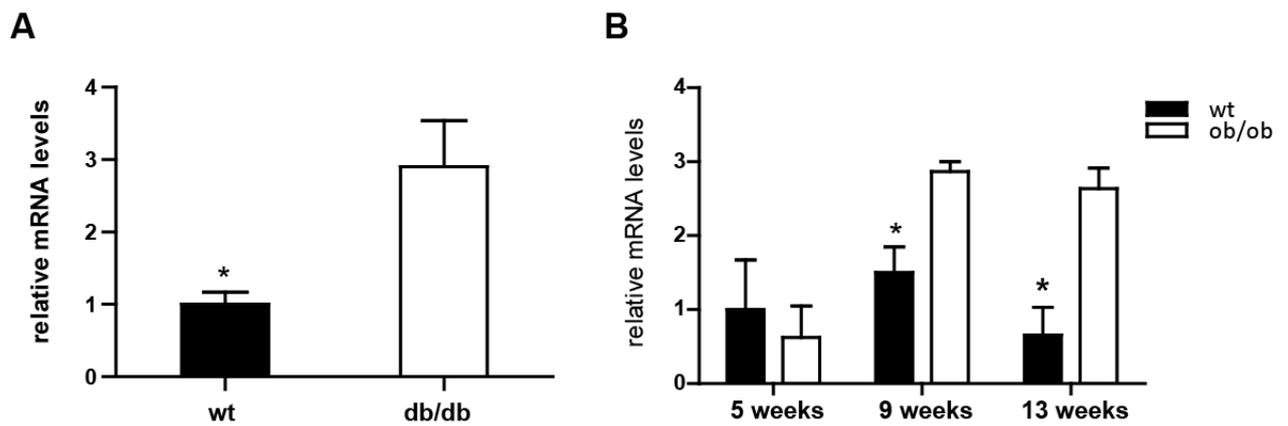
Fig 13: TSC22D1 expression is increased in obese mice. *A) TSC22D1 expression was determined in random fed db/db and C57BL/J (wt) mice. B) TSC22D1 expression was determined in, 9 or 13 week old ob/ob mice and control wt mice. Liver mRNA was analyzed by qPCR. (n=4-5), (means ± SEM). (*) indicates significance; p < 0.05.*

4.2.7 TSC22D1 expression is reduced in aged mice

Aging is characterized by an overall impairment of cellular function, resulting in common metabolic, inflammatory, cardiovascular and neurodegenerative diseases. Pathways that are altered in aged mice include glucose and fatty acid metabolism and redox homeostasis (R.H. Houtkooper *et al.*, 2011). In 22 month old mice which were refed for 6h after 24h of fasting TSC22D1 mRNA levels were 70% lower compared to refed 12 week old mice. Further, they did not exhibit down-regulation of TSC22D1 expression after fasting as seen in young mice (Fig 14). These results point towards an altered function of TSC22D1 in aged mice.
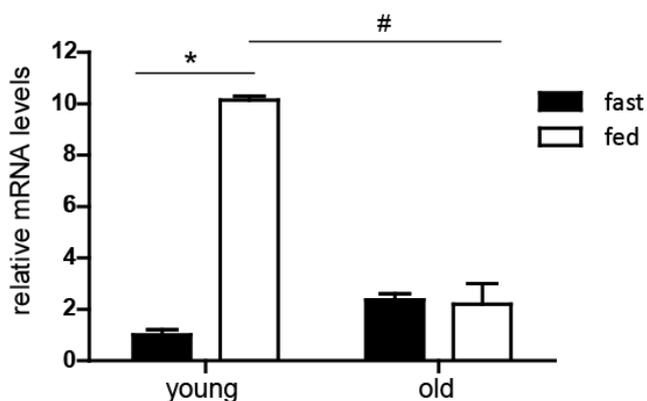
Fig 14: TSC22D1 expression is reduced in old mice. *TSC22D1 expression in 22 month old mice and 12 week old mice which were fasted for 24h hours, one group was sacrificed directly and the other*

group was refed for 6h. Liver mRNA was analyzed by qPCR. (n=5), (means ± SEM). (*) indicates significance p≤0.05 for nutritional status, (#) indicates significance p≤0.05 for age

4.2.8 TSC22D1 expression is induced by TGF-beta1 *in vivo* and *in vitro*

Signaling by the transforming growth factor TGF-β has various functions including the control of development, growth or function of diverse cell types (Y. Shi and J. Massague, 2003). *In vitro* TSC22D1 expression was shown to be induced by TGF-β1 stimulation (M. Shibanuma *et al.*, 1992, T. Kawa-Uchi *et al.*, 1995, R. A. Gupta *et al.,* 2003). We could recapitulate these findings in primary hepatocytes (Figure 15A), where expression started to increase 6h after stimulation and peaked after 24h. Furthermore, *in vivo* application of TGF-β1 to C57BL/6 mice increased hepatic TSC22D1 expression (Figure 15B). Interestingly, TGF-β1 levels correlate with obesity in mice (Figure 15C) and humans (H. Yadav *et al.*, 2011).
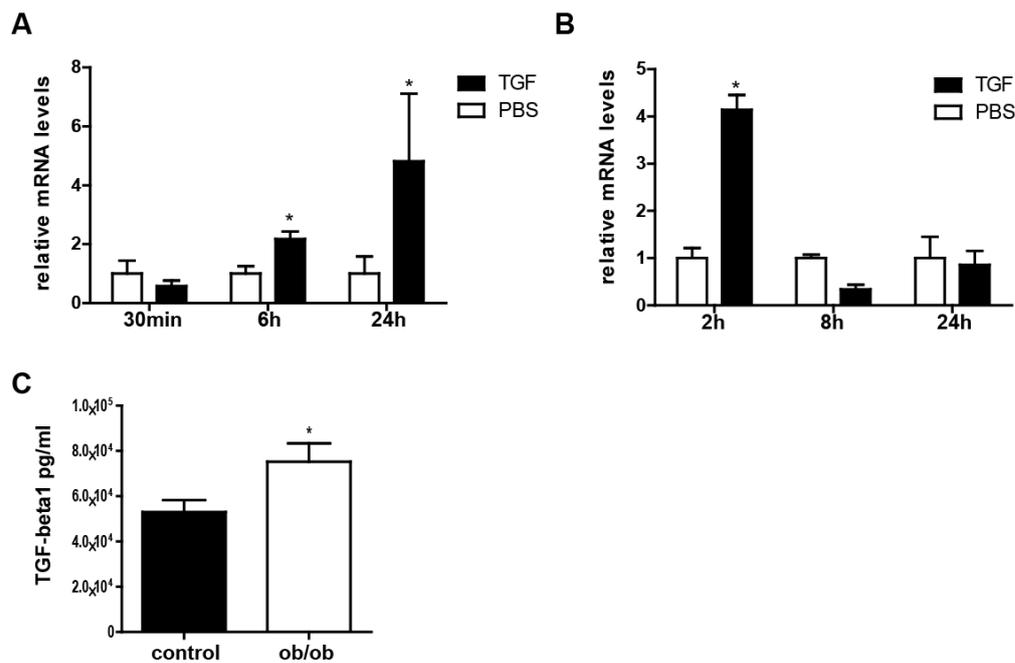
Fig 15: TSC22D1 expression is induced by TGF-ß1 stimulation. (A) TSC22D1 expression in primary hepatocytes after stimulation with 10 ng human recombinant TGF-ß1 for the indicated time. Primary hepatocyte mRNA was analyzed by qPCR. (n=3), (means ± SEM). (B) TSC22D1 expression in C57BL/6 mice injected with either PBS or 5µg human recombinant TGF-ß1. Mice were sacrificed at indicated time points after injection. (n=4), (means ± SEM). (C) Serum TGF-ß1 levels in ob/ob mice compared to wildtype control mice (wt). TGF-ß1 levels were determined by ELISA. (n=4), (means ± SEM). (*) indicates significance p≤0.05

4.2.9   Summary of TSC22D1 expression data

Altogether, we found hepatic TSC22D1 levels to be strongly altered in mouse models of metabolic disorders (Table 3). Whereas TSC22D1 expression was up-regulated in mouse models of obesity, it was strongly downregulated in models for wasting, cancer cachexia and upon fasting. These results point towards an important role of TSC22D1 in liver metabolism in different states of energy supply.

Table 3: Summary of hepatic TSC22D1 expression under different metabolic conditions

Mouse Model / Condition	Regulation
Fasting	↓
MCD diet	↓
Cachexia	↓
HFD	↑
db/db	↑
ob/ob	↑
TGFβ1	↑
Aging	↑

↑: indicates up-regulation, ↓ indicates down-regulation compared to respective controls

4.3   Phenotypic analysis of TSC22D1 deficient C57BL/6J mice

4.3.1   Adenoviral mediated knockdown of TSC22D1 in vivo

Adenoviruses are commonly used as vectors to transfer exogenous DNA to cells or whole organs *in vivo* or *in vitro*. If adenovirus is injected into the tail vain it is transported through the capillary system into the liver. Thus, mainly liver cells get infected and other tissues are hardly affected by the transgene. In this study an adenoviral vector system was used to deliver short hairpin RNAs (shRNA) or a cDNA into the mouse liver. Adenoviral vectors can only be used for short term experiments, as the virus is cleared from the system after approximately 14 days. The ideal time point for phenotypic analysis has been shown to be 7 days post infection (U. Lemke *et al.*, 2008) and has thus been used for all adenovirus experiments described in this work.

Specific shRNA sequences targeting TSC22D1 were cloned into the Invitrogen pENTR-DEST vector. Their knockdown efficiency was tested by co-transfecting Hepa1c1 cells with shRNAs targeting TSC22D1 or a scrambled control and a TSC22D1 overexpression construct. TSC22D1 depletion was analyzed by luciferase assay and Western blot (Fig 16). Sequence 395 performed efficiently in both assays and was subsequently sub-cloned into the Invitrogen pAD-BLOCK-IT vector. This vector contains most of the viral genome, but lacks

for safety reasons E1 and E3 genes which are required for viral replication. Adenovirus was propagated in HEK293A cells which express the missing genes in *trans*. Next, virus was purified by the cesium chloride method (U. Lemke *et al.*, 2008) and the titer was determined for *in vivo* application.
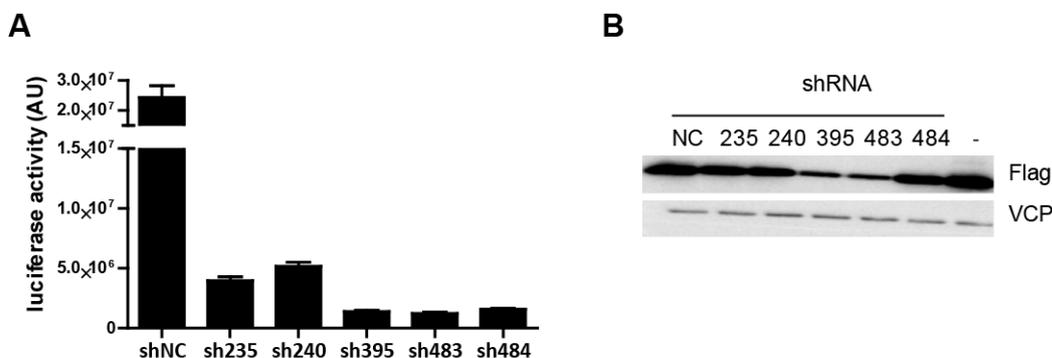
Fig 16: Cloning of adenoviral expression construct for TSC22D1 knockdown. A) HEK293A cells were transfected with plasmids containing the TSC22D1 sequence in frame with the luciferase coding sequence and co-transfected with plasmids expressing either a scrambled shRNA sequence (shNC) or different TSC22D1 targeting sequences (sh235-484). Luciferase activity is normalized to β-galactosidase and plotted relative to control shRNA. (n=3), (means ± SEM). B) HEK293A cells were transfected with plasmids overexpressing flag-tagged TSC22D1 and co-transfected with plasmids expressing either a scrambled shRNA sequence (NC) or different TSC22D1 targeting sequences (sh235-484) or nothing (-). Protein levels were analyzed by immunoblot using flag-antibody and VCP-antibody as loading control. Representative results from 3 experiments are shown.

In order to investigate the effects of reduced TSC22D1 expression in livers of C57BL/6J mice, 2 x 10^9 viral particles expressing either a scrambled shRNA sequence (shNC), or the sequence targeting the TSC22D1 (shD1) mRNA were administered via tail vein injection.

Over the time of the experiment, mice were housed in a TSE phenotyping system for indirect calorimetry. Mice were kept at 22°C with free access to food and water. Six days post injection animals were fasted for 24 hours. Then, half of the mice were sacrificed directly and the other group was refed for 6h. TSC22D1 knockdown efficiency was assessed at mRNA level by qPCR and at protein level by Western blot (Fig 17A-B). As also seen before (Fig 9), TSC22D1 expression was strongly downregulated by fasting.
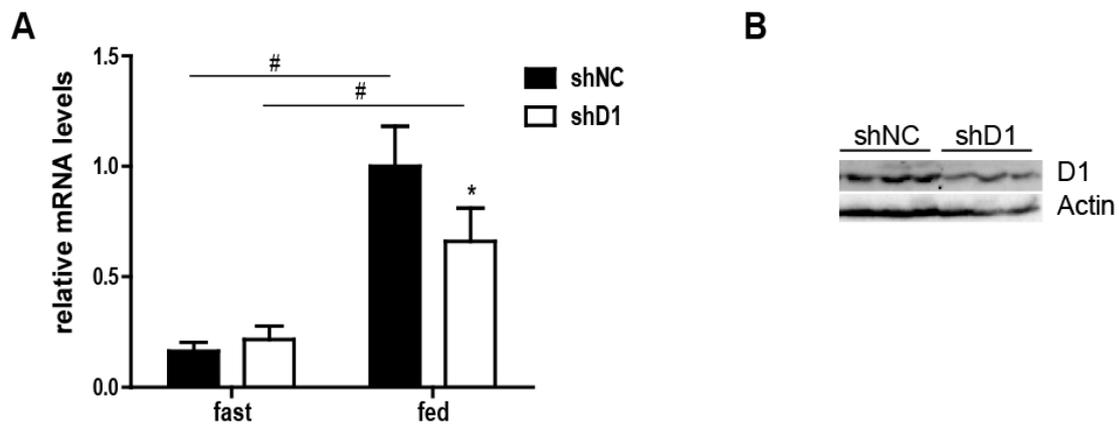
Fig 17: ShRNA mediated knockdown of TSC22D1. *(A) TSC22D1 expression in C57BL/6J mice treated with control or TSC22D1 shRNA adenovirus. Mice were fasted for 24h and one group was directly sacrified and the other was refed for 6h. Liver mRNA levels were determined by qPCR. (B) Representative Western Blot of liver extracts from same mice as in A, using TSC22D1 (D1) or actin (loading control) specific antibodies. (means ± SEM). (*) indicates significance p≤0.05*

4.3.2   TSC22D1 deficiency does not alter body or liver weight

To asses if TSC22D1 knockdown affects body weight, mice were weight prior to injection and during the course of the experiment. There was no difference detectable between the TSC22D1 knockdown group and the control group. After 24h fasting, both groups lost approximately 15% of their body weight. After 6h refeeding, the TSC22D1 depleted animals gained slightly less weight, which was 10% of their body weight (Fig 18A). During dissection of the mice, liver and abdominal fat weight was determined, which remained unchanged by TSC22D1 knockdown (Fig 18B-C). Moreover, indirect calorimetry revealed no differences in oxygen consumption (Fig 18D). Also respirator exchange ration (RER), which is an indicator for preferences in substrate (lipid/carbohydrate) utilization, was similar in both experimental groups (Fig 18E).
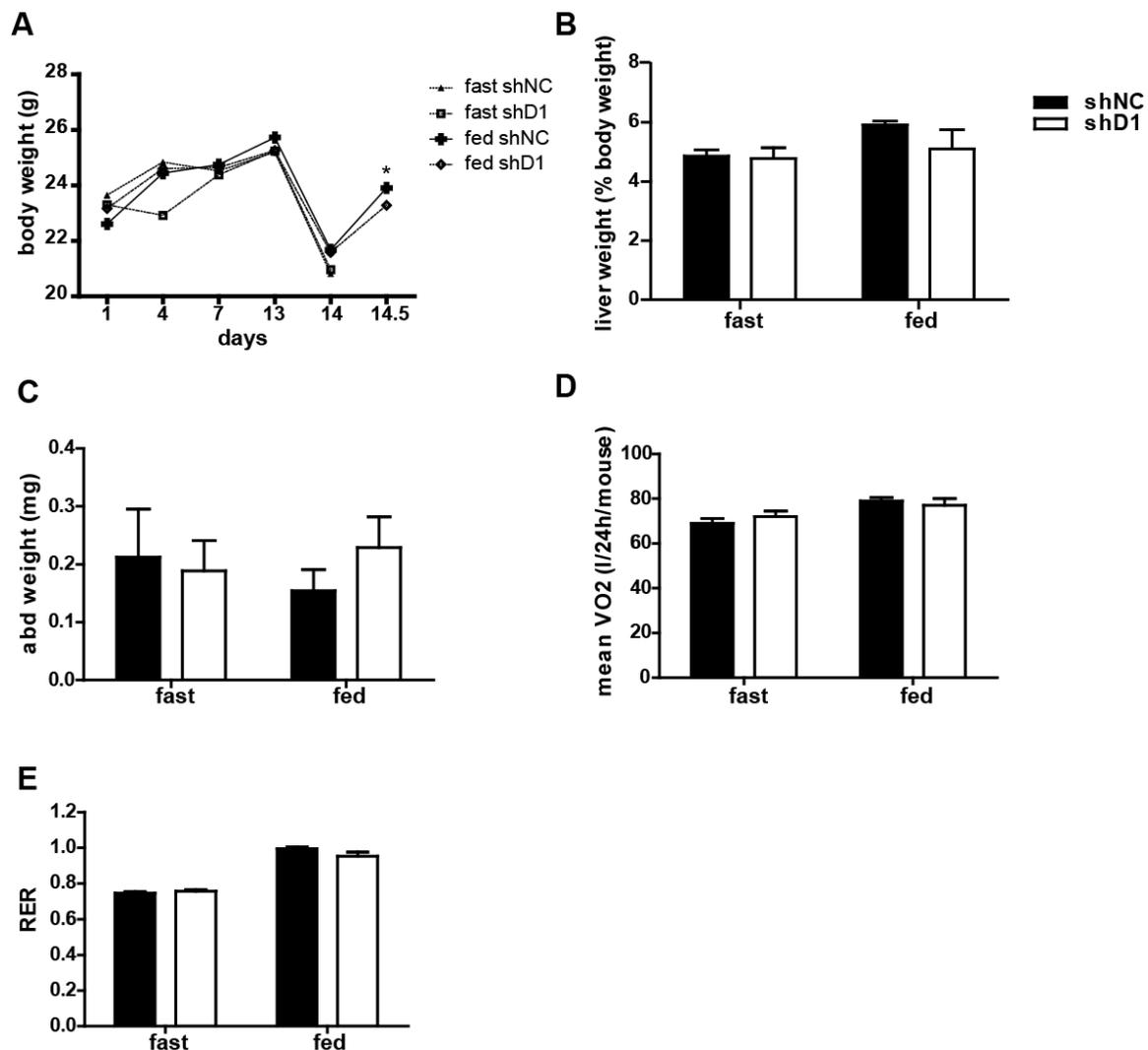
Fig 18: Body, liver and abdominal fat weight are not affected by TSC22D1 knockdown. *A) Body weight of mice treated with control (shNC) or TSC22D1 shRNA (shD1) adenovirus. Mice were fasted for 24h and one group was directly sacrified and the other was refed for 6h. (B) Liver weight of same mice as in A. Weight was determined after dissection. (C) Abdominal fat weight in same mice as in A. Weight was determined after dissection. (D) Oxygen consumption in same mice as in A, as determined by indirect calorimetry. (E) Respiratory exchange ratio in same mice as in A, as determined by indirect calorimetry. (n=5) (means ± SEM)*

4.3.3 Hepatic glycogen and blood glucose are not affected by TSC22D1 knockdown

In the fed state, excess glucose is stored in the liver in the form of glycogen, whereas in the fasting state the glycogen is broken down to maintain normoglycemia. As TSC22D1 is downregulated in the fasted state, we wanted to asses if that influences the emptying or refilling of liver glycogen stores or blood glucose levels. However, there was no difference between both groups neither in the fasted nor in the fed state (Fig 19).
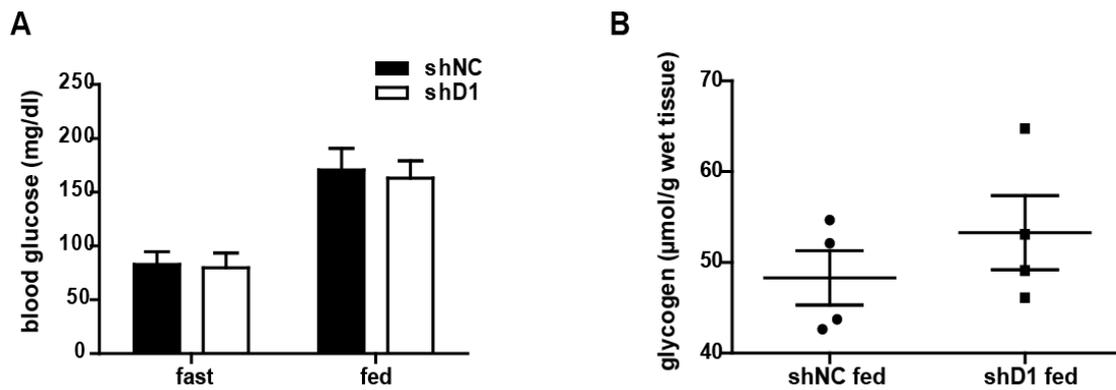
Fig 19: Glycogen and blood glucose are unaltered by TSC22D1 knockdown. *(A) Blood glucose of mice treated with control (shNC) or TSC22D1 shRNA (shD1) adenovirus. Mice were fasted for 24h and one group was directly sacrified and the other was refed for 6h. (B) Hepatic glycogen of same mice as in A. (n=5) (means ± SEM)*

4.3.4 TSC22D1 knockdown significantly reduces serum triglycerides

In order to investigate if TSC22D1 knockdown in the liver alters the levels of circulating non-esterified free fatty acids (NEFA), ketone bodies and triglycerides, these parameters were measured in mouse serum using commercially available colorimetric assays.

Hydrolysis of triglycerides by hormone sensitive lipase liberates NEFAs and glycerol. After uptake into hepatocytes, they can be used for energy production, re-packaged into triglycerides for secretion or storage or converted to ketone bodies. In the fasting state, serum NEFA levels are elevated due to increased breakdown of adipose tissue to meet the energy demands (M. Lafontan and D. Langin, 2009). In the present experiment, NEFA levels were up-regulated by fasting as expected but not affected by TSC22D1 knockdown (Fig 20A).

In case of prolonged fasting, the brain blood glucose levels are not high enough to supply the brain with energy, and ketone bodies can serves as an alternative energy source. The liver is the only organ that can produce ketone bodies as a by-product of beta-oxidation (H.A. Krebs *et al.*, 1999). In this experiment, the level of serum ketone bodies was higher in the fasted state as expected but remained unaffected by TSC22D1 knockdown (Fig 20B).

Most of the fats digested by humans are triglycerides. They can be stored and as well as synthesized by fat and liver cells. In case of energy deprivation hormonal signaling as by epinephrine results in the breakdown of triglycerides to free fatty acids, which can be used for energy production.

In the fasting state, serum TGs were below the detection limit in both experimental groups. Interestingly, however, in the fed state serum TGs were significantly lower (60%) in TSC22D1 deficient mice (Fig 20C). These results hint at a role of TSC22D1 in lipid metabolism. As the liver can also store excessive triglycerides, hepatic TG levels were analyzed by lipid isolation and oil-red-o staining (Fig 20D). TSC22D1 knockdown did not alter liver lipid levels. Interestingly, fasting liver cholesterol levels were significantly increased by TSC22D1 knockdown (Fig 20E).
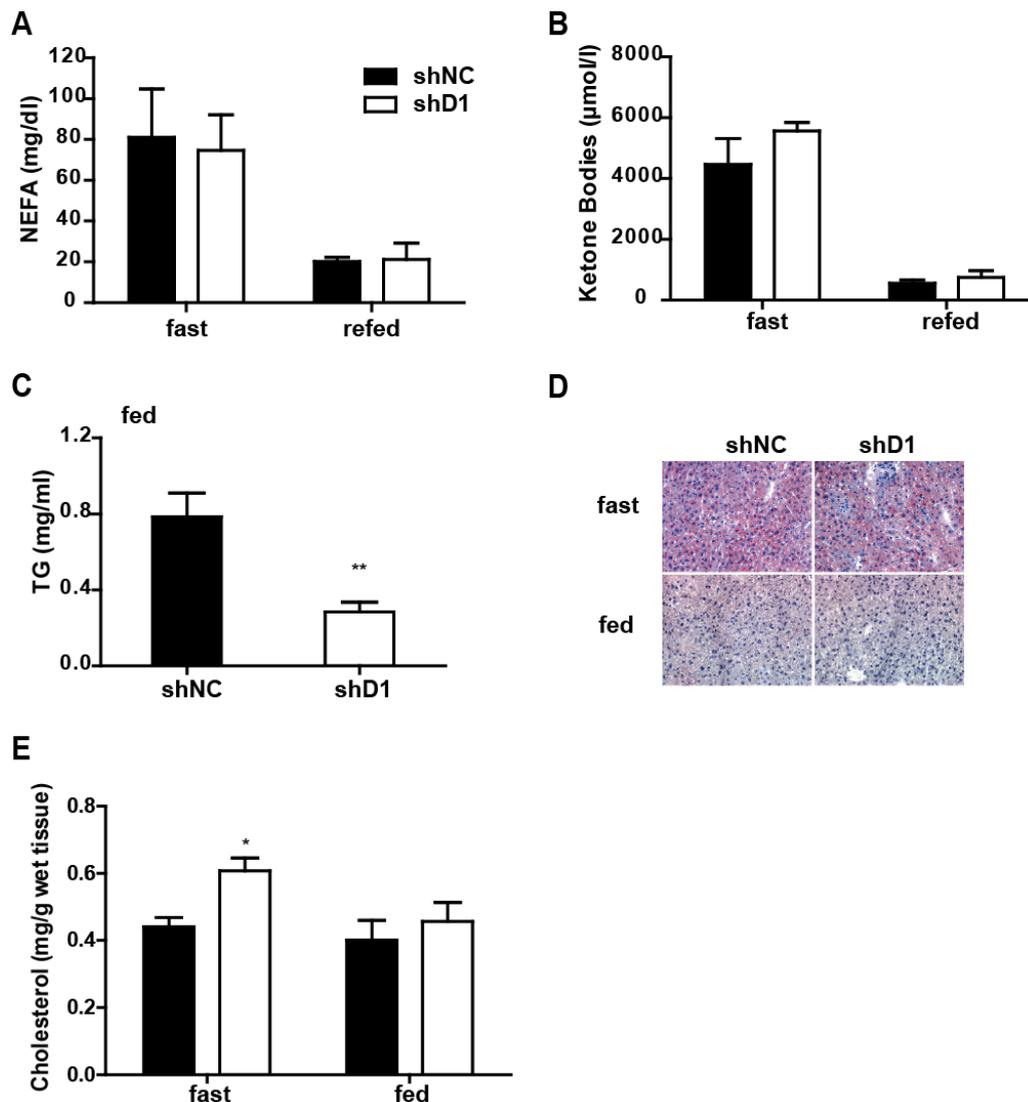
Fig 20: Serum triglycerides are significantly reduced by TSC22D1 knockdown. *(A) Serum non-esterified free fatty acids (NEFA) in C57BL/6J mice treated with control or TSC22D1 shRNA adenovirus. Mice were fasted for 24h and one group was directly sacrified and the other was refed for 6h. (B) Serum ketone bodies in the same mice as in A. (C) Postprandial serum triglycerides (TG) in same mice as in A. Triglycerides in the fasted group were below the detection limit. (D Representative liver cryosections from same mice as in A. Lipids were stained red using Oil Red O. (E) Liver cholesterol from same mice as in A (means ± SEM). (*) indicates significance p ≤0.05*

4.3.5 TSC22D1 deficient mice have reduced circulating VLDL triglycerides and HDL cholesterol

As triglycerides and cholesterol are water-insoluble, they are transported as part of lipoproteins through the blood stream. Triglycerides are mainly associated with very low density lipoproteins (VLDL) whereas cholesterol is transported by low densitiy (LDL) and high density (HDL) lipoproteins (H. N. Ginsberg *et al.*, 2005).

As a significant decrease in serum TG levels was observed in mice after TSC22D1 knockdown, we analyzed the different lipoprotein species in regard to their TG and cholesterol content. For this purpose, total serum was fractionated by fast protein liquid chromatography on a Superose 6 10/300 GL column. According to their size, VLDL particles are collected first, followed by LDL and finally HDL particles.

Indeed, the observed decrease in serum TGs in the fed mice could be attributed to the VLDL fraction, as the corresponding peak (fraction number 21) was significantly lower than in the control group (Fig 21A).

Cholesterol is mainly transported in HDL particles. Cholesterol is a component of cellular membranes and serves as a substrate for the production of hormones and bile acids. In the fasted state the peak corresponding to HDL particles (fraction 36) was nearly gone in the shTSC22D1 treated group compared to the control group. In the refed state the peak was only mildly reduced (Fig 21B).
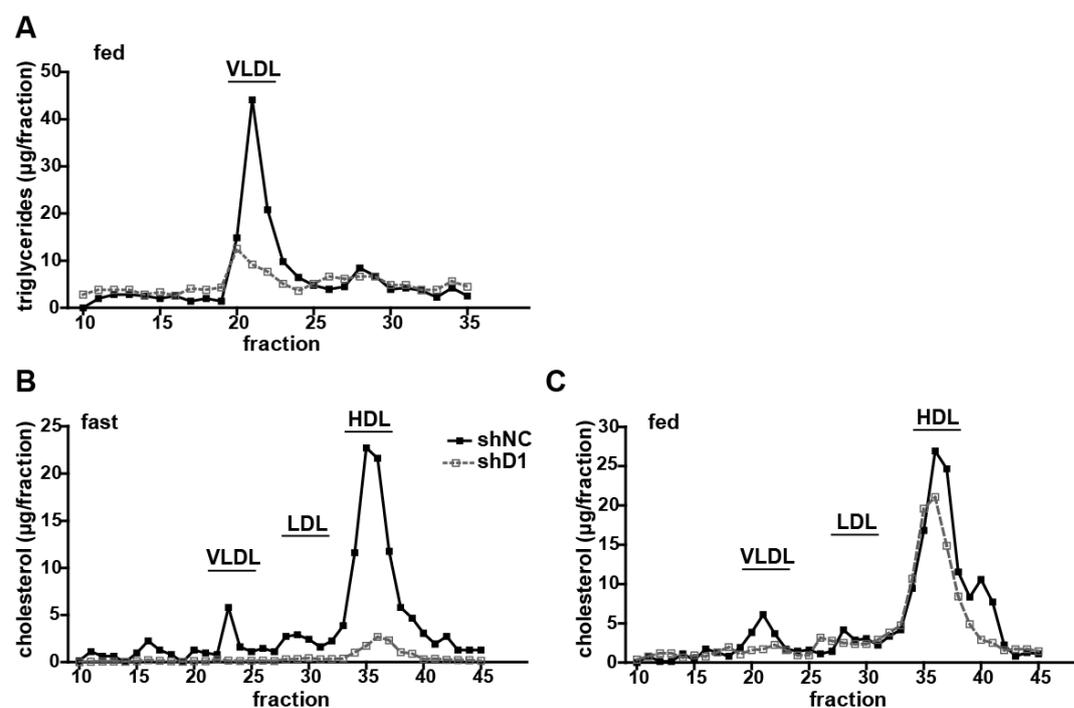
Fig 21: TSC22D1 knockdown lowers circulating VLDL triglycerides and HDL cholesterol. *Lipoprotein-associated serum triglyceride (TG) and cholesterol levels as measured by fast protein liquid chromatography (FPLC). Serum from 24 hour fasted (B) or 6 hour refed (A and C) mice treated with either control or TSC22D1 shRNA adenovirus was pooled and applied to a Superose 6 10/300 GL column; shown are concentrations of triglycerides (A) and cholesterol (B and C) (n=5).*

4.3.6 TSC22D1 knockdown alters gene expression of key genes involved in VLDL assembly and HDL cholesterol metabolism

To determine the mechanism responsible for the reduction in serum VLDL triglycerides and HDL cholesterol, lipoprotein lipase (LPL) activity in white adipose tissue, VLDL uptake and secretion and gene expression was analyzed.

4.3.7 TSC22D1 knockdown does not affect LPL activity in white adipose tissue

Lipoprotein lipase (LPL) is the rate-limiting enzyme for the hydrolysis of TGs from chylomicrons or VLDL particles. It is expressed in heart, adipose tissue and muscle and sits on the periphery of these tissues. The hydrolysis of a triglyceride molecule yields three fatty acids and a molecule of monoglycerol. These products are taken up by the tissues locally and serve different purposes. A reduced activity in adipose tissue LPL leads to an accumulation of VLDL triglycerides in the blood stream (H. Wang and R. H. Eckel, 2009). As serum VLDL triglycerides were significantly reduced in TSC22D1 knockdown mice, we wanted to determine if LPL activity was increased. To this end, the enzyme was isolated from white adipose tissue. A subsequent activity assay was performed using radiolabeled glyceryl tri-[14C] oleate. No significant changes were observed in LPL activity upon TSC22D1 knockdown (Fig 22) revealing that LPL activity is not responsible for the decrease in VLDL triglyceride levels.
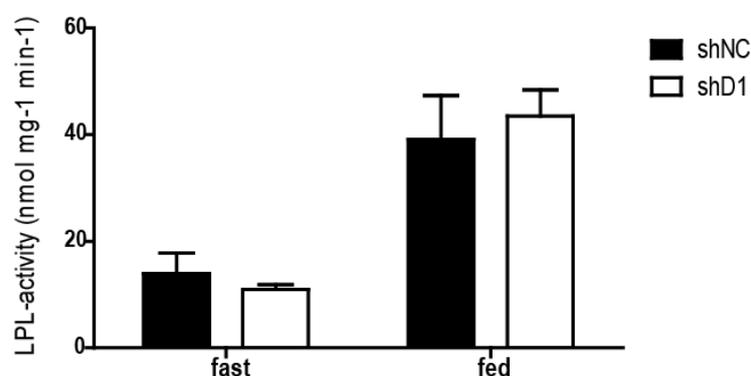
Fig 22: LPL activity is not affected by TSC22D1 knockdown. White adipose tissue LPL activity was determined in C57BL/6J mice injected with control or TSC22D1 shRNA adenovirus. Mice were fasted for 24h and one group was directly sacrified and the other was refed for 6h. (n=3-5), (means ±SEM)

4.3.8 Hepatic TG release is not changed upon TSC22D1 knockdown

To investigate the rate of TG production, a Tyloxapol assay was performed. Tyloxapol is a non-ionic detergent which upon injection results in complete inhibition of LPL. (S. Mandard *et al.,* 2006). Inhibition of LPL continually leads to an accumulation of VLDL particles released from the liver into the blood stream over time. For this experiment, wt C57BL/6J mice were injected *via* tail vein with 2 x 10^9 viral particles expressing either a scrambled shRNA sequence (shNC), or the sequence targeting the TSC22D1 (shD1) mRNA. On day 6 after injection, mice were fasted for 16 hours and then injected with 20% w/v Tyloxapol. Blood was drawn at specific time points and TG levels were determined colorimetrically (Fig 23). Even though serum TG levels were slightly higher 50 and 100 min after Tyloxapol injection, there was no significant difference between both experimental groups at the final time point. Thus, TSC22D1 knockdown does not alter hepatic TG release.
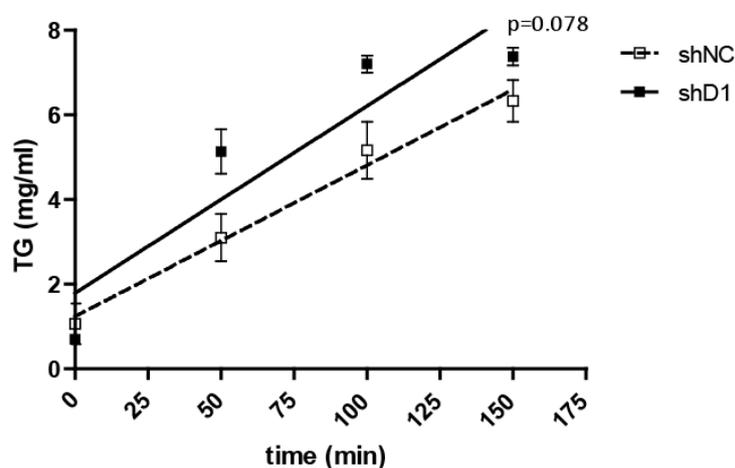
Fig 23: TSC22D1 knockdown does not alter VLDL secretion by the liver. Serum TG levels after tyloxapol injection in control or TSC22D1 shRNA adenovirus injected wild-type C57BL/6J mice. (n=6), (means ± SEM).

4.3.9 TSC22D1 knockdown increases VLDL triglyceride clearance

Apolipoprotein B is the main apolipoprotein of VLDL and it is present as one molecule per lipoprotein particle (H. N. Ginseberg *et al.*, 2005). Thus, the determination of the amount of

ApoB directly yields the amount of VLDL particles. Excessive VLDL particles as occurring after a meal are cleared by the liver to prevent accumulation in the blood stream. In order to investigate if the clearance of VLDL particles is affected by TSC22D1 knockdown, a VLDL clearance assay was performed. To this end, mice were fasted for 4 hours and injected with purified human VLDL *via* the tail vein. Blood was taken at distinct time points and human apolipoprotein B (ApoB) levels in the serum were determined *via* enzyme-linked immunosorbent assay (ELISA) (Fig 24A), for human ApoB. In this experiment, VLDL clearance was significantly increased in TSC22D1 knockdown mice, which is in line with the observed phenotype. Further, Western blot analysis of livers from wild-type C57BL/6J mice injected with control or TSC22D1 shRNA adenovirus showed increased levels of ApoB in the liver of TSC22D1 knockdown mice (Fig 24B). As ApoB needed to enable clearance of VLDL from the blood, higher abundance of AboB protein in the liver are in accordance with higher clearance.
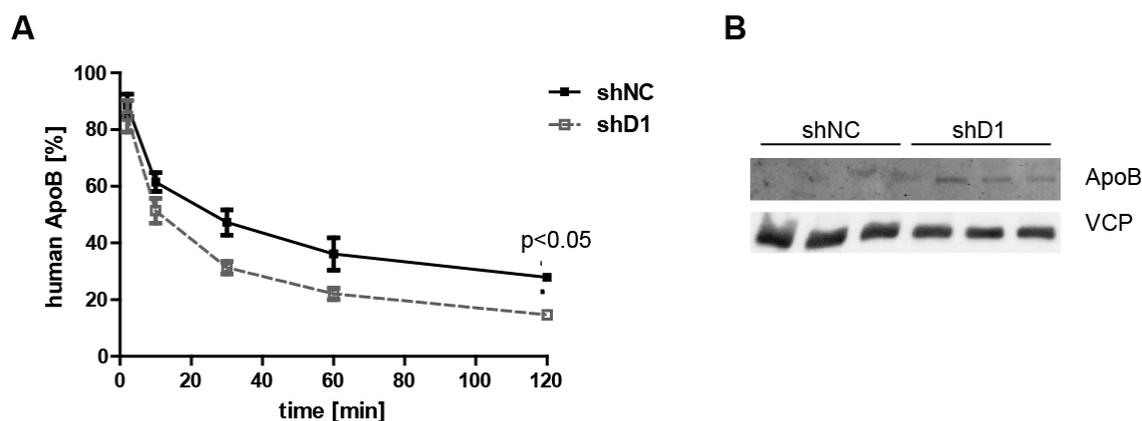
Fig 24: TSC22D1 knockdown increases VLDL triglyceride clearance. *Clearance of human ApoB from serum of control or TSC22D1 shRNA adenovirus injected C57BL/6J mice. 20µg of human VLDL were injected into each animal and serum samples were taken at the indicated time points. Human ApoB levels were determined by human-specific ELISA (n=5) (means ± SEM) Two Way ANOVA RM. (B) Representative Western blot of liver extracts from C57BL/6J mice injected with control (shNC) or TSC22D1 shRNA adenovirus. Protein was detected using ApoB and VCP (loading control) antibodies. n=3*

4.3.10 TSC22D1 knockdown leaves pFoxo1 levels unchanged

Forkhead box (Fox)O1 is a transcription factor that has been shown to be a regulatory factor in VLDL metabolism. It can transcriptionally activate microsomal triglyceride transfer protein (MTP), which is required for VLDL assembly (A. Kamagate *et al.*, 2008). FoxO1 is inactivated by Akt-mediated phosphorylation. In regards to the observed reduction in VLDL-TGs by TSC22D1 ablation, FoxO1 and Akt levels in the liver were analyzed by Western

blotting. Neither total Akt or phosphorylated Akt nor FoxO1 or phosphorylated FoxO1 levels were altered upon TSC22D1 knockdown (Fig 25) indicating that FoxO1 is not responsible for the observed phenotype.
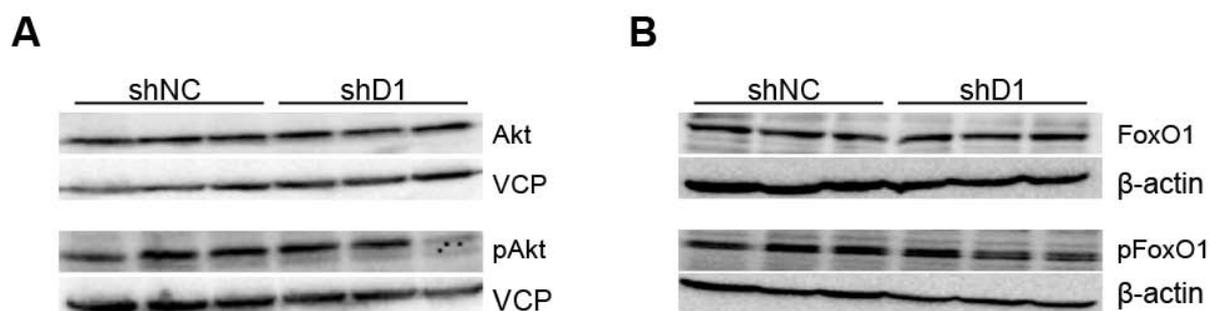
Fig 25: TSC22D1 knockdown does not alter pFoxo levels. Representative Western blots of liver extracts from C57BL/6J mice injected with control (shNC) or TSC22D1 shRNA adenovirus. Protein was detected by (A) Akt, pAkt and VCP antibodies,(B) FoxO1, pFoxO1 and β-actin (loading control) antibodies.n=3

4.3.11 TSC22D1 knockdown decreases expression of genes involved in cholesterol metabolism and VLDL synthesis

Knockdown of TSC22D1 resulted in decreased serum VLDL triglycerides and HDL cholesterol. It was likely that expression of genes involved in lipid or cholesterol metabolism were altered to account for the observed phenotype. Quantitative real time PCR was used to analyze a panel of putative target genes for changes in gene expression (Fig 26). The investigated genes are grouped according to the functions or metabolic pathway they are involved in. A short description of their hepatic function is listed in Table 4.

Table 4: List of analyzed genes involved in hepatic lipid and cholesterol metabolism

Gene Name	Abbreviation	Function	Pathway regulated / cellular function
Liver X Receptor	**LXR**	Transcription factor regulating cholesterol, fatty acid and glucose metabolism.	Nuclear Receptors
Peroxisome proliferator-activated receptor alpha	**PPARα**	Transcription factor regulating hepatic lipid metabolism	
ATP-citrate lyase	**ACLY**	Acetyl CoA synthesis	Lipogenesis
Fatty acid synthase	**FANS**	Fatty acid elongation	
Stearoyl-CoA desaturase-1	**SCD1**	Production of desaturated fatty acids	
Fatty acid binding protein	**FABP1**	Binding of long chain fatty acids	
Angiopoietin-like 3 and 4	**ANGPTL3/4**	Inhibition of lipoprotein lipase and endothelial lipase	LPL-Activity
Scavenger Receptor B1	**SRB1**	HDL Receptor	
Low density lipoprotein receptor-related protein 1	**LRP1**	Apolipoprotein E acceptor	
Low-Density Lipoprotein	**LDLR**	Apolipoprotein B receptor	

Receptor			
Lipolysis-stimulated lipoprotein receptor	**LSR**	Receptor for triglyceride-rich lipoproteins	Lipoproteins/Receptor/ Transporter
Cluster of Differentiation 36	**CD36**	Uptake of long-chain fatty acids	
Apolipoprotein B	**ApoB**	Primary apolipoprotein of VLDL	
Tribbles homolog 1	**TRIB1**	Regulator of VLDL Production	TG/VLDL synthesis and assembly
diacylglycerol *O*-acyltransferase 1 and 2	**DGAT1/2**	Catalyzationof the formation of triglycerides from diacylglycerol and Acyl-CoA.	
Perilipin 2	**PLIN2**	Associated to lipid droplets	
Microsomal triglyceride transfer protein	**MTTP**	Lipoprotein assembly	
Lipin1	**LPIN1**	Involved in VLDL production	
Fat specific protein 27	**FSP27**	Associated to lipid droplets	
Cell death-inducing DNA fragmentation factor A-like effector B	**CIDEB**	Associated to lipid droplets	
ATP-binding cassette transporter ABCA1	**ABCA1**	Mediation of cholesterol and phospholipid efflux	Cholesterol Metabolism
ATP-binding cassette sub-family G member 1	**ABCG1**	Transport of cholesterol into endosome	
ATP-binding cassette sub-family G member 5 and 8	**ABCG5/8**	Excretion of sterols into bile	
Apolipoprotein A1/2	**APOA1/2**	Major protein components of HDL	
Lecithin-cholesterol-acyltransferase	**LCAT**	Conversion of free cholesterol into cholesteryl ester	
Phospholipid transfer protein	**PLTP**	Transfer of phospholipids from triglyceride-rich lipoproteins to HDL	
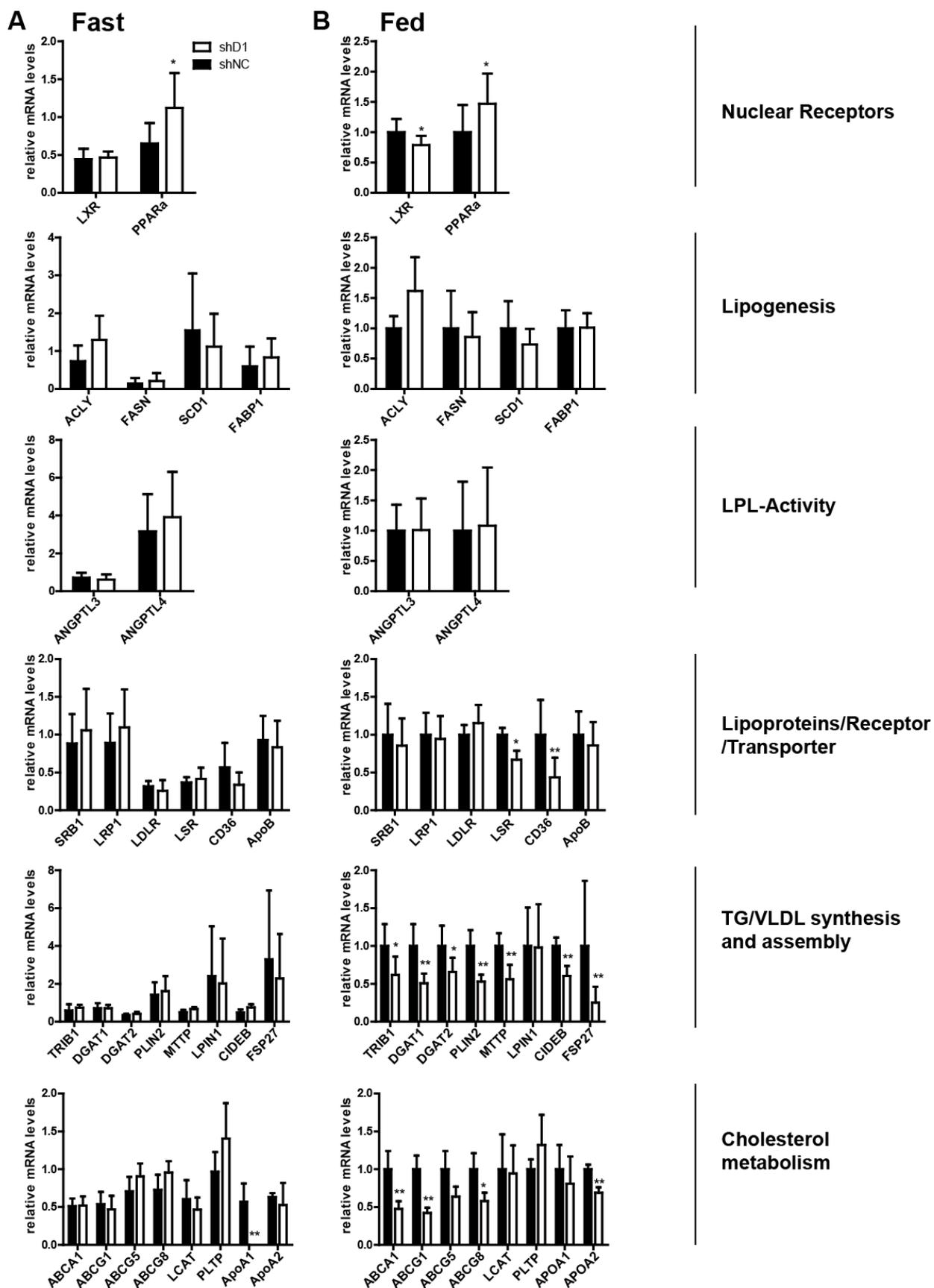
Fig 26: TSC22D1 knockdown results in decreased expression of key genes involved in cholesterol metabolism. *TSC22D1 expression in C57BL/6J mice treated with control or TSC22D1 shRNA adenovirus. Mice were fasted for 24h and one group was directly sacrificed (Panel A) or refed for 6h*

(Panel B). Liver mRNA levels of depicted genes (Table 2) were analyzed by qPCR. (n=5) (means ± SEM). (*) indicates significance; p < 0.05; (**)p < 0.01

Firstly, gene expression analysis (Fig 26) revealed that most of the observed changes in gene expression occurred in the postprandial state. In the fed state, nuclear receptor LXR was slightly down-regulated, whereas PPARα was slightly up-regulated. Expression of key genes involved in lipogenesis as fatty acid synthase was not altered. Also expression of ANGPTL3 and 4, which inhibit lipoprotein lipase were unchanged, which is in line with the results of LPL activity measurement (Fig 22). When it comes to lipid metabolism, receptors for lipoproteins and their receptors play an important role in mediating the transport and uptake of lipids. Expression of LSR, which is a receptor for the TG-rich lipoproteins, was down-regulated as well as CD36 which mediates the uptake of long chain fatty acids. Moreover, genes involved in key steps in TG and VLDL synthesis and assembly as DGAT1 and 2 or MTTP were significantly down-regulated by TSC22D1 knockdown. Genes for key mediators of cholesterol metabolism as ABCA1 which mediates cholesterol efflux, or ABCG1 which is responsible for cholesterol transport, were significantly less expressed in TSC22D1 knockdown animals as compared to control mice. In the fasted state, only PPARa was slightly up-regulated and expression of ApoA1 was nearly fully blunted. Altogether, these results are in line with the observed phenotype regarding decreased levels of VLDL-triglycerides (Fig 21A) and decreased levels of HDL-cholesterol (Fig 21B) in TSC22D1 knockdown animals compared to control mice particulary during fasting.

4.4 Overexpression of TSC22D1 increases circulating VLDL triglycerides and HDL cholesterol

As we observed that short term knockdown of TSC22D1 resulted in significant decrease of circulating VLDL triglycerides and HDL cholesterol, we wanted to investigate if overexpression of TSC22D1 could reverse that phenotype. For this purpose, an adenovirus encoding the TSC22D1 cDNA sequence in frame with the Flag peptide under the control of the constitutively active CMV promoter was cloned and produced.

4.4.1 Overexpression of TSC22D1 in fasted and refed mice

For the overexpression study, 1×10^9 infectious units of either TSC22D1 overexpression virus, or an empty control virus incorporating the CMV promoter were injected via tail vein into C57BL/6J mice. As endogenous TSC22D1 expression is altered by fasting, 6 days after infection half the mice were fasted for 24h and sacrificed directly, whereas the other half was refed for 6h.

Overexpression in the liver was analyzed by qPCR and Western blotting (Fig 27A-B). In the fasted as well as in the refed state, TSC22D1 was significantly overexpressed. Other than expected, TSC22D1 overexpression was higher in the fasted than in the refed state, which does not match the endogenous regulation. This is probably due to an activation of the CMV promoter by fasting signals, which has been observed in other experiments before (unpublished observation Maria Rohm, Allan Jones Herzig Lab). In order to see if TSC22D1 overexpression was tissue specific, TSC22D1 levels were determined in abdominal fat (abd), inguinal fat (ing), kidney and gastrocnemius muscle (GC). Expression in these tissues was not changed by TSC22D1 overexpression in liver (Fig 27C).
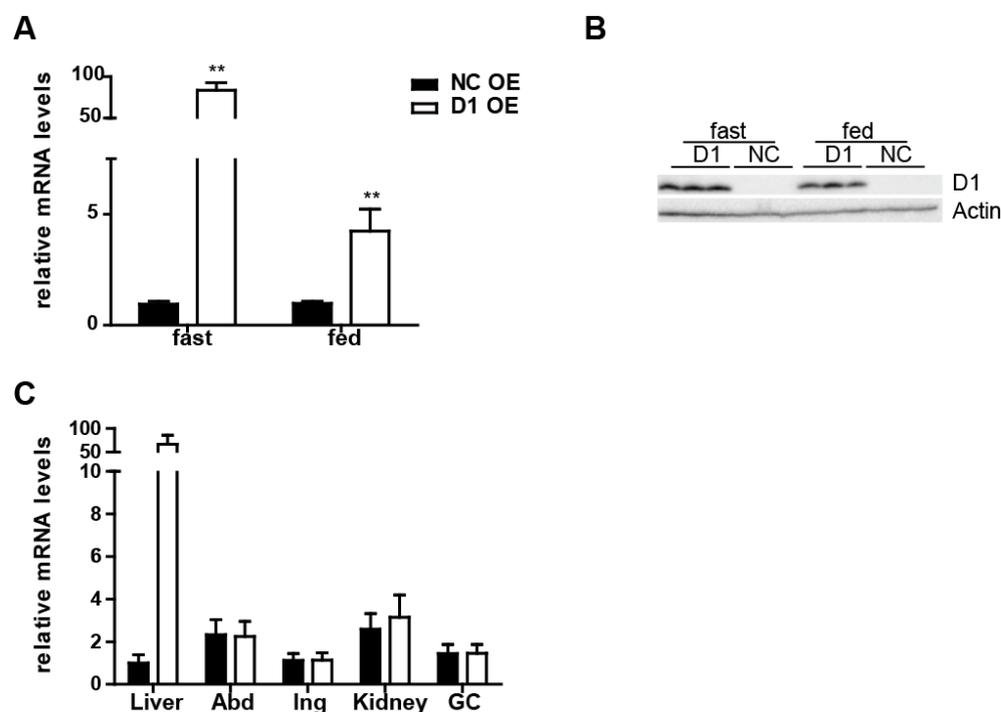
Fig 27: Hepatic overexpression of TSC22D1 in fasted and refed mice. TSC22D1 expression in C57BL/6J mice treated with control or TSC22D1 overexpression adenovirus. Mice were fasted for 16h and directly sacrificed or refed for 6h. (A) Liver mRNA levels of TSC22D1 were analyzed by qPCR. (B) Western blot of liver extracts from representative mice using TSC22D1 and β-actin (loading control) antibodies. n=3 (C) TSC22D1 expression in liver, abdominal fat (abd), inguinal fat (ing), kidney or

gastrocnemius muscle (GC) in the fasted state in same mice as in A. (means ± SEM, n=7). (**) indicates significance p<0.01

4.4.2 TSC22D1 overexpression does not alter body or liver weight

To asses if TSC22D1 overexpression affects body weight, mice were weight before injection and during the course of the experiment. There was no difference between the TSC22D1 overexpression group and the control group. After 24h fasting both groups lost approximately 15% of their body weight. After 6h refeeding both experimental groups gained back 10% of their body weight (Fig 28A). During dissection of the mice, liver and abdominal fat weight were determined, which remained unchanged by TSC22D1 overexpression (Fig 28B-C).
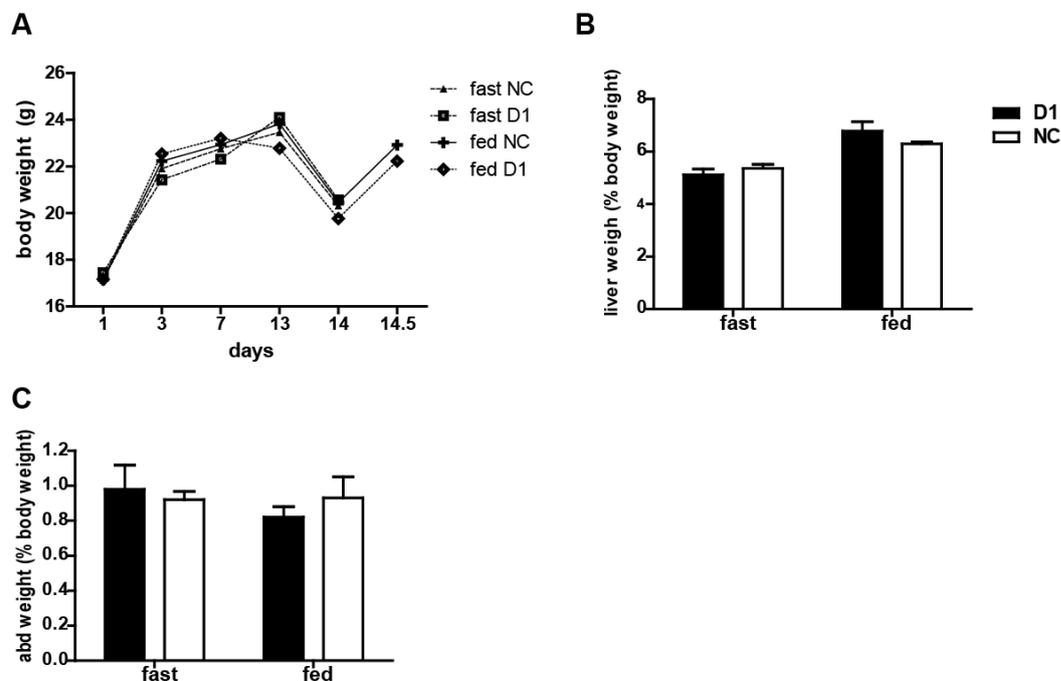
Fig 28: Body, liver and abdominal fat weight are not affected by TSC22D1 overexpression. (A) Body weight (B) liver and (C) abdominal fat weight of mice treated with control (NC) or TSC22D1 overexpression (D1) adenovirus. Mice were fasted for 24h and one group was directly sacrified and the other was refed for 6h. n=7 (means ± SEM)

4.4.3 Hepatic glycogen and blood glucose are not affected by TSC22D1 overexpression

Knockdown of TSC22D1 did not affect hepatic glycogen and blood glucose (Fig 19), as expected there were also no differences in blood glucose levels observed between TSC22D1 overexpressing and control mice neither in fasted nor in the fed state (Fig 29A). For hepatic

glycogen, levels could only be determined in the fed animals, also blood glucose levels were unchanged (Fig 29B).
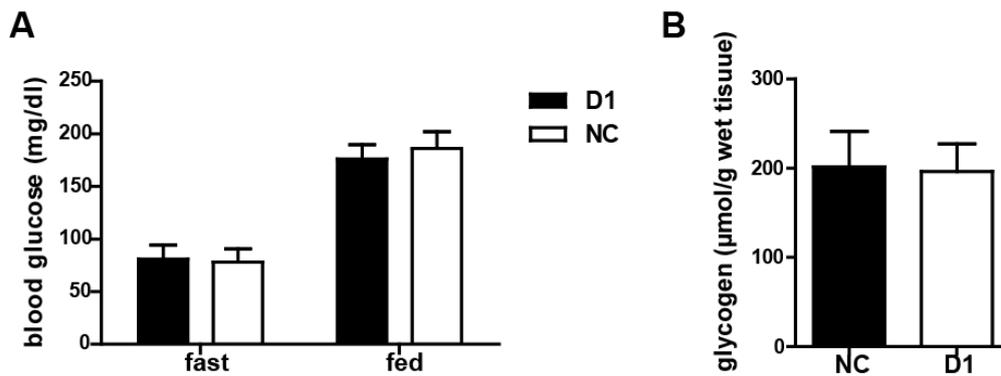
Fig 29: Glycogen and blood glucose are unaltered by TSC22D1 overexpression. *(A) Blood glucose and (B) hepatic glycogen in mice treated with control (NC) or TSC22D1 overexpression (D1) adenovirus. Mice were fasted for 24h and one group was directly sacrified and the other was refed for 6h. (n=7) (means ± SEM)*

4.4.4 TSC22D1 overexpression alters circulating VLDL triglycerides and HLD cholesterol levels

The strong phenotype regarding serum parameters including circulating VLDL TGs in TSC22D1 knockdown mice prompted us to analyze the same parameters in TSC22D1 overexpressing mice.

As in the knockdown experiment, levels of circulating NEFAs and ketone bodies were unchanged (Fig 30A-B). Levels of circulating TGs were reduced in the fasted state but unaltered in the refed state (Fig 30C). Liver triglycerides were unchanged as well (Fig 30D).
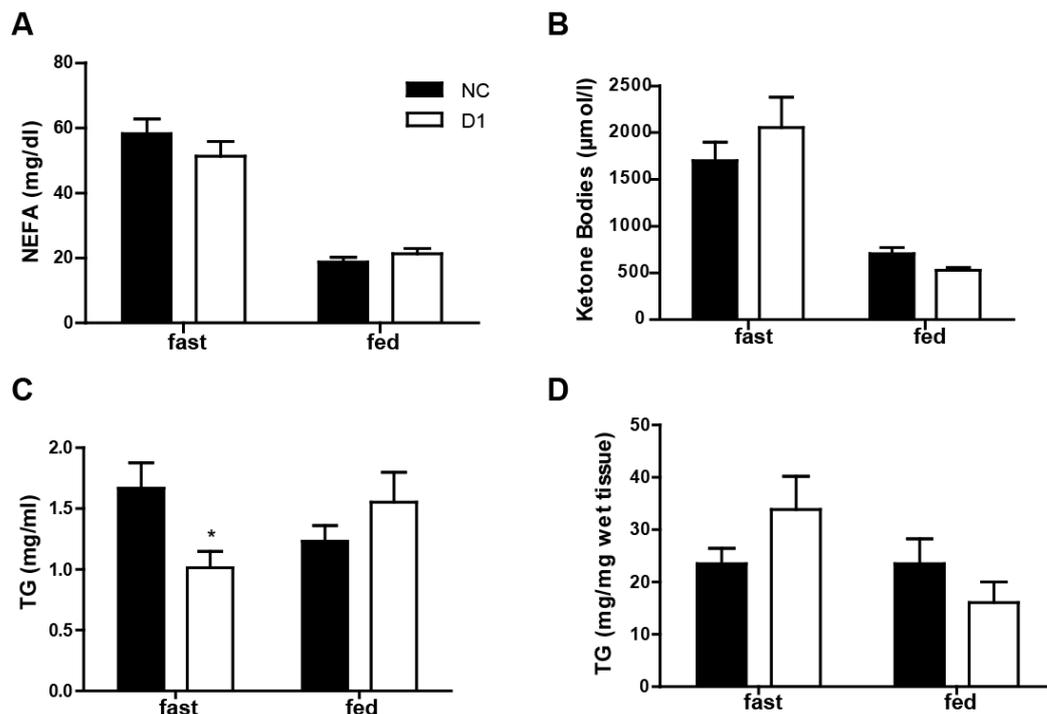
Fig 30: Serum parameters are unchanged by TSC22D1 overexpression*. (A) Serum non-esterified free fatty acids in C57BL/6J mice treated with control (NC) or TSC22D1 (D1) overexpression adenovirus. Mice were fasted for 24h and one group was directly sacrified and the other was refed for 6h (B) Serum ketone bodies in the same mice as in A. (C) Serum triglycerides in same mice as in A. (D) Liver triglyceride (TG) content in same mice as in A. (n=5) (means±SEM)*

FPLC analysis allows rapid separation by size and purification of the different lipoprotein fractions present in the serum. This allows a more detailed analysis of the serum lipid composition (W. Marz *et al.*, 1993). In this study, FPLC analysis revealed a significant elevation in the VLDL peak in mice overexpressing TSC22D1 in the fasted state as compared to the control mice and also a mild elevation in the VLDL peak in the fed state (Fig 31A-B). Cholesterol levels in the fasting state were unchanged whereas in the refed state TSC22D1 overexpression resulted in an elevated HDL peak (Fig 31C-D). These results are opposing to the effects seen by TSC22D1 knockdown, which strengthens the idea that TSC22D1 is involved in regulating levels of serum VLDL and HDL.
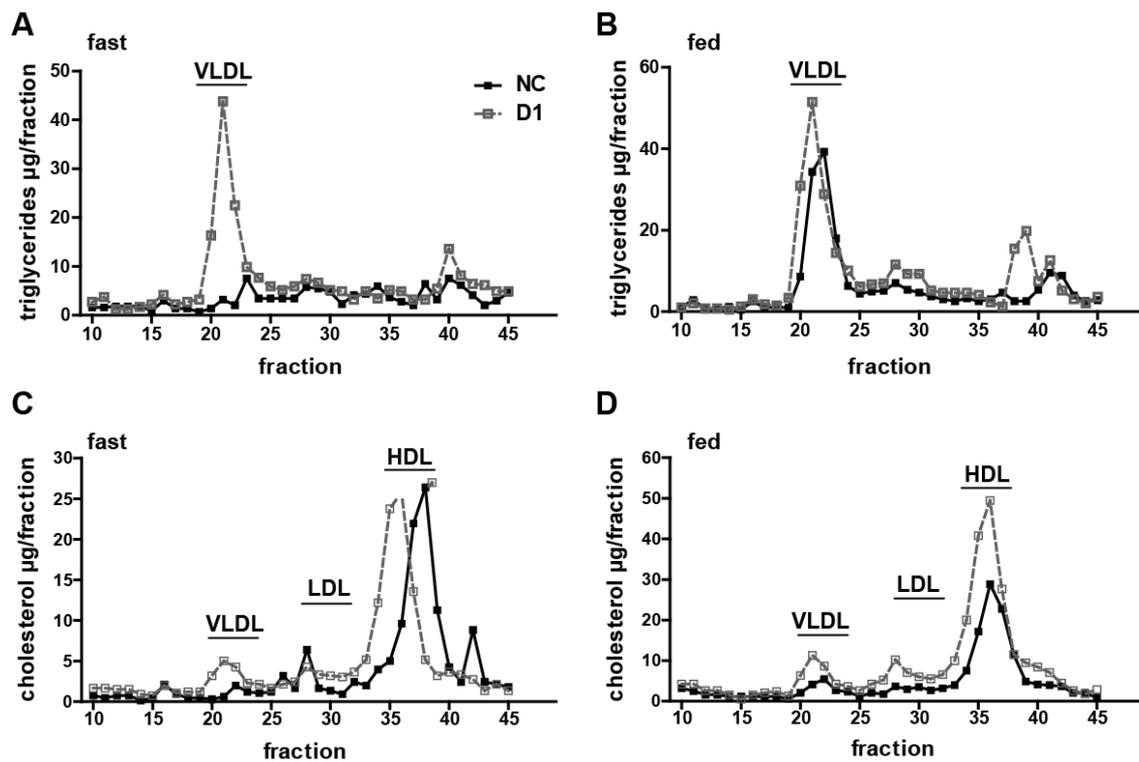
Fig 31: TSC22D1 overexpression increases circulating VLDL triglycerides and HDL cholesterol. *Lipoprotein-associated serum triglyceride (TG) and cholesterol levels as measured by fast protein liquid chromatography (FPLC). Serum from 24 hour fasted or 6 hour refed mice treated with either control or TSC22D1 overexpression adenovirus was pooled and applied to a Superose 6 10/300 GL column; (A) TGs fasted, (B) TGs fed, (C) cholesterol fasted, (D) cholesterol fed. (n=5)*

4.4.5 TSC22D1 overexpression significantly induces ABCG1 expression

In order to see if TSC22D1 overexpression changes the expression of genes that were affected by TSC22D1 knockdown (Table 4 and Fig 26), mRNA levels were analyzed by qPCR (Fig 32A-B). As observed before (Fig 26A), in the fasted state gene expression was not changed (Fig 30A). In the fed state, TSC22D1 overexpression resulted in a significant increase of FSP27 expression, which is opposite of what was detected in the case of TSC22D1 knockdown. For DGAT1 and 2 it is less clear, as DGAT1 expression is unregulated, whereas DGAT2 is down-regulated. Regarding the genes involved in cholesterol metabolism, ApoA1 and A2 expression was surprisingly down-regulated. Nevertheless, ABCG1 expression, which is a key factor for cholesterol shuttling, is up-regulated, which is in line with the FPLC results (Fig 31) and opposite of what is seen for TSC22D1 knockdown (Fig 21).

Fig 32: TSC22D1 overexpression induces FSP27 and ABCG1 expression. *TSC22D1 expression in C57BL/6J mice treated with control or TSC22D1 cDNA adenovirus. Mice were fasted for 24h and one group was directly sacrificed (Panel A) or refed for 6h (Panel B). Liver mRNA levels of depicted genes (Table 4) were analyzed by qPCR. (n=5), (means ± SEM). (*) indicates significance; p < 0.05; (**)p < 0.01*

4.5 Chronic knockdown of TSC22D1 results in reduced HDL cholesterol

4.5.1 Chronic hepatocyte specific TSC22D1 knockdown

As the short term knockdown as well as overexpression of TSC22D1 affected lipid metabolism, we wanted to confirm these results in an independent system. To investigate if chronic knockdown results in a similar phenotype as the short-term knockdown, a miRNA targeting TSC22D1 was cloned in an AAV vector system. Adenoviruses can only be used for short-term experiments as they are cleared from the body by the immune system. Adeno-associcated viruses (AAV) do not evoke an immune-response and hence, can be used for long term knockdown experiments (N. Chirmule *et al.*, 1999). Furthermore, the AAV serotype that was used (AAV2/8) was designed to preferentially infect hepatocytes and the inserted mRNA was under the control of the hepatocyte-specific LP1 promoter, which is not active in other liver cells such as Kupffer cells (P. Kulozik *et al.*, 2011). Specific miRNA sequences targeting TSC22D1 were cloned into the Invitrogen pcDNA6.2-GW/EmGFP-miR vector. Their knockdown efficiency was tested by co-transfecting Hepa1c1 cells with

miRNAs targeting TSC22D1 or a scrambled control and a TSC22D1 overexpression construct. TSC22D1 depletion was analyzed by luciferase assay and Western blot (Fig 33A-B). Sequence 4.2, performed efficiently in both assays and was subsequently sub-cloned into the pdsAAV-LP1-EGFPmut AAV (P. Kulozik *et al.*, 2011). The plasmids encoding the miRNA constructs were contransfected into HEK293T cells with the pDGΔVP helper plasmid (D. Grimm *et al.*, 1998) and a mutated p5E18-VD2/8 expression vector (G.P. Gao *et al.*, 2002) encoding AAV2 rep and a mutated AAV8 cap protein. The generated virus particles were purified via Iodixanol gradient and titered for *in vivo* application.
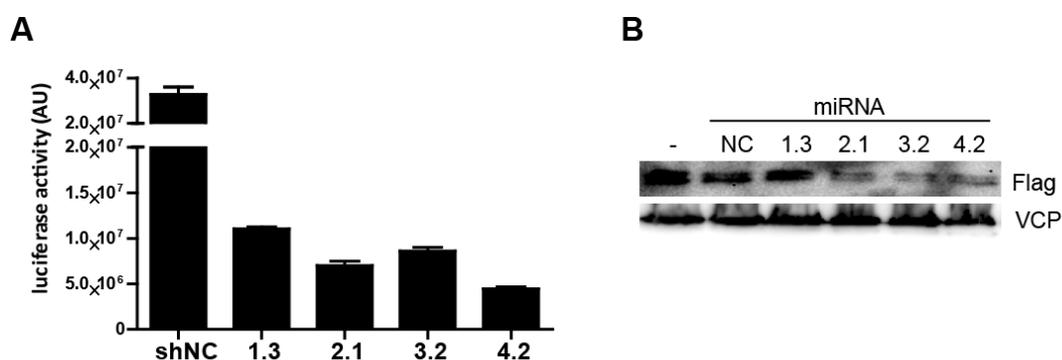
Fig 33: Cloning of AAV miRNA expression construct for long term TSC22D1 knockdown. *(A) HEK293A cells were transfected with plasmids containing the TSC22D1 sequence in frame with the luciferase coding sequence and co-transfected with plasmids expressing either a scrambled miRNA sequence (miNC) or different TSC22D1 targeting sequences. Luciferase activity is normalized to β-galactosidase and plotted relative to control miRNA. (n=3), (means ± SEM). (B) HEK293A cells were transfected with plasmids overexpressing flag-tagged TSC22D1 and co-transfected with plasmids expressing either a scrambled miRNA sequence (NC) or different TSC22D1 targeting sequences (1.3-4.2) or nothing (-). Protein levels were analyzed by immunoblot using flag-antibody and VCP-antibody as loading control. Results from 3 independent experiments are shown.*

4.5.2 TSC22D1 expression is significantly reduced in a chronic knockdown experiment

C57BL/6N mice were injected with 5×10^{11} viral particles into the tail vein. Mice were kept for 34 days and sacrificed in a random fed state. TSC22D1 expression was analyzed by qPCR (Fig 34A) and Western blot (Fig 34B). TSC22D1 mRNA and protein levels were significantly reduced. In order to see if chronic TSC22D1 knockdown was tissue specific, TSC22D1 levels were determined in abdominal fat (abd), inguinal fat (ing), kidney and gastrocnemius muscle (GC). Expression in these tissues was not changed by miRNA mediated TSC22D1 knockdown in the liver (Fig 34C).
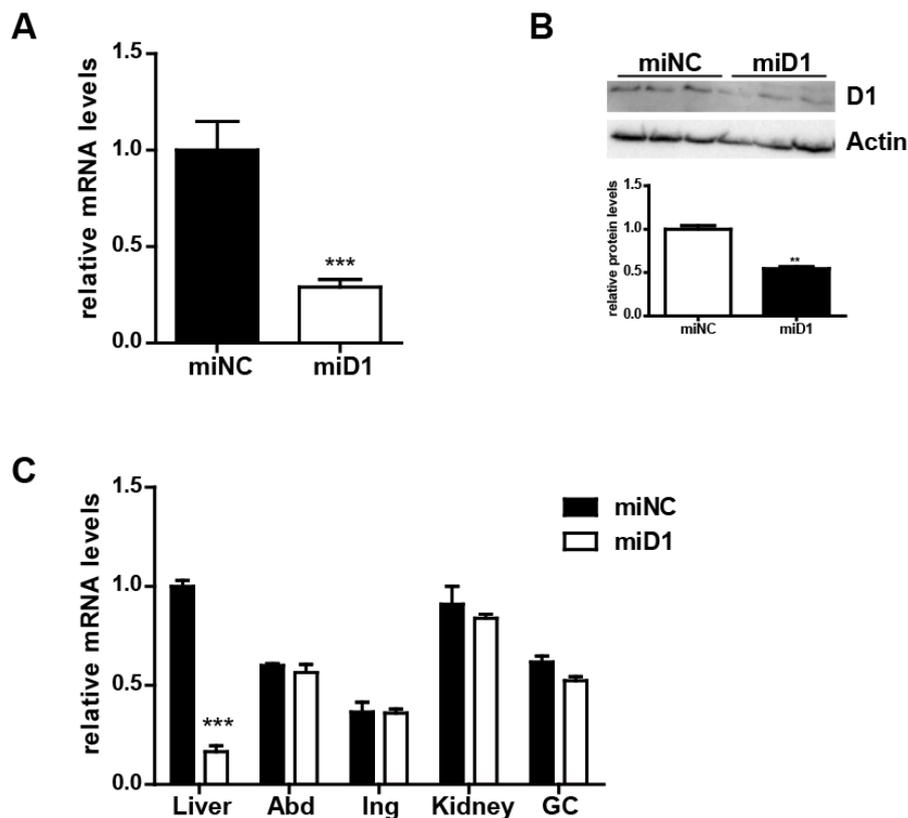
Fig 34: AAV mediated TSC22D1 knockdown. *TSC22D1 expression in C57BL/6N mice treated with control (NC) or TSC22D1 overexpression (miD1) AAV. (A) Liver mRNA levels of TSC22D1 were analyzed by qPCR. (B) Western blot and quantification of liver extracts from representative mice using TSC22D1 and β-actin (loading control) antibodies.(n=3) (C) TSC22D1 expression in liver, abdominal fat (abd), inguinal fat (ing), kidney or gastrocnemius muscle (GC) in same mice as in A. (means ± SEM, n=7). (***) indicates significance; p<0.001*

4.5.3   Long-term TSC22D1 knockdown reduces liver weight

During the course of the experiment different weight parameters and blood glucose concentration were monitored. 25 days after injection mice were challenged with 24h fasting to see if fasting glucose was changed. There was no difference between the groups (Fig 35A). After sacrifice, abdominal fat and liver weight was measured. Interestingly, whereas body weight was not changed, TSC22D1 knockdown mice showed a slightly reduced liver weight, which could be correlated to TSC22D1 expression (Fig 35D-E).
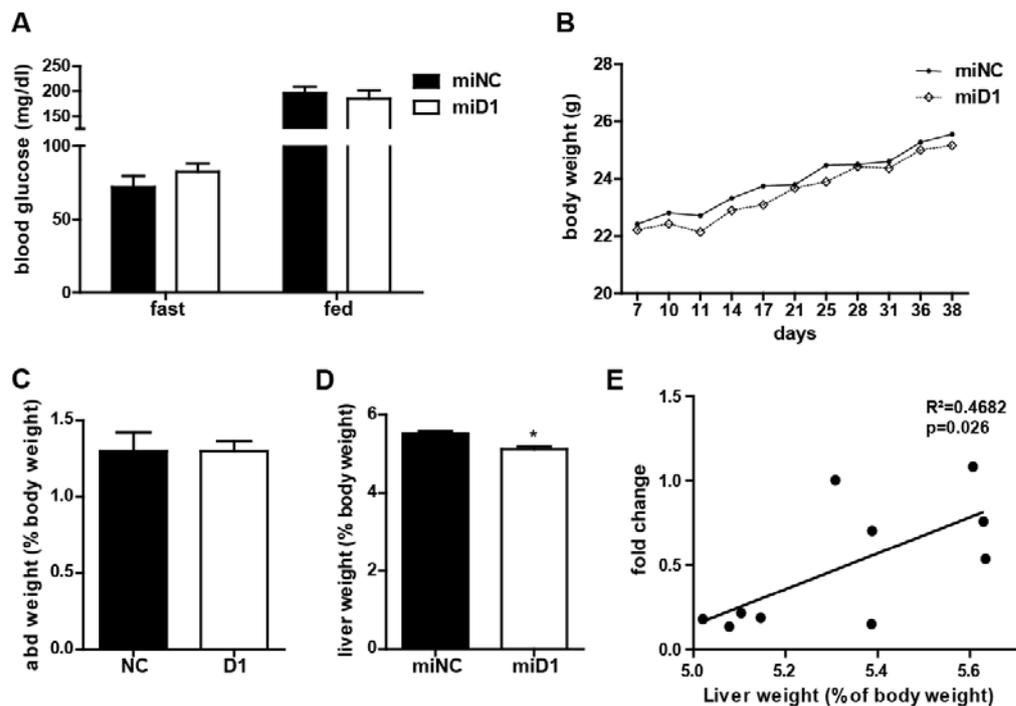
Fig 35: Chronic TSC22D1 knockdown reduces liver weight. *(A) Blood glucose of mice treated with control (miNC) or TSC22D1 miRNA (miD1) AAV. Mice were fasted for 24h refed for 6h, (B) body weight, (C) abdominal fat weight (D) and liver weight after sacrifice (E) Pearson's correlation of log(2) of TSC22D1 expression and liver weight. n=5 (means ± SEM) (*) indicate significance p < 0.05*

4.5.4 HDL cholesterol is reduced by chronic TSC22D1 knockdown

As short term knockdown of TSC22D1 as well as its overexpression, altered the serum profile regarding VLDL triglycerides and HDL cholesterol, this effect was analyzed in more detail. Different to the other two studies the mice were in a random fed state at the time of sacrifice. Serum NEFAS were unchanged, whereas, ketone bodies were reduced in the TSC22D1 knockdown animals compared to control mice (Fig 36A-B). Circulating TGs were not altered, and liver TGs were slightly but not significantly reduced (Fig 36C-D). As seen before by acute knockdown (Fig 20) liver cholesterol levels were significantly increased in TSC22D1 depleted mice as compared to control mice (Fig 36E).
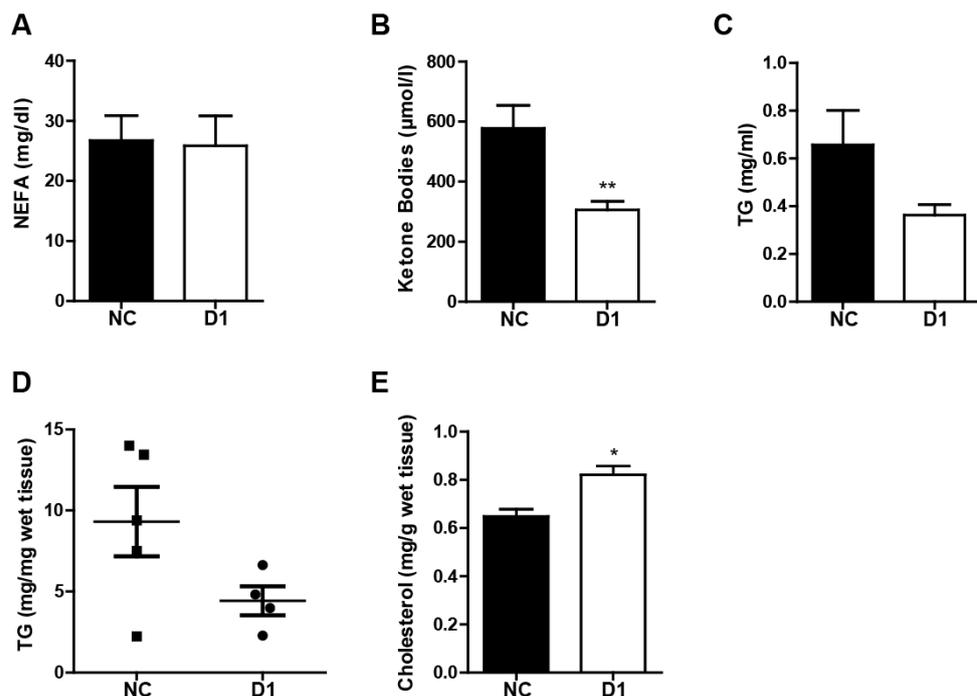
Fig 36: Serum ketone bodies are reduced by long term TSC22D1 knockdown. *(A) Serum non-esterified free fatty acids in BL56C/6N mice treated with control (miNC) or TSC22D1 miRNA AAV (miD1). Mice were sacrified in refed state. (B) serum ketone bodies, (C) serum triglyceride, (D) liver triglyceride (TG) content, (E) liver cholesterol content in same mice as in A. (n=5) (means±SEM)*

To characterize the lipoprotein fractions we again performed an FPLC analysis. In contrast to acute TSC22D1 knockdown, the VLDL TG peak was unchanged (Fig 37A). However, we observed again a 25% reduction in the HDL cholesterol peak (Fig 37B). This is in line with the results from the acute knockdown study (Fig 20) and the hypothesis that TSC22D1 plays a role in regulating levels of circulating HDL cholesterol.
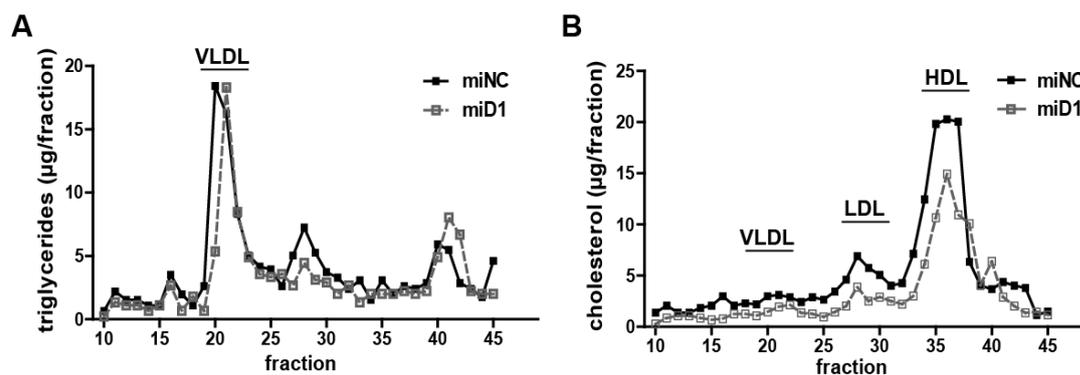
Fig 37: Long term TSC22D1 knockdown lowers circulating HDL cholesterol. *Lipoprotein-associated serum triglyceride (TG) and cholesterol levels as measured by fast protein liquid chromatography (FPLC). Serum from random fed mice treated with either control (miNC) or TSC22D1 miRNA AAV (miD1) was pooled and applied to a Superose 6 10/300 GL column; (A) TGs (B) cholesterol (n=5).*

4.5.5 Chronic knockdown of TSC22D1 alters expression of key cholesterol metabolism genes

Chronic TSC22D1 knockdown reduced HDL cholesterol but left VLDL TGs unaltered (Fig 37A-B). In order to investigate if that can be explained by changes in gene expression, we performed qPCR analysis on genes involved in VLDL assembly and cholesterol metabolism (Table 4). Other than for the short term knockdown (Fig 26) chronic TSC22D1 ablation did not change expression of DAGT1 or 2 or MTTP (Fig 38A). Again, however, genes involved in cholesterol metabolism as ApoA1 or ABCG5 and 8 were significantly down-regulated in TSC22D1 knockdown mice as compared to control mice (Fig 38B). These results are in line with the FPLC analysis (Fig 37).
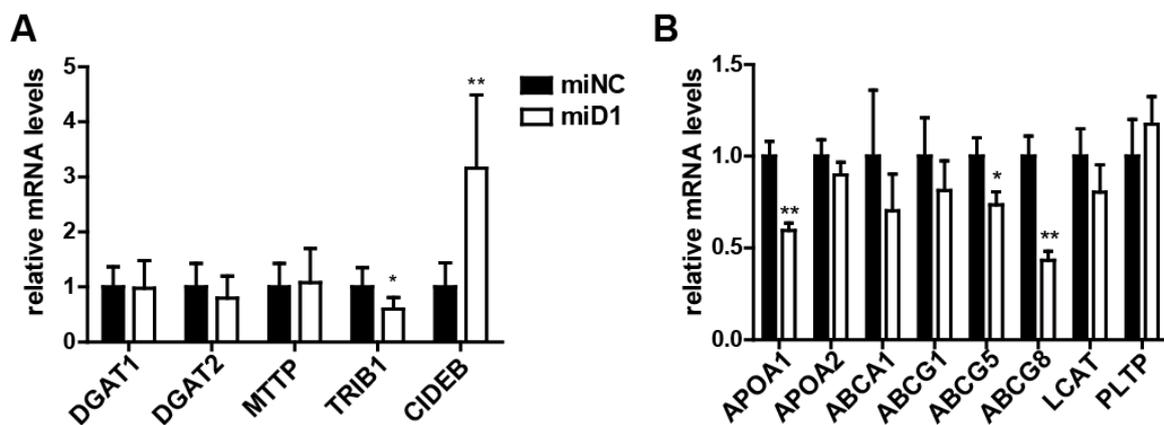
Fig 38: Chronic TSC22D1 knockdown alters expression of cholesterol metabolism genes. TSC22D1 expression in C57BL/6N mice treated with control or TSC22D1 AAV. Liver mRNA levels of depicted genes involved in (A) VLDL assembly, (B) cholesterol metabolism (Table 4) were analyzed by qPCR. (n=5) (means ± SEM). (*) indicates significance; $p < 0.05$; (**)$p < 0.01$

In order to get a comprehensive analysis of changes in gene expression by chronic TSC22D1 ablation, microarray analysis was performed using RNA extracts isolated from the livers of control or TSC22D1 deficient mice. As seen from the hierarchical heat map (Fig 39A), the four groups were very homogenous but distinct from one another. In total, more than 1600 genes were differentially regulated. The volcano plot (Fig 39B) shows all genes on the microarray, all genes above the threshold are considered as significantly altered in expression ($p < 0.05$). Genes shown on the left are less expressed and on the right more expressed in the TSC22D1 knockdown mice as compared to negative control mice. The volcano plot indicates, that TSC22D1 knockdown up- as well as downregulates a comparable amount of genes. As expected, TSC22D1 was among the most strongly down-

regulated genes. Furthermore ABC transporters, as ABCA1, or apolipoproteins as ApoA4, which is a part of HDL cholesterol were among the down-regulated genes. Gene set enrichment analysis (GSEA) was performed to find groups of genes that are regulated together. Among the top regulated pathways were steroid synthesis and PPAR signaling, but also pathways as cytosolic DNA-sensing pathway or TGFbeta signaling. Microarray analysis proved that hepatocyte specific TSC22D1 knockdown changes the expression of a large set of genes. It did not give new insight, however, in regards to the observed cholesterol phenotype.
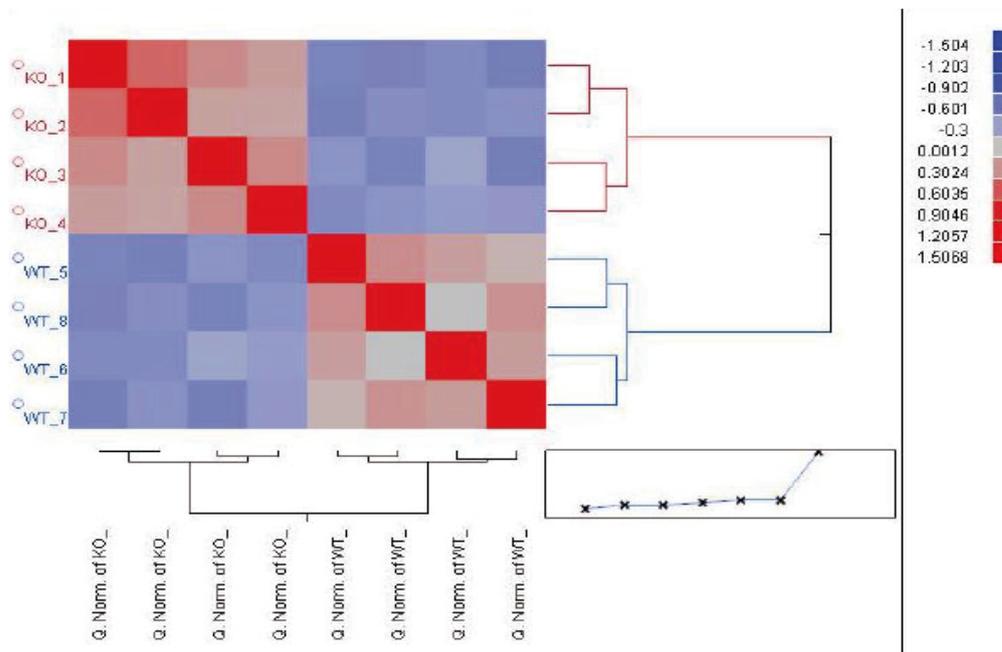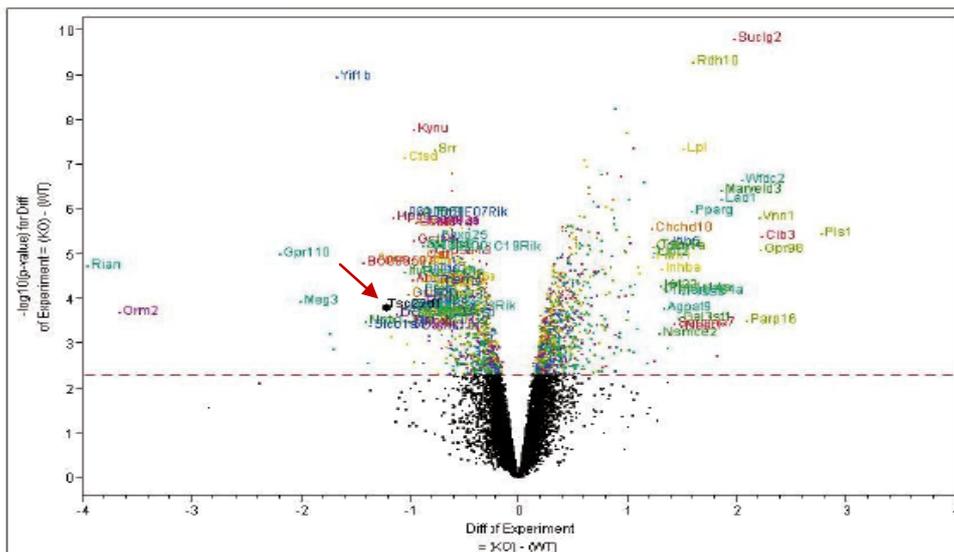
Fig 39: Gene expression profiling of C57BL/6J mice treated with control or TSC22D1 AAV. (A) Hierarchical heat map cluster of the samples, (B) Volcano Plot of control vs. TSC22D1 miRNA treated animals.The red arrow indicates TSC22D1. (n=4)

4.6 Effects of TSC22D1 knockdown in cultured cells

Next, we wanted to see if TSC22D1 ablation can as well change the expression of some of the genes involved in cholesterol metabolism in a cell culture model. For this purpose, Hepa1c1 cells, a mouse hepatoma cell line, were infected with either control or TSC22D1 shRNA adenovirus and harvested 48h post transfection. Gene expression was analyzed by qPCR (Fig 40). TSC22D1 mRNA levels were reduced by 80%. Hepa1c1 cells do not express ABCG1 and ABCG8, nevertheless, ABCG5 and ApoA1 mRNA levels were reduced by TSC22D1 knockdown, which is in line with the results seen *in vivo* (Fig 38B).
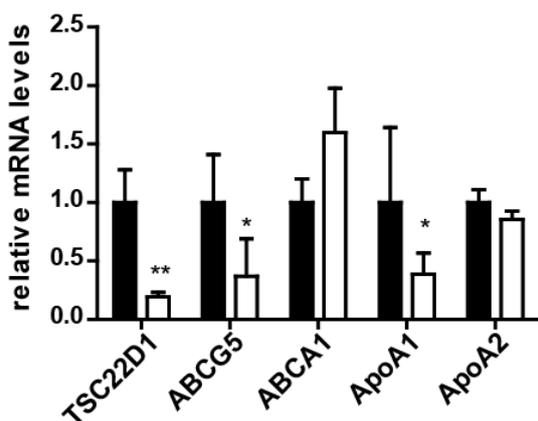
Fig 40: TSC22D1 knockdown reduces ApoA1 expression. Expression of genes involved in cholesterol metabolism (Table 4) in Hepa1c1 cells infected with either control (shNC) or TSC22D1 shRNA expressing adenovirus at an MOI of 500. mRNA levels were analyzed by qPCR. (n=3-4) (means ± SEM). (*) indicates significance; p < 0.05;

4.7 TSC22D1 knockdown reduced HDL cholesterol in a mouse model of obesity

TSC22D1 expression was shown to be up-regulated in mouse models of obesity, such as ob/ob mice (Fig 12A). These mice have a mutation in the leptin gene (Y. Zhang *et al.*, 1994). Furthermore, they exhibit increased levels of cholesterol (P. Hahn, 1980). Having in mind the reduction of HDL cholesterol by TSC22D1 knockdown in wildtype C57BL/6J mice, we expected that TSC22D1 knockdown also reduces cholesterol in *ob/ob* mice.

4.7.1 TSC22D1 can be efficiently knocked down in ob/ob mice

The AAV system was used to deliver control or TSC22D1 specific miRNAs to knockdown TSC22D1. For this purpose, mice were injected with 5×10^{11} viral particles into the tail vein and housed for 3 weeks, body weight and blood glucose were monitored. On day 20 after injection mice were fasted for 24h, one group was sacrificed directly and the other was refed for 6h. Liver TSC22D1 mRNA levels were determined by qPCR (Fig 41A) and Western blot analysis (Fig 41B). TSC22D1 mRNA and protein level were significantly lower in the miD1 group compared to the control group. Also, in the control group TSC22D1 expression was down-regulated by fasting again.
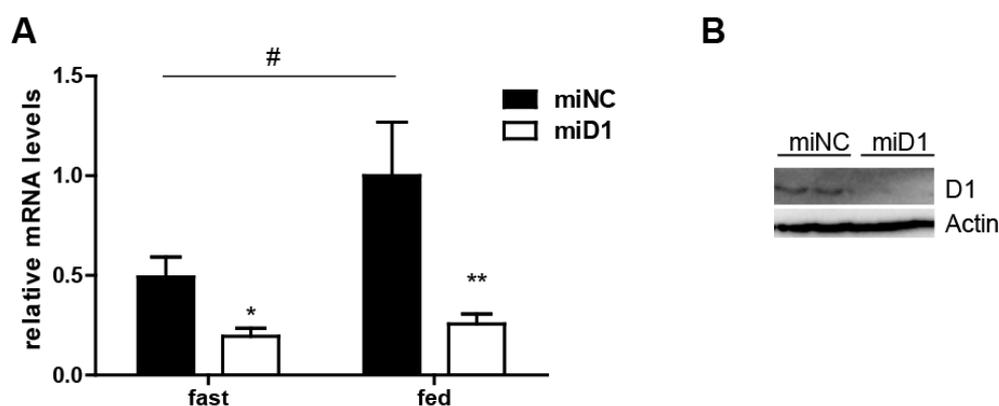
Fig 41: AAV mediated TSC22D1 knockdown. *(A) TSC22D1 expression in ob/ob mice treated with control (NC) or TSC22D1 overexpression (miD1) AAV. Mice were fasted for 24h and either directly sacrificed or refed for 6h. Liver mRNA levels of TSC22D1 were analyzed by qPCR. (B) Western blot of liver extracts from representative mice using TSC22D1 and β-actin (loading control) antibodies. (n=7), (means ±SEM), (*) indicates significance p<0.05 and (**) p<0.01 for genotype and (#) indicates significance p<0.05 for nutritional status*

4.7.2 Body weight, blood glucose and liver weight are unaltered by TSC22D1 knockdown in ob/ob mice

As already observed in the previous experiments, body weight and liver or abdominal fat weight were not changed (Fig 42A-C). It should be noted, that the blood sugar concentration was in a physiological range in all groups and under all conditions (Fig 42D), which indicates that the ob/ob mice were not yet in a diabetic state.
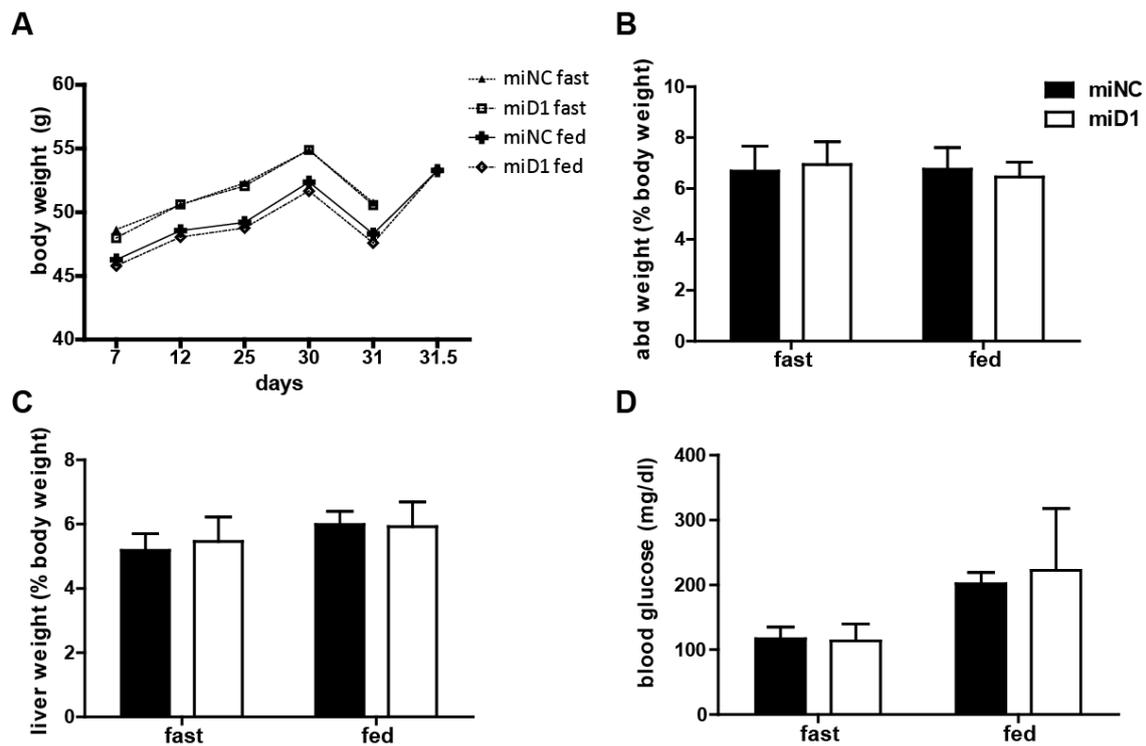
Fig 42: No change of body weight, blood glucose or liver weight by TSC22D1 knockdown. *(A) Body weight of ob/ob mice treated with control (miNC) or TSC22D1 miRNA (miD1) AAV. Mice were fasted for 24h and sacrificed or refed for 6, (B) abdominal fat weight, (C) liver weight and (D) blood glucose. n=7 (means ± SEM) (*)*

4.7.3   HDL cholesterol is reduced by TSC22D1 knockdown in ob/ob mice

Based on the other three studies, serum parameters were analyzed for the fasted and the fed state. Serum NEFAS, ketone bodies and serum TGs were unchanged (Fig 43A-C). Livers of ob/ob mice contained a lot of lipid droplets, but fat content was not changed by TSC22D1 knockdown as shown by liver lipid isolation and Oil-red-o staining (Fig 43D). As observed before (Fig 36) cholesterol was increased in livers of fed TSC22D1 knockdown mice as compared to control mice (Fig 43E).
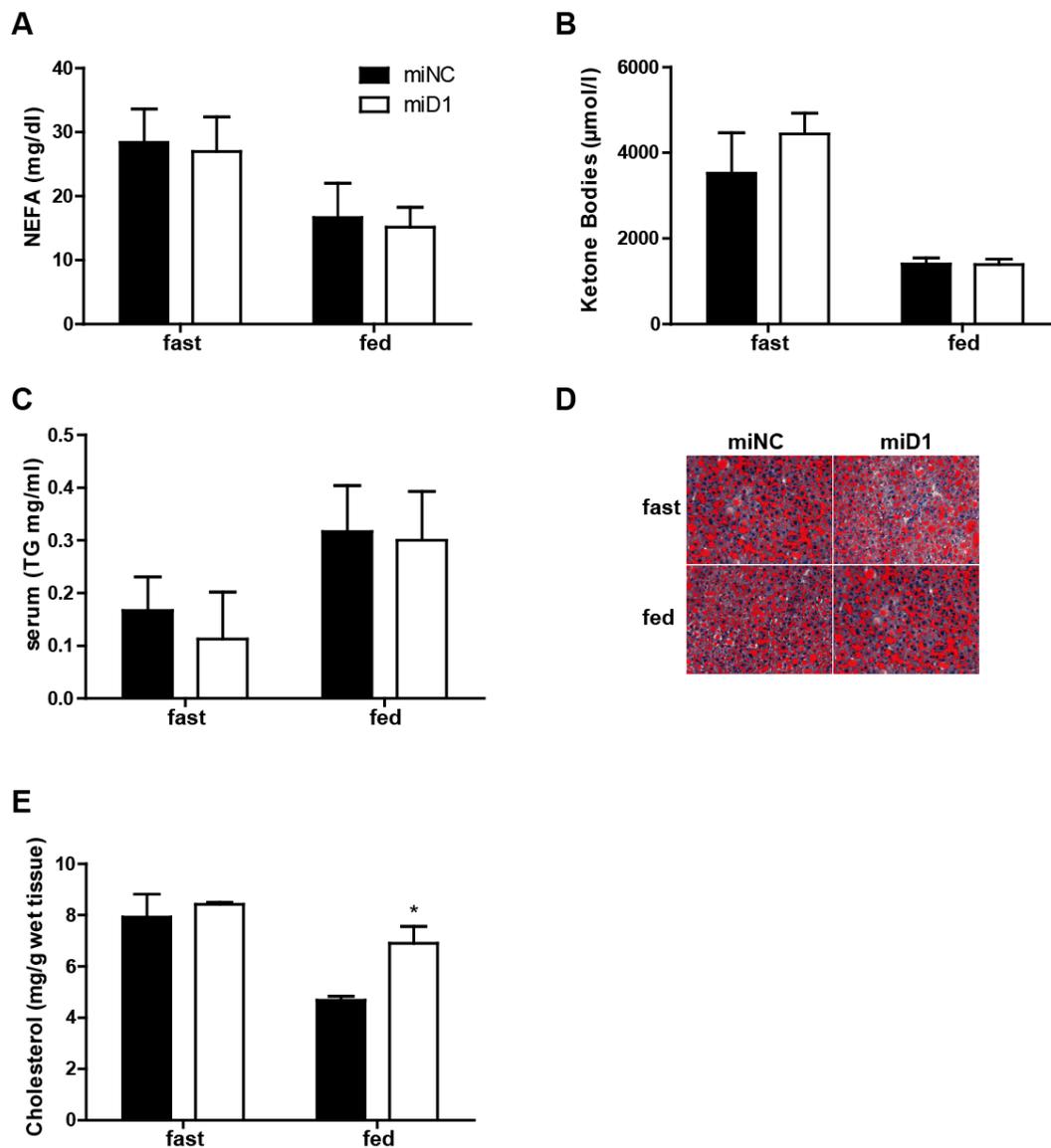
Fig 43: No change in circulating TGs by TSC22D1 knockdown in ob/ob mice. *Ob/ob mice were treated with control (miNC) or TSC22D1 miRNA AAV (miD1). Mice were fasted for 24h, one group was sacrified directly and the other refed for 6h. (A) Serum non-esterified free fatty acids (NEFA), (B) serum ketone bodies, (C) serum triglycerides, (D) liver triglyceride (TG) as shown by representative Oil-red-O staining of cryosections and (E) liver cholesterol. (n=7) (means±SEM), (*) indicates significance p<0.05*

The FPLC analysis of circulating VLDL-TGs or HDL-cholesterol revealed no difference in VLDL TGs in fasted or refed animals (Fig 44A-B). However, a substantial reduction in fasting HDL and LDL cholesterol and a slight reduction of HDL cholesterol in the fed state by TSC22D1 knockdown could be shown (Fig 44C-D). This data is in line with the results of the prior studies of acute and chronic TSC22D1 knockdown.
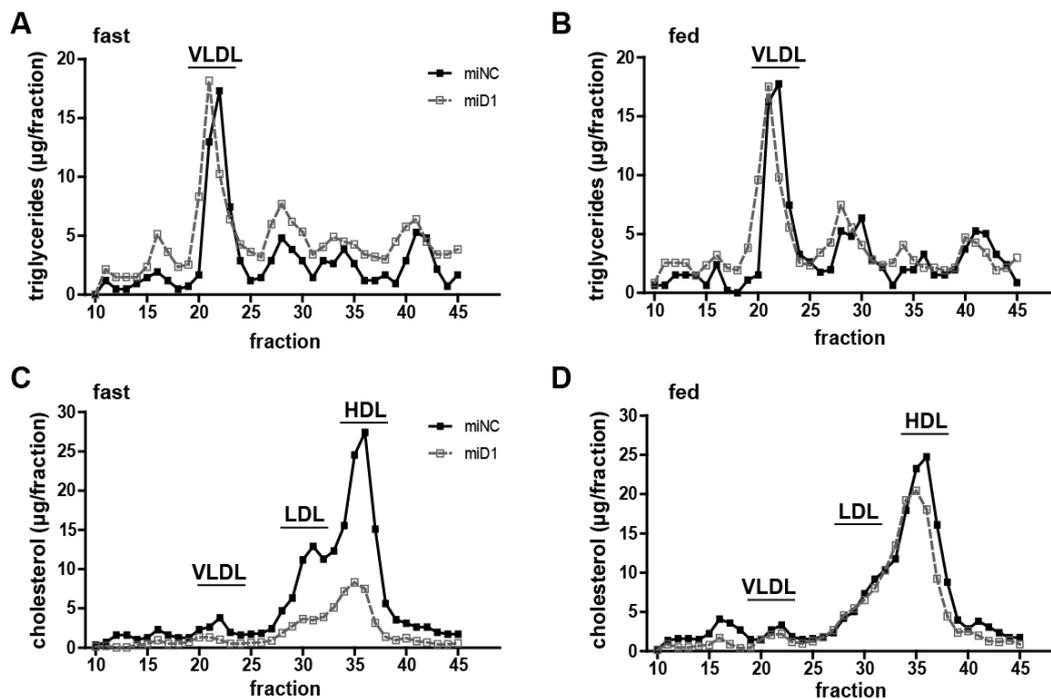
Fig 44: TSC22D1 knockdown in ob/ob mice lowers circulating HDL cholesterol. *Lipoprotein-associated serum triglyceride (TG) and cholesterol levels as measured by fast protein liquid chromatography (FPLC). Serum from 24h fasted or 6h refed ob/ob mice treated with either control (miNC) or TSC22D1 miRNA AAV (miD1) was pooled and applied to a Superose 6 10/300 GL column; (A) fasting TGs, (B) fed TGs, (C) fasting cholesterol and (D) fed cholesterol (n=7).*

4.7.4 TSC22D1 knockdown can decrease expression of cholesterol metabolism linked genes in ob/ob mice

As hypothesized, TSC22D1 knockdown in ob/ob mice could reduce HDL cholesterol (Fig 44). Again, we analyzed expression of genes involved in VLDL assembly and cholesterol metabolism (Table 4) by qPCR. Expression of MTTP, DGAT1/2 and FSP27 (Fig 45A-B) was not altered. For the panel of genes involved in cholesterol metabolism different genes were altered depending on the feeding status of the mice (Fig 45A-B). In fasted animals, ABCA1 and LCAT and PLTP showed reduced expression in TSC22D1 ablated mice as compared to controls. In the fed state, as seen before (Fig 26, 28 and 38) expression of ApoA1 and 2 and ABCG51, 5 and 8 was significantly reduced. The expression data is in line with the previous results and strengthens the idea of TSC22D1 as a mediator of cholesterol metabolism.
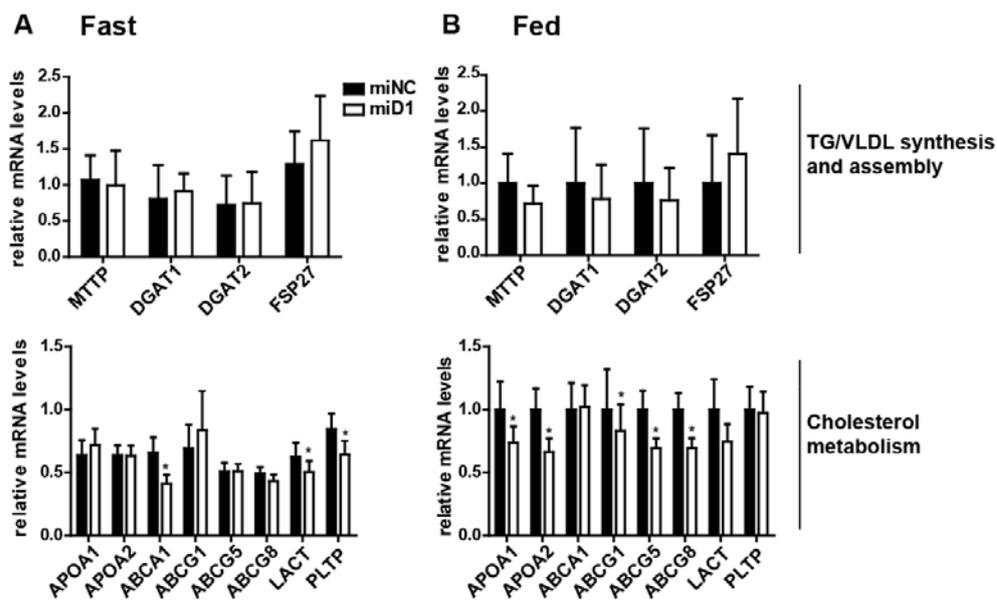
Fig 45: TSC22D1 knockdown reduces expression of cholesterol metabolism genes. *TSC22D1 expression in C57BL/6J mice treated with control or TSC22D1 cDNA adenovirus. Mice were fasted for 24h and one group was directly sacrificed (Panel A) or refed for 6h (Panel B). Liver mRNA levels of depicted genes (Table 4) was analyzed by qPCR. (n=7) (means ± SEM). (*) indicates significance; p < 0.05; (**)p < 0.01*

4.8 Comprehensive overview of all conducted mouse experiments

A summary of phenotypes and biochemical parameters resulting from acute or chronic TSC22D1 knockdown or overexpression in the liver of wild-type or *ob/ob* mice is shown in Table 5.

Table 5: Summary of phenotypic changes in mice with altered hepatic TSC22D1 expression

Mouse Strain	TSC22D1 Status	Nutritional Status	Weight			Serum					Liver		FPLC		Expression of key genes
			Body	Abd	Liver	NEFA	Ketone	TG	Glc	TG	C	Gly	VLDL	HDL	
C57BL/6	KD acute	Fast	-	-	-	-	-	ud	-	-	↑	ud	↓↓	↓↓	↓APOA1
C57BL/6	KD acute	Fed	-	-	-	-	-	↓↓	-	-	-	-	↓↓	↓	↓DGAT1/2, MTTP, TRIB1, PLIN2, CIDEB, FSP27, ABCA1, ABCG1, ABCG8, APOA2
C57BL/6	OE acute	Fast	-	-	-	-	-	↓	-	-	nd	ud	↑↑	-	
C57BL/6	OE acute	Fed	-	-	-	-	-	-	-	-	nd	-	↑	↑↑	↑DGAT2, FSP27, ABCG1, PLTP, ↓ APOA1, APOA2
C57BL/6	KD chronic	Fed	-	-	↓	-	↓↓	-	-	-	↑	-	-	↓↓	↓APOA1, ABCG5/8
ob/ob	KD chronic	Fast	-	-	-	-	-	-	-	-	-	nd	-	↓↓	↓ABCA1
ob/ob	KD chronic	Fed	-	-	-	-	-	-	-	-	↑	nd	-	↓	↓APOA1, APOA2, ABCG1, ABCG5/8

Abd: abdominal fat; NEFA: non esterified fatty acids; Ketone: ketone bodies; TG: triglycerides; Glc: glucose; C: cholesterol; Gly: Glycogen: FPLC: fast protein liquid chromatography; VLDL: very low density lipoprotein; HDL: high density lipoprotein; KD: knockdown; OE: overexpression, -: no change;↓ reduced levels; ↑ increased levels both as compared to control mice; ud: undetectable; nd: not determined

5   Discussion

5.1   TSC22D1 regulates systemic HDL cholesterol metabolism

Cardiovascular diseases (CVDs) are the leading cause of death worldwide. In 2008 an estimate of 17.3 million people died from CVDs, and the numbers are on the rise (WHO fact sheet No 317, 2013). Prevention of atherosclerosis requires life style changes, but several drugs have also been developed with statins representing the most widely used group. They are HMG-CoA reductase inhibitors which work primarily by reducing LDL cholesterol levels, as elevated serum LDL levels are shown to be atherogenic. Nevertheless, HDL cholesterol remains a predictor for cardiovascular events in statin treated patients besides their LDL levels (H. Soran *et al.*, 2012). Further, various studies in humans present an inverse correlation between plasma concentrations of HDL, and the risk for atherosclerotic cardiovascular disease (G.F. Lewis and D.J. Rader, 2005).

5.1.1   TSC22D1 knockdown alters cholesterol efflux by changes in gene expression

In the present study we found that TSC22D1 has a promoting effect on systemic HDL cholesterol levels in mice (Table 5). Although mice are highly resistant to atherosclerosis; they represent a good and widely used model system to study HDL cholesterol metabolism *in vivo,* especially because of their high levels of HDL (J. Jawien *et al.*, 2004). It has to be noted, that mice and humans have different blood profiles when it comes to cholesterol. Humans carry about 75% of their plasma cholesterol in LDL, mice, however, carry most of their cholesterol in form of HDL (J. Jawien *et al.*, 2004). FPLC analysis showed a reduction of HDL cholesterol in an acute as well as in a chronic TSC22D1 loss of function experiment (Fig 21 and 37) in C57BL/6 mice. Overexpression of TSC22D1 could in turn elevate plasma HDL cholesterol (Fig 31). We explain these findings by changes in gene expression of some key genes in the cholesterol metabolism pathway, which will be discussed in the following.

Apoliprotein A1 is the most abundant apoliprotein in the human plasma and it is secreted by the liver and the intestine. Like HDL, ApoA1 plasma concentration is inversely correlated to atherosclerosis (G.F. Lewis and D. J. Rader, 2005). Mice lacking ApoA1 have significantly lower plasma HDL cholesterol levels (A. S. Plump *et al.,* 1997), reflecting our findings with TSC22D1 ablated mice showing lower expression of ApoA1 (Table 5). As ApoA1 levels are mainly transcriptionally regulated (S. Malik, 2003), reduced expression of ApoA1 by

TSC22D1 knockdown would then translate to lower levels of serum ApoA1. However, serum analysis for ApoA1 levels has not been performed so far.

ATP binding cassette transporter 1 (ABCA1) is often described as the most important mediator for the efflux of cholesterol from macrophages to HDL in the reverse cholesterol transport. Patients with Tangier disease, who carry a mutated and thus defective ABCA1, have very low plasma HDL (M. Maricil *et al.,* 1999). ABCA1 expressed in hepatocytes is involved in the generation of HDL particles (E. Tarling *et al.,* 2013). Thus, liver specific ABCA1 deficiency reduces serum HDL by 80% (J. Y. Lee and J.S. Parks, 2005). In the present study, ABCA1 expression in TSC22D1 ablated mice was decreased as compared to control mice (Table 5), indicating that this may contribute to the reduced levels of HDL cholesterol in these mice and increased liver cholesterol.

Additionally, expression of ABCG5 and/or 8 is reduced by TSC22D1 knockdown (Table 5). ABCG5 and 8 are expressed in liver as well as in intestine and they function as a heterodimer in efflux of plant sterols. It was shown that ABCG5/8 knockout mice (ABCG5/8-/-) fed a normal chow diet containing 0.02% cholesterol, had highly reduced serum cholesterol levels compared to control mice (L. Yu *et al.,* 2002). These mice exhibited however reduced liver cholesterol, which is contradicting the increased hepatic cholesterol content of TSC22D1 ablated mice (Table 5). This discrepancy may possibly be explained through the observed decrease of ApoA1 expression, which might reduce HDL efflux and thereby result in higher cholesterol levels in the liver. ABCG5/8-/- mice have higher cholesterol concentrations in their gallbladder (L. Yu *et al.,* 2002). The excretion of cholesterol into bile is important for cholesterol excretion out of the body and thus limits the reuptake of cholesterol by the intestine. In our studies the cholesterol content of the bile was not measured. The decrease in ABCG5/8 gene expression hints at a reduction of bile cholesterol in TSC22D1 ablated mice compared to control mice.

In summary, TSC22D1 knockdown seems to specifically alter cholesterol efflux as presented in Fig 46. Apparently, cholesterol efflux from the liver mediated by the ABCA1 transporter is reduced as is ApoA1 expression, resulting in a decreased HDL particle formation. Furthermore, reduction of the levels of ABCG5/8 results in lowered transport of cholesterol to the intestine. Uptake appears to be unaffected as indicated by unchanged expression of scavenger receptor B1 (SR-B1) (Table 5), the major HDL receptor (S. Acton *et al.*, 1996).
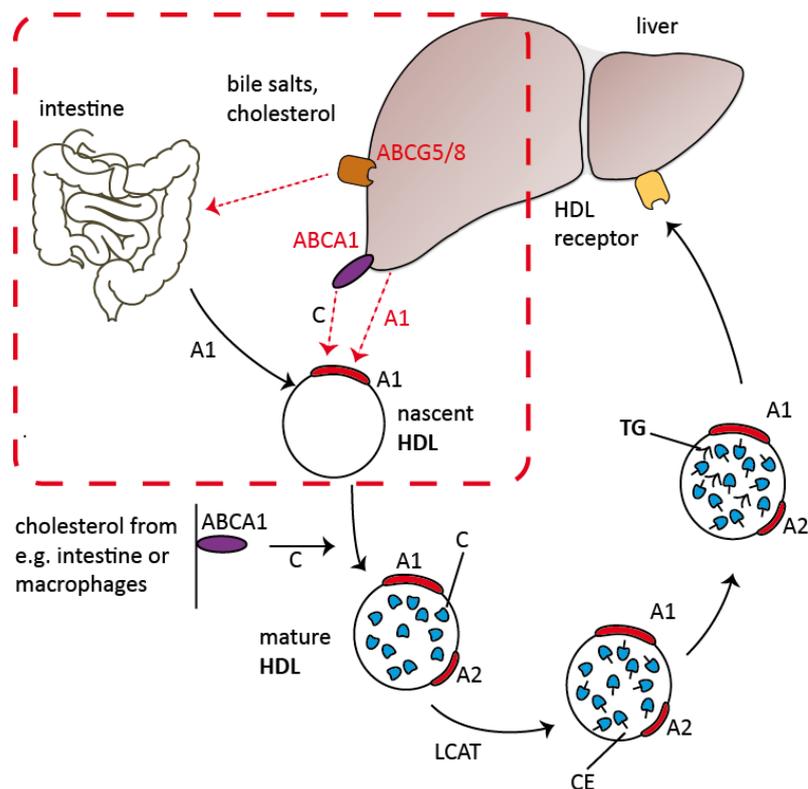
Fig 46: Altered cholesterol metabolism by reduced TSC22D1 expression. *Hepatic knockdown of TSC22D1 in wild-type as well as in ob/ob mice specifically alters expression of genes involved in cholesterol efflux. Lower expression of hepatic ABCA1 results in decreased cholesterol efflux from the liver. Additionally, reduced ApoA1 expression decreases HDL particle formation. Finally, lower levels of ABCG5/8 reduce transport of cholesterol into the intestine for re-shuttling or final secretion from the body. Uptake of HDL into the liver or particle maturation is presumably not altered.*
A1/2: ApolipoproteinA1/2; C: cholesterol; LCAT: lecithin-cholesterol acetyltransferase; CE: cholesterol-ester, HDL: high density lipoprotein; ABC A1/G5/G8: ATP-binding cassette protein A1, G5, G8; TG: triglycerides
The part of the cholesterol metabolism which is directly affected by reduced TSC22D1 expression is mareked with a red dotted line.

ApoA1, as well as ABCG5 and 8 are also expressed by the intestine, where they play a substantial role in regulating system cholesterol homeostasis. TSC22D1 expression levels in intestine have been shown to be even higher than in the liver (P. Jay *et al.,* 1996). Given the putative function of TSC22D1 to regulate expression of ApoA and ABCG5/8, it would be very interesting to analyze the effect of TSC22D1 knockdown in the intestine. One can speculate that a combined ablation of TSC22D1 liver and intestine function would have an even higher impact on systemic cholesterol homeostasis. We cannot rule out that TSC22D1 exerts its function in a tissue specific manner, as is the case for TBL1 and TBLR1 which are expressed in various different tissues including liver and white adipose tissue and both play a major role in regulating liver lipids (P. Kulozik *et al.*, 2011). Nevertheless, only TBLR1 not

TBL1 acts on lipolysis in white adipose tissue. (M. Rohm *et al.*, 2013, and M. Rohm PhD thesis, Herzig Lab)

We made an interesting observation regarding cholesterol metabolism and the regulation of TSC22D1. Apparently, regulation of TSC22D1 expression by fasting or feeding signals is impaired in aged mice (Fig 14). It has been described that cholesterol efflux is impaired with aging (H. Berrougui, *et al.* 2007) and also concentrations of ApoA1 decrease with age (H. Berrougui and A. Khalil, 2009). Hence, it is tempting to speculate, that a decrease in the expression levels of TSC22D1 correlates with impairment of cholesterol regulation in aging.

5.1.2 Overexpression of TSC22D1 increases HDL cholesterol

Currently, we cannot explain why overexpression of TSC22D1 leads to an increase in HDL cholesterol. When it comes to gene expression analysis (Fig 32), we saw a reduced expression of ApoA1 as also seen before in case of TSC22D1 knockdown. Expression of phospholipid transfer protein (PLTP) was slightly increased, a gene that was not affected by acute TSC22D1 ablation. PLTP is responsible for the transfer mainly of phospholipids from VLDL to HDL particles. A recent publication demonstrated that liver specific overexpression of PLTP resulted in an increase in non-HDL cholesterol and VLDL-TGs, rather than in HDL cholesterol. These findings regarding cholesterol levels are not in line with our study. Interestingly, however we saw a similar increase in VLDL-TG levels (Fig 31). Another gene upregulated by hepatic TSC22D1 overexpression, was ABCG1, which is responsible for the efflux of cholesterol to already lipid rich HDL. Liver-specific overexpression of ABCG1 resulted in decreased serum HDL rather than increased levels as seen in our study. Further analysis is required to explain the HDL cholesterol phenotype seen by TSC22D1 overexpression, including PLTP enzyme activity or ApoA1 protein abundance.

5.1.3 TSC22D1 knockdown in a mouse model of obesity

Given the promoting effect of TSC22D1 on systemic HDL cholesterol levels in C57BL/6 mice, we hypothesized that the observed upregulation of TSC22D1 under obesity conditions (Fig 12-13) reflects a counter-regulatory mechanism to maintain high levels of HDL cholesterol. Compared to C57BL/6 mice ob/ob mice exhibit an abnormal blood profile they show higher levels of HDL as well as less dense HDL particles and LDL, both appearing as a shoulder on the HDL peak in an FPLC analysis and are referred to as HDL1/LDL (own observation and D.L. Silver *et al.*, 1999). Interestingly, we could see that chronic knockdown of TSC22D1

resulted in significantly reduced levels of HDL cholesterol and also lowered the HDL1/LDL shoulder in ob/ob mice (Fig 44). As observed before, TSC22D1 knockdown in ob/ob mice resulted in a decreased expression of ABCA1, ApoA1, ABCG5 and 8 (Fig 45). Additionally, expression of ApoA2 was reduced. It is the second most abundant Apoliporotein on HLD particles, and interestingly, it is especially high expressed in ob/ob mice (D.L. Silver *et al.*, 1999). Due to the increased levels of HDL cholesterol, ob/ob mice are protected against atherosclerosis as compared to C57BL/6 mice (M.R. Plummer A. H. Hasty*., 2008). Our data indicate that TSC22D1 might be involved in such a protection mechanism.

5.1.4   Liver TSC22D1 expression is reduced in a mouse model of atherosclerosis

LDL receptor knockout mice (LDLR-/-) represent one of the most used mouse models for studies regarding atherosclerosis. They present low levels of HDL and increased levels of LDL and develop atherosclerosis on a high cholesterol diet (J. Jawien, 2004). LDL and as well as VLDL levels are further increased in streptozotocin-induced (STZ) type 1 diabetic mice (R.K Vikramadithyan *et al.*, 2005 and unpublished observation K. Genreith, Herzig Lab). Diabetes exaggerates development of vascular lesions in these mice. Interestingly, we found hepatic TSC22D1 levels significantly reduced in livers of STZ treated LDLR-/- mice, as compared to non-diabetic LDLR-/- controls (own observation, data not shown). Furthermore, liver TSC22D1 mRNA levels tended to negatively correlate with the degree of plaque formation in STZ treated or non-treated LDLR-/- mice (own observation, data not shown). These findings strengthen the idea that TSC22D1 plays a role in atheroprotection. In this respect, it would be highly interesting to see if hepatic TSC22D1 overexpression in LDLR-/- mice would help to normalize the blood profile by increasing HDL cholesterol and thus, decrease atherogenic plaque formation.

5.1.5   Atherosclerosis and TGFbeta

TSC22D1 expression was initially found to be induced by TGFbeta1 in mouse osteoblastic cells (M. Shibanuma *et al.*, 1992). We could recapitulate this finding *in vitro* in primary hepatocytes (Fig 15) as well as *in vivo*, where systemic introduction of TGFbeta induced hepatic TSC22D1 expression. It has recently been shown that systemic TGFbeta levels were elevated in obese patients (H. Yadav *et al.*, 2011) and obese mice (Fig 15 and H. Yadav *et al.*, 2011), which interestingly is in accordance with higher TSC22D1 expression in ob/ob mice. Intriguingly, there is evidence that TGF beta is anti-atherogenic. It has been shown

that there is an inverse relationship between serum TGFbeta levels and the development of atherosclerosis (N.N. Singh D.P. Ramji, 2006). Serum levels of TFGbeta were found to be severely reduced in advanced atherosclerosis (D. J. Grainger *et al.*, 1995). TSC22D1 knockdown resulted in decreased levels of HDL cholesterol, which is a risk for development of atherosclerosis. It is tempting to speculate that there is a correlation between low TGFbeta levels in atherosclerosis, low levels of TSC22D1 expression and reduced atheroprotection by reduction of HDL cholesterol.

5.1.6   Beyond cholesterol

There are several other important aspects prompting to understand HDL metabolism. HDL has a lot of additional functions apart from its importance as the "good cholesterol", as it is termed in the laymen press (C. Mineo, 2013). For instance, HDL and its component ApoA1 can promote insulin secretion by pancreatic beta cells (S. J. Peterson *et al.*, 2008). Other *in vivo* studies suggest, that HDL can bind and neutralize bacterial lipololysaccharide (LPS) and thereby prevent proinflammatory gene expression (H. Soran *et al.*, 2012). There is also evidence that HDL can enhance endothelial cell proliferation, which is important an important response to vascular injury (C. Mineo, 2013). The present study did not consider a role of TSC22D1 for HDL besides cholesterol metabolism. But these few examples demonstrate that it might be worthwhile to have a look beyond cholesterol.

5.2   TSC22D1 as a transcriptional co-regulator

Transcriptional regulators represent critical checkpoints in the regulation of liver energy homeostasis, as exemplified by several nuclear receptor co-factors, e.g. peroxisome proliferator-activated receptor co-activator (PGC) 1, receptor interaction protein (RIP) 140 and transducing beta-like (TBL1) (J.N. Feige and J. Auwerx, 2007; P. Kulozik *et al.*, 2011, M. Berriel Diaz *et al.*, 2008).

In the present study, we could demonstrate with co-immunoprecipitation studies that TSC22D1 indeed interacts with TBL1 (Fig 8). This interaction, however, could neither be recapitulated nor further mapped by GST-pulldowns. These findings indicate that TBL1 and TSC22D1 do not interact directly but may be associated in a complex with several other proteins. This assumption could be experimentally verified by immunoprecipitation of

TSC22D1 directly from liver tissue and subsequent analysis using mass spectrometry to identify endogenous interaction partners.

Other than TSC22D4, TSC22D1 did not co-immuoprecipitate with TBRL1, which early on indicated that TSC22D1 and TSC22D4 might be present in different complexes and thus, will also have different functions in liver metabolism. Previous studies on the common *Drosophila melanogaster* TSC22D precursor *bunched* also indicated that TSC22D4 and TSC22D1 may at least in part have antagonizing effects in regard to cell proliferation (X. Wu *et al.*, 2008; S. Gluderer *et al.*, 2008). This data is in line with our findings from gene expression analysis for TSC22D1 and TSC22D4. Whereas TSC22D1 expression is reduced in states of energy deprivation and increased in energy surplus situations (Table 3) TSC22D4 is regulated in the opposite direction (A. Jones, PhD thesis, Herzig Lab).

TSC22D1 has to be present in the nucleus to act as a transcriptional co-factor. However, a nuclear localization signal is missing (M. Shibanuma *et al.*, 1992; S. Ohta *et al.*, 1997) but a nuclear export signal (NES) is present at its N-terminus (P. Jay *et al.*, 1996). As the molecular weight of human as well as rodent TSC22D1 is about 16-18 kDa (P. Jay *et al.*, 1996; M. Shibanuma *et al.*, 1992) and intracellular proteins of 50 kDa or less can freely permeate through micropores in the nuclear membrane (J.E. Hinshaw *et al.*, 1992). TSC22D1 may nevertheless be able to enter the nucleus. Additionally, translocation of TSC22D1 from the cytoplasm to the nucleus has been implicated, as flag-tagged TSC22D1 was present in the cytoplasm under steady-state conditions and Ras activation could induce nulear translocation (M. Nakamura *et al.*, 2011).

The intracellular localization of TSC22D1 in hepatocytes is presently unknown. Recently, a Western blot analysis detected TSC22D1 in the nuclear, but not in the cytoplasmic fraction of liver lysates (own observation). This preliminary observation requires a more in depth analysis to draw sound conclusion regarding the localization of TSC22D1. Furthermore, it would be interesting to see if its subcellular localization is altered under different metabolic conditions.

5.2.1 TSC22D1 and LXR?

We consider TSC22D1 to be a transcription co-regulator, nevertheless, we did not perform studies so far to determine DNA binding interaction partners. Based on its role in liver

metabolism, we assume that TSC22D1 would interact with a nuclear receptor because nuclear receptors are pivotal for integrating nutritional, metabolic and endocrine signals.

In respect to the changes in gene expression seen by TSC22D1 knockdown (Table 5), liver receptor X (LXR) would be a likely candidate. There are two LXRs, LXRalpha, which is highly expressed in metabolic active tissues as liver, white adipose tissue or macrophages and LXR beta which is ubiquitously expressed (A. C. Calkin and P. Tontonoz, 2012). LXR functions as an obligate heterodimer with retinoid X receptor (RXR). Activation of gene transcription requires ligand binding. LXR can be activated by cholesterol derivatives as oxysterols (B. A. Janowski *et al.*, 1996) or by synthetic agonists. Thus, direct target genes of LXR include genes involved in reverse cholesterol transport, cholesterol uptake, cholesterol absorption and secretion. Indeed, in our study TSC22D1 knockdown resulted in decreased expression of ABCA1 and ABCG5/8, which are direct targets of LXR (J. J. Repa *et al.*, 2000). Along these lines, acute knockdown of TSC22D1 in C57BL/6 mice, as well as chronic TSC22D1 ablation in ob/ob mice, reduced expression of cholesterol 7 alpha hydroxylase (Cyp7a) (own observation). Cyp7a is the key enzyme in the conversion of cholesterol to bile acid, and is a further LXR target gene. It would be interesting to see if the presence of TSC22D1 can alter LXR activity and if so, under which conditions this occurs. Luciferase promoter assays could be conducted to address this question. A putative model for TSC22D1 function is shown in Fig 46.
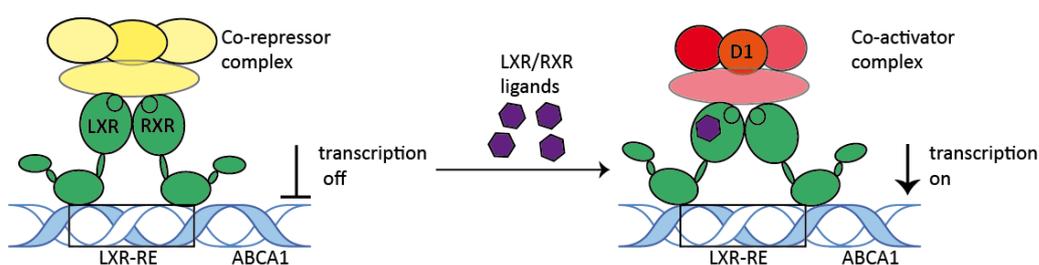
Fig 47: Putative TSC22D1 action on nuclear receptor LXR.
LXR/RXR dimer and their co-repressor complex are bound to the DNA and transcription is repressed. Upon ligand binding conformational changes are induced and co-activator complexes can bind and activate target gene transcription e.g. of ABCA1 transcription. TSC22D1 (D1) protein is part of the co-activator complex. In case TSC22D1 levels are reduced, as by knockdown or by fasting, activation is less efficient and target gene transcription is reduced.
LXR: liver X receptor; RE: response element; RXR: retinoid X receptor; ABCA1: ATP binding cassette protein A1; D1: TSC22D1

As discussed before, Apolipoprotein A1 expression was also shown to be reduced by TSC22D1 knockdown (Table 5). ApoA1 is not a direct target gene of LXR. Interestingly, however, ApoA1 is a farnesoid x receptor (FXR) target, which as LXR also heterodimerizes with RXR, indicating that TSC22D1 might act on RXR in combination with LXR rather than on LXR alone.

In rodents, synthetic LXR ligands can inhibit the development of atherosclerosis, in part by upregulating expression of ABCA1, ABCG1, ABCG5/8 and thus lowering liver and serum cholesterol levels. Still, LXR agonist treatment also induces genes involved in fatty acid and TG regulation as FASN or ANGPTL3, resulting in high TG levels (J.R. Schultz, 2000) which limits a pharmacological success of LXR agonists. Intriguingly, in our study lipogenic gene expression was unaltered (Fig 26, 38 and 45). It is tempting to speculate that TSC22D1 action might regulate the expression of a subset of LXR target genes beneficial for atheroprotection. Nuclear receptors exert different functions depending on their co-repressor or activator complexes. Thus, these co-factors represent an interesting platform for the development of drugs, which alter expression of only a specific subset of genes thus limiting side effects.

5.3 Open questions

TSC22D1 seems to very specifically affect cholesterol metabolism, as indicated by the performed *in vivo* studies. Physiological parameters as body weight, blood glucose or serum non-esterified fatty acids remained mostly unchanged by manipulations in TSC22D1 expression levels (Table 5). Nevertheless, analysis of all presented data leaves some obvious open questions.

We observed a strong reduction of postprandial serum TGs upon acute TSC22D1 knockdown (Fig 20). This reduction was due to a decrease in VLDL, as shown by FPLC analysis. In line with that, VLDL TGs were elevated by acute TSC22D1 overexpression (Fig 21). Gene expression analysis revealed that some key genes involved in TG metabolism as microsomal triglyceride transfer protein (MTTP) or diaglyceride acetyltransferases 1 and 2, were downregulated by TSC22D1 knockdown. Additionally, acute TSC22D1 knockdown resulted in increased clearance of VLDL, whereas TG secretion was not altered (Fig 24). However, in chronic knockdown of TSC22D1 alterations in VLDL TG levels could not be

recapitulated (Fig 37). We cannot rule out that over time TSC22D1 function for TG metabolism can be compensated by other unknown factors. A similar phenomenon has been observed for TSC22D4 depletion which results in high serum and liver TG levels, this effect is, however, lost over time (A. Jones, Phd thesis, Herzig Lab). A time course study to monitor the effects of TSC22D1 knockdown could provide experimental evidence in that direction.

Hepatic TSC22D1 expression was shown to be altered by the energy status (Table 3). Our findings about TSC22D1 function in cholesterol metabolism provide evidence that upregulation of TSC22D1 in an obese situation might help to maintain HDL levels. Another aspect of TSC22D1 regulation is the downregulation of TSC22D1 expression in situations of energy deprivation as cachexia or fasting. In fasting there is no uptake of exogenous cholesterol and thus less transport throughout the body required for final excretion. At least expression of ABCA1 and ApoA1 in control mice was reduced by fasting as well (Fig 16, 32 and 45). Interestingly, in cachectic mice HDL cholesterol is slightly reduced (A. Jones *et al.*, 2013), which cannot be explained so far. In cancer cachexia, cholesterol metabolism is of course not important in regards to atherosclerosis. Nevertheless, as mentioned before, HDL has more functions as being anti-inflammatory (C. Mineo, 2013) and cholesterol itself is important as a part of cell membranes or precursor of steroid hormones. The function of hepatic TSC22D1 in situations of energy deprivation requires further experimental analysis, which will help to understand the importance of TSC22D1 for systemic HDL metabolism.

5.4 Conclusions

In summary, we could demonstrate that hepatic TSC22D1 expression is found to be differentially regulated in mouse models of opposing energy supply. Intriguingly, we have identified hepatic TSC22D1 as a novel regulator of systemic cholesterol metabolism. Acute or chronic knockdown of TSC22D1 in livers of wild-type and obese mice resulted in a marked decrease of serum HDL cholesterol. Overexpression of TSC22D1, on the contrary, increased HDL cholesterol. TSC22D1 is a putative transcriptional co-regulator. Indeed, TSC22D1 ablation resulted in a significantly decreased expression of key genes involved in cholesterol efflux, namely ApoA1, ABCA1 and ABCG5/8. These changes can at least in part explain the observed reduction in serum HDL (Fig 46). HDL/ApoA1 plasma concentrations

inversely correlate with the risk for atherosclerotic cardiovascular disease. Thus, hepatic TSC22D1 transcription factor complex may represent an interesting new pharmaceutical target for manipulation of HDL cholesterol levels.

6   Methods

6.1   Molecular Biology

6.1.1   Transformation of *Eschericha Coli*

Top 10, XL-1 blue and Sure2 chemical competent E. coli strains were transformed by chemical transformation. 50 µl of competent cells were thawed on iced. Either 0.1-1 µg plasmid DNA or 1-5 µl of ligation reaction was added and cells were incubated for 20-30 min on ice. Following a heat shock for 45 s at 42°C, 250 µl LB- (for TOP 10 and XL-1 blue) or SOC- (for Sure2), medium was added. Cells were kept for 30-60 min at 37°C in a table top shaker with 300 rpm. After the incubation period, 100-200 µl of cell suspension was spread on Agar-plates containing the required antibiotic. Plates were incubated at 37°C overnight for bacterial growth and stored at 4°C.

6.1.2   Bacterial liquid cultures

Small scale liquid cultures

Single colonies were inoculated into 5 ml LB medium supplemented with the appropriate antibiotic. The cultures were incubated over night at 37°C under vigorous shaking (~160 rpm).

Larger scale liquid cultures

Depending on the required DNA yield, 200-2000 ml cultures were inoculated with a small scale liquid culture that had been pre-incubated for 5-8h. The cultures were incubated over night at 37°C under vigorous shaking (~160 rpm).

6.1.3   Preparation of plasmid DNA from Eschericha Coli

Small scale plasmid preparation (Mini Prep)

Plasmid preparation from small scale bacterial liquid cultures was performed using the Qiaprep Plasmid Miniprep Kit provided by Qiagen following the manufacturer's instruction. The DNA was eluted with 50 µl H_2O. Plasmid DNA was stored at -20°C.

Large scale plasmid preparation (Maxi or Mega Prep)

Plasmid preparation from large scale bacterial liquid cultures was performed using the PureLink HiPure Plasmid Maxiprep Kit provided by Invitrogen or the Qiaprep Plasmid Megaprep Kit provided by Qiagen following the manufacturer's instruction. The DNA was eluted with 200 µl H_2O or 800 µl of H_2O, respectively. Plasmid DNA was stored at -20°C.

6.1.4   Purification of plasmid DNA

For the purification of plasmid DNA phase trap A tubes (Peqlab) were used. 800 µl phenol/chlorophorm/isoamylalcohol (25:24:1) was added to 1 ml plasmid DNA in a phase trap tube. The sample was inverted and centrifuged for 10 min at 13000 rpm. The aqueous phase was transferred to a fresh phase trap tube. 800 µl chloroform was added and the sample was inverted again and centrifuged for 10 min at 13000 rpm. The aqueous phase was transferred to a new 2 ml Eppendorf tube and 700 µl Isopropanol and 100 µl Sodium acetate (3M, pH 5.2) was added. The sample was centrifuged for 10 min at 13000 rpm. After removal of the supernatant, the DNA pellet was washed once with 70 % Ethanol and centrifuged for another 10 min at 13000 rpm. The pellet was dried and the DNA was dissolved in 800 µl H_2O.

6.1.5 Preparation of genomic DNA from liver tissue samples

Liver tissue was digested in 500 µl proteinase K lysis buffer containing 0.5 mg/ml proteinase K for 3 hrs at 60°C and overnight at 56°C, shaking. Genomic DNA was extracted by phenol chloroform extraction adding 500 µl phenol/chlorophorm/isoamylalcohol (25:24:1), vortexing and centrifugation at 13.000 rpm, 4°C, 10 min. The upper phase was transferred to a new tube and the extraction step was repeated. The upper phase was transferred to a new tube and 500 µl chloroform were added. After spinning, DNA was pelleted by adding the upper phase to 500 µl isopropano, vortexing and incubation at -20°C for 1 h, followed by spinning at 13.000 rpm, 4°C, 45 min. Pellet was washed with 75% ethanol, dried, and resuspended in 100 µl TE buffer. Complete resuspension was accomplished by incubation for 2 h at 60°C. Genomic DNA was stored at 4°C until use.

6.1.6 Determination of DNA concentration

DNA concentrations were determined by using the NanoDrop ND-1000 spectrophotometer. The concentration was determined by measuring the absorption at 260 nm wavelength, contamination with salts or proteins was assessed by measuring the absorbance spectrum between 220 and 300 nm. A 1.5 µl DNA sample was used for each measurement

6.1.7 DNA sequencing

Plasmids were sequenced by the company LGC genomics (Berlin).

6.1.8 PCR

DNA from plasmids, cDNA or a genomic DNA was amplified by polymerase chain reactions using a thermocycler (PTC 200) and Phusion polymerase (Finnzymes). The primers used are listed in the material section.

A typical PCR rection is shown below:

	Amount	Final concentration
5X Phusion polymerase buffer	10 µL	1 X
10 mM dNTP mix	1 µL	0.2 mM
Forward primer (100 µM)	1µL	2 µM
Reverse primer (100 µM)	1 µL	2 µM
DNA Template		~ 5 ng
Phusion polymerase	1 µL	2 U
Double distilled water	ad 50 µL	

A typical PCR reaction was programmed as followed:

Step	Temperature	Time
1. Denaturation	95°C	30 sec
2. Denaturation	95°C	10 sec
3. Primer annealing	55 – 65°C	30 sec
4. Extension	72°C	60 sec
5. Go to 2		30x
6. Extension	72°C	5-10 min
7. Hold	4°C	∞

The annealing temperature was adjusted depending on the length and G/C content of the primers. The extension time was adjusted depending on the size of the desired PCR product.

6.1.9 Purification of PCR fragments

DNA from PCR reactions was purified using the QIAquick PCR purification kit provided by Qiagen following the manufacturer's instructions. DNA was eluted in 30 µl H2O. Alternatively, fragments were purified by gel extraction as described.

6.1.10 Agarose gel electrophoresis

DNA fragments were separated by agarose gel electrophoresis using 1-2% agarose and 1 µg/ml ethidium bromide in TBE. DNA samples were mixed with 1x Orange G loading dye and separated at 80-100 V. Gel pictures were taken under UV light (254 nm) with the Gel imager (Intas).

6.1.11 Gel extraction of DNA

DNA fragments were excised from agarose gels under a UV lamp using a scalpel and purified using the QIAquick Gel Extraction Kit, according to the manufacturer's instructions.

6.1.12 DNA restriction

DNA restriction was performed by using restriction enzymes (10-20 U per µg DNA) and corresponding buffer provided by New England Biolabs. Reactions were incubated at the required temperatures for 1-12 h.

6.1.13 DNA ligation

Ligation of insert and vector DNA was performed using a T4 DNA ligase (NEB or Fermentas). The molar ratio of insert to vector was adjusted to 3:1 applying the following formula:

ng insert = (100 ng vector x bp insert / bp vector) x 3

1 U enzyme was used in 1x ligase buffer for the ligation reactions according to the manufacturer's protocol. The reactions were performed in 20 µl total volume and incubated for 2-12 h at room temperature. After the ligation reaction, the enzyme was heat inactivated (10 min 65°C).

6.1.14 RNA isolation

RNA isolation from cell culture samples

Adherent cells were treated according to experimental needs. The medium was removed and the cell monolayer was washed once with sterile PBS. The buffer was aspirated and 800-1000 µL Qiazol™ Lysis reagent was added per well. The cells were released from the plate using a pipette and transferred into DNase/RNase-free reaction tubes, in which they were incubated for 5 min at room temperature. The samples were vortexed vigorously, until all cells were solubilised. The obtained cell lysates were stored at -80°C or immediately used for RNA isolation, as described below.

RNA isolation from tissue samples

20-50 mg of snap frozen tissue were transferred into a 2 ml RNase/DNase-free reaction tube containing a stainless steel bead. 1 ml of Qiazol™ Lysis (Qiagen) reagent was added directly. The samples were lysed using the TissueLyser™ for 30-60 s at a frequency of 30 Hz. Lysates were incubated at room temperature for 5 min to release nucleoprotein complexes before they were transferred, excluding the stainless steel bead, into a fresh 1.5 ml RNase/ DNase-free safe-lock tube. Subsequently, 200 µl of chloroform was added. Mixtures were vigorously inverted 15 times and then centrifuged for 30 min at 13,000 rpm. The upper aqueous solution, containing the RNA, was

carefully transferred into a fresh reaction tube containing 500 µl of iso-propanol and incubated at room temperature for 10 min, followed by a 10 min centrifugation step at 12,000 rpm. The supernatant was aspirated and the pellet was washed once with 1 ml of 75% ethanol. The solvent was discarded, and the remaining ethanol was removed using a pipette. The pellet was briefly air-dried and re-solubilised in water (30-50 µl). To increase solubilisation, the RNA solution was incubated at 55-60°C for 10 min. The samples were stored at -80

For microarray analysis, RNA isolated using Qiazol™ Lysis reagent was purified using the RNeasy Mini purification kit provided by Qiagen. RNA was transferred to into a fresh reaction tube containing 525 µl of 100 % ethanol. RNA was then purified following the manufacturer's instruction. The optional DNA digestion step was included. RNA was eluted in 30-50 µl H2O.

6.1.15 Determination of RNA concentration

RNA concentrations were determined by using the NanoDrop ND-1000 spectrophotometer. The concentration was determined by measuring the absorption at 260 nm. In parallel, the ratio 260 nm/280 nm was detected in order to determine protein impurities in the samples.

6.1.16 cDNA Synthesis

For synthesis of complementary DNA, 800-2000 ng of RNA was used. cDNA synthesis was performed using the cDNA synthesis kit (Fermentas) following the manufacturer's instructions. After completion, cDNA samples were diluted 10-fold in RNase free water and stored at -20°C.

6.1.17 Quantitative PCR

5 µl of the diluted cDNA samples obtained from reverse transcription, see above, were used for quantitative PCR. A master mix was prepared containing 10 µl *TaqMan* Gene Expression Assay Supermix, 4.5 µl DNase/RNase free water and 0.5 µl *TaqMan* probe per individual reaction. Water was used as a negative control and samples containing no reverse transcriptase served as controls for genomic DNA contamination. 20 µl PCR reactions were transferred per well onto a MicroAmp Optical 96 well reaction plate. All reactions were performed as technical duplicates. Quantitative PCR was performed using the StepOnePlus Real Time PCR System (Applied Biosystems).

6.1.18 Gene expression profiling

Gene expression profiling was performed with RNA extracted from livers with knockdown or overexpression of TSC22D1 and respective control livers, depending on the experiment in fasted, refed or random fed state.

Total RNA was extracted using TRIzol method according to manufacturer's protocol (Invitrogen Life Technologies). cDNA synthesis was performed using the SuperScript Choice System (Invitrogen Life Technologies, Invitrogen Corporation) according to manufacturer's protocol. Biotin-labeled cRNA was produced using ENZO BioArray HighYield RNA Transcript Labeling Kit. Standard protocol from Affymetrix (Santa Clara, CA) with 3.3 µL of cDNA was used for the in vitro transcription (IVT). Cleanup of the IVT product was done using CHROMA SPIN-100 columns (Clontech, USA). Spectrophotometric analysis was used for quantification of cRNA with acceptable A260/A280 ratio of 1.9 to 2.1. After that the cRNA was fragmented using Affymetrix defined protocol. Labeled and fragmented cRNA was hybridized to Affymetrix Mouse430_2 microarrays for 16 hrs at 45° C using Affymetrix defined protocol. Microarrays were washed using an Affymetrix fluidics station 450 and stained initially with streptavidinphycoerytherin. For each sample the signal was further enhanced by incubation with biotinylated goat anti-streptavidin followed by a second incubation with

streptavidinphycoerytherin and a second round of intensities were measured. Microarrays were scanned with Affymetrix scanner controlled by Affymetrix Microarray Suite software.

Microarry processing and statistical analysis

Gene expression profiling was performed using arrays of Mouse430_2 -type from Affymetrix (Santa Clara, CA, USA). cDNA and cRNA synthesis and hybridization to arrays were performed according to the recommendations of the manufacturer. A Custom CDF Version 14 with Entrez based gene definitions was used to annotate the arrays. The Raw fluorescence intensity values were normalized applying quantile normalization. Differential gene expression was analysed based on loglinear mixed model ANOVA (W. P. Hsieh, 2003; J. Roy, 2007), using a commercial software package SAS JMP7 Genomics, version 4, from SAS (SAS Institute, Cary, NC, USA). A false positive rate of a=0.05 with FDR correction was taken as the level of significance.

The overrepresentation analysis (ORA) is a microarray data analysis that uses predefined gene sets to identify a significant overrepresentation of genes in data sets (A. Subramanian *et al.*, 2005; T. Manoli *et al.*, 2006). Pathways belonging to various cell functions such as cell cycle or apoptosis were obtained from public external databases (KEGG, http://www.genome.jp/kegg/). A Fisher's exact test was performed to detect the significantly regulated pathways. Gene Set Enrichment Analysis (GSEA), was used to determine whether defined lists (or sets) of genes exhibit a statistically significant bias in their distribution within a ranked gene list (see http://www.broadinstitute.org/gsea/for details (A. Subramanian *et al.*, 2005). Pathways belonging to various cell functions such as cell cycle or apoptosis were obtained from public external databases (KEGG, http://www.genome.jp/kegg/).

6.2 Cell Biology

6.2.1 Cell culture conditions

All experiments with eukaryotic cells were performed under sterile conditions. Cells were cultivated at 37°C, 5% CO2 and 95% humidity. All media and additives were warmed to 37°C prior to use. Cells were cultivated in 6-well, 12-well, 24-well, 96-well, chamber slides 10 cm or 15 cm cell culture dishes. A list of the media used for cell culture experiments is shown in tabel 6.

Media used for cell culture and virus experiments

Name	Medium	Serum	Antibiotic	Further additives
HEK293	DMEM	10% FCS	1% P/S	
HEK293A	DMEM	10% FCS	1% P/S	1% NAA
HEK293T	DMEM	10% FCS	1% P/S	1% NAA
HEK293A virus titration	DMEM	2% FCS	1% P/S	1% NAA
Hepa1c1	DMEM	10% FCS	1% P/S	
Freeze medium	DMEM	20% FCS		10% DMSO

6.2.2 Thawing of cells

Eukaryotic cells were stored in liquid nitrogen tanks in 1 ml aliquots containing about $1*10^6$ cells in freeze medium. Following thawing at 37°C, cells were carefully mixed with 10ml pre-warmed culture medium and centrifuged for 3 min at 2000 rpm, to remove DMSO. The pellet was resuspended in 10 ml medium. Those 10 ml were distributed to two 15 cm tissue culture plates (3 ml and 7 ml) containing 25 ml culture medium.

6.2.3 Cultivation of Human Embryonic Kidney (HEK), HEK293A and HEK293T cells

HEK 293 cells were maintained and propagated in Dulbecco's Modified Eagle Medium with high glucose (DMEM), 10 % fetal calf serum (FCS) and 1 % penicillin/ streptomycin. HEK293A and HEK293T cells also required 1 % Non-Essential Amino Acids (NAA). Cells were passaged by the factor 1:10 – 1:20 two times per week.

For passaging, the cells were first washed in 1x PBS and then washed from the plate with 10 ml of culture medium. Cells were pelleted by centrifugation at 2000 rpm for 3 min and subsequently resuspended in 10 ml fresh medium and distributed to 15 cm plates. Cells were split by the factor 1:10 – 1:20 two times per week.

6.2.4 Cultivation of Hepa1c1 mouse hepatoma cells

Hepa1c1 cells were maintained and propagated in DMEM containing 10 % FCS, 1 % penicillin / streptomycin and 1% NAA. For passaging, the cells were first washed in 1x PBS and trypsinized, then the detached cells were resuspended in 10 ml of fresh medium. Cells were pelleted by centrifugation at 2000 rpm for 3 min and subsequently resuspended in 10 ml fresh medium. Cells were split by the factor 1:10 two times per week

6.2.5 Determination of cell number

To determine the cell count and viability for subsequent seeding of cells or for cell numer assays the Countess® automated Cell Counter (Life technologies) was used. According to the manufactures protocol, 10 µl of sample was mixed with 10 µl of trypan blue, and pipetted into Countess® chamber slide and inserted into the machine.

6.2.6 Transient transfection of HEK cells

Transfection with calcium phosphate

Cells were seeded 24 h prior to transfection and transfected at 60-80% confluency. DNA was mixed with 0.25 M CaCl2 and the same volume of 2x BBS, the amounts used are listed in table. After 15-20 min at RT, the mixture was added to the cells in fresh medium. Medium was changed 12 h after transfection. Experiments were performed 48-72 hrs after transfection.

Format	Cell number	DNA	CaCl2	2x BBS
6-well plate	2×10^5	100 ng -1 µg	100 µl	100 µl
12-well plate	1×10^5	100 ng -1 µg	80 µl	80 µl

Lipofectamin 2000

For higher transfection efficiency HEK293 cells were transfected with Lipofectamine 2000 transfection reagent (Invitrogen). 3 µl of the reagent were added to 250 µl of serum free Opti-MEM medium. The mixture was combined with DNA which was diluted in the same medium, and the mixture was incubated at RT for 20 min to allow complex formation. The DNA/Lipofectamine complexes were added dropwise to the cells in antibiotic-free medium. Medium change to the normal culture medium was performed the following day.

6.2.7 Transient transfection of Hepatoma cells

Hepa1c1 were transfected using polyethylenimine (PEI) reagent, a substance with low cytotoxicity For transfection with the PEI method cells were plated at a concentration of 1.4x105 cells/ml on a 12-well plate one day prior to transfection. The amount of PEI needed was calculated with respect to the amount of DNA that was used for the individual transfection. Generally, 8 µl of PEI were

applied per µg of DNA. Per well a maximum of 1.5 µg DNA could be used. Each condition was done at least in duplicates.

The following mixes were prepared as followed:

Mix1: DNA xµl; yµg

Water add ½ total of volume mix1

NaCl ½ total of volume mix1

Mix2: PEI (8µl/µg DNA)

Water add ½ total of volume mix2

NaCl ½ total of volume mix2

(total volume at least 16 µl x µg DNA)

After preparation Mix 2 was added to Mix1 and incubated for 10 min at RT. In the meantime, medium of the cells was changed. Afterwards, the mixture was added drop wise to the cells. After incubation of cells for 24h hours at 37°C the medium was changed. Cells were harvested 48 hours post-transfection.

6.2.8 Luciferase assay

The luciferase assay is one form of reporter gene assay. It was used to determine the promoter activities of the transfected reporter gene vectors. The enzyme Luciferase catalyzes the oxidation of its substrate luciferin in the presence of ATP and Mg2+. By formation of the product molecule oxyluciferin light is produced which can be measured. Under experimental conditions the amount of emitted light is proportional to the amount of luciferase in the cell lysate, which gives conclusions about the promoter activity.

Transfected cells were harvested 48 h post transfection. Medium was removed and the cells were washed with PBS. Then 150 µl harvest buffer was added and the cells were shaken on a vortex device at the lowest strength about 20-30 min to allow detachment of cells from dish. Following, the cell-lysate was transferred into an Eppendorf tube and centrifuged at 13.000 rpm for 3 min at 4°C to sediment cell debris. The supernatant was transferred into a new Eppendorf tube and stored at -20°C until subjected to the luciferase reporter knockdown assay.

For the assay 30 µl of cell lysate from transfected cells were transferred into one well of a black 96-well-plate. The lysate was diluted with 100 µl assay buffer and the plate was placed into a luminometer (Mithras 940 Luminescence). The automatic injection of 100µl luciferin buffer per well started the reaction. Light emission was measured at a wavelength of 569nm. Assay buffer was used as control. Triplicates were done and each value was normalized against β-galactosidase values.

For determination of transfection efficiency the reactions were co-transfected with the pCMV-β-galvector, which constitutively expresses β-galactosidase. The measured β-galactosidase activity directly correlates with the amount of DNA incorporated during transfection. As a substrate ortho-nitrophenyl-β- galactopyranosid (ONPG) was provided with the assay buffer, prior to use 13.5 µl beta-mercaptoethanol was added per 5 ml. For the assay 50 µl cell lysate and 50 µl buffer per well was added to a 96-well plate. The plate was incubated until the samples developed a clear yellow color. The absorption was measured at 405 nm, which is the maximum absorption of the ortho-nitrophenylat ion.

6.2.9   Infection of cells with adenovirus

1-2x 10^5 HEK293 or 2-4x10^4 Hepa1c1 cells were seeded on 6- or 12-well plates or 2.4x10^4 Hepa1c1 cells on chamber slides and infected with different amounts of adenovirus 6-12 h after plating. MOIs of 10-500 were used depending on the experiment. fibroblasts. The desired amounts of virus were diluted in DMEM culture medium and added to the cells. Cells were incubated 24-72 h until harvest.

6.2.10 Primary hepatocyte experiments

Primary mouse hepatocytes were isolated and cultured as described (U. Klingmueller *et al.*, 2006). Male 8-12 week old C57Bl/6J mice were anesthetized by intraperitoneal injection of 5 mg 10% ketamine hydrochloride / 100 mg body weight and 1 mg 2% xylazine hydrochloride / 100 mg body weight. After opening the abdominal cavity, the liver was perfused with HANKS I buffer via the portal vein for 5 min at 37°C and subsequently with HANKS II buffer for 5-7 min until disintegration of the liver structure could be observed. The liver capsule was removed and the cell suspension was filtered through a 100 µm mesh. Cells were washed and, subsequently, viability of cells was determined by trypan blue staining. 500,000 living cells / well were seeded on collagen I-coated 6- or 12-well plates. Cells were infected with recombinant adenoviruses (multiplicity of infection = 100) 24 hours after seeding and harvested for mRNA analysis 48 hours later.

6.3   Virus Biology

6.3.1   Cloning of adenoviruses

The BLOCKiT™ Adenoviral RNAi Expression System was used to generate adenoviruses expressing shRNA sequences against murine TSC22D1 as well non-specific shRNAs. Oligonucleotide sequences were chosen using Invitrogen's RNAi Designer tool. Forward and reverse oligonucleotides against the target gene sequence were annealed and cloned into the pENTR™/U6 vector according to the manufacturer's instructions. The resulting constructs were recombined with the pAd/BLOCK-iT™ DEST vector, which contains the adenovirus serotyp 5 DNA, but lacks the E1 and E3 genes that are required for viral replication. The viral vector containing the shRNA sequence was linearized by restriction digest using the enzyme PacI and transfected into HEK 239A cells using Lipofectamine reagent according to the manufacturer's instructions. HEK293A cells express the viral E1 and E3 genes necessary for viral outbreak, allowing the virus to expand in this cell line. Viral plaques appeared 6 to 10 days after transfection and cells started to detach from the cell culture dish. Once about 70% of cells were floating, they were harvested. The same procedure was used to generate a virus overexpressing TSC22D1. The TSC22D1 cDNA was cloned into a pENTR vector harbouring the CMV promoter and subsequently recombined with the pAd/BLOCK-iT™ DEST vector. An empty adenovirus was used as a negative control in over expression experiments.

6.3.2   Adenovirus harvest

HEK293A cells were harvested, when 70-90% were rounded up and had detached from the plate. Remaining adherent cells were washed of the plate with the medium from the plate. The medium was collected from twenty 15 cm cell culture plates per virus and centrifuged for at 2,000 rpm for 10 min. The supernatant was discarded and the cell pellet was resuspended in 3 ml PBS-TOSH buffer. The cell suspension was stroed at -80°C. The virus was released from the cell, by three freeze and thaw cycles. For that, the cell suspension was thawed at 37°C with vigorous vortexing and then

frozen in liquid nitrogen. After cell lysis the mixture was centrifuged at 3,000 rpm for 5 min, to remove cell debris. The supernatant containing the crude virus lysate was used for purification by cesium chloride gradient or for further infection of HEK293A cells.

6.3.3 Adenovirus purification using cesium chloride gradient

Cesium chloride (CsCl) gradient centrifugation is a type of density gradient centrifugation for the purification of viral particles. Confluent HEK293A on twenty 15 cm cell culture dishes were infected with crude virus lysate or purified adenovirus (1 µl per plate) and grown until 70-80% of the cells were rounded and lost adhesion, then they were harvested and lysed as described before. PBS-TOSH was added to the crude lysate to a final volume of 20 ml. All solutions were adjusted to pH 7.2. The first gradient was layered with 9 ml 4.4 M CsCl, 9 ml 2.2 M CsCl and 20 ml virus in PBS-TOSH. After ultracentrifugation (2 hrs, 4 °C, 24,000 rpm, SW28 rotor) a clear virus band was visible. The virus band was removed by piercing the tube with a 5 ml syringe. To the obtained virus (3-3.5ml) the same volume of saturated CsCl was added. The second gradient was layered with 6-7 ml virus in CsCl, 2 ml 4.4 M CsCl und 2 ml 2.2 M CsCl. Following the second ultracentrifugation (3 hrs, 4 °C, 35,000 rpm, SW40Ti rotor) the virus band was removed by syringe in the smallest possible volume and dialysed twice against PBS-glycerol, 1 hour and over night at 4°C. 10% glycerol was added to the purified virus and aliquots were stored at -80°C.

6.3.4 Virus Titration using the Tissue Culture Infectious Dose 50 (TCID$_{50}$) method

The Tissue Culture Infectious Dose 50 (TCID50) assay was used to titrate adenovirus. For that purpose, 104 HEK293A cells were seeded in 100 µl virus titration medium in each well of a 96 well plate and infected with decreasing amounts of virus after 2-4 hrs of adhesion. Serial dilutions of the virus from 10-7 to 10-14 were prepared in titration medium and added to the cells. Double measurements were performed for each virus. 10-12 days after infection and incubation at 37°C the plaques were counted using a microscope and the titer was calculated by the following formula:

T = 10 1+(s-0.5) x 10 pfu / ml

(s = sum of positive wells starting from the 10-1 dilution; 10 positive wells per dilution = 1)

6.3.5 Cloning of AAV

The BLOCKiT™ Pol II miR RNAi Expression System was used to generate adeno-associated viruses expressing miRNA sequences against murine TSC22D1 as well non-specific miRNAs. Oligonucleotide sequences were chosen using Invitrogen's RNAi Designer tool. Forward and reverse oligonucleotides against the target gene sequence were annealed and cloned into the pcDNA6.2-GW/EmGFP-miR vector according to the manufacturer's instructions. Following, they were transferred into the previously described double stranded pdsAAV-LP1-EGFPmut AAV vector (P. Kulozik *et al.*, 2011) using the restriction enzymes BglII and SalI. The plasmids encoding the miRNA constructs were contransfected into HEK293T cells with the pDGΔVP helper plasmid (D. Grimm *et al.*, 1998) and a mutated p5E18-VD2/8 expression vector (G.P. Gao *et al.*, 2002) encoding AAV2 rep and a mutated AAV8 cap protein (aa 589-592: QNTA to GNRQ).

6.3.6 AAV production

For virus production, HEK293T cells from six 80-90% confluent 15 cm plates were suspended in 1100 ml medium. 1,000 ml of the cell suspension was transferred to a 10x cell-stack chamber and 100 ml were transferred to a 1x-cell stack chamber (control chamber for analysis under the microscope). 24 h after plating, the cells were approximately 70-80% confluent and were

transfected with the plasmids encoding the viral genes using the PEI method in the amounts stated below.

Plasmid	Amount
AAV-miRNA expression vector	436 µg
p5E18 VD2/8 helper plasmid	550 µg
pDGΔVP helper plasmid	1579 µg

Once the cell monolayer was approximately 90% confluent, cells were washed with PBS, before they were released from the plate using 10 ml (1x cell stack) or 100 ml (10x cell stack) trypsin-EDTA for 5 min at 37°C. Fresh medium was added (40 ml or 350 ml respectively) and the cells were transferred to a 50 ml falcon tube, or a 500 ml conical tube. The chambers were washed with PBS and used for a second round of transfection. Cells were centrifuged at 2,000 rpm for 10 min. The supernatant was removed and the pellets were resuspended in 8 ml lysis-buffer containing 150 mM NaCl and 50 mM Tris-HCL, pH 8.5. The lysates were transferred into 15 ml falcons, vortexed, snap-frozen in liquid nitrogen and stored at -80°C.

6.3.7 AAV purification

AAV lysates were thawed at 37°C under vigorous vortexing and then centrifuged at 3,500 g for 10 min. The supernatant was collected and the pellets were resuspended in 4 ml lysis buffer and snap-frozen. The freeze-thaw cycle was repeated three times. The final pellet was solubilised using a sonicator in a water bath at 48 W for 1 min. The pooled suspension was then digested with benzonase (50 U/ml) for 30 min at 37°C. This solution was then centrifuged at 4°C and 3,500 g for 10 min. The virus was stored at -80°C until further use.

1st Iodixanol gradient

Purifying virus by iodixanol gradient leads to a separation of packed and unpacked AAV capsids, as they migrate differentially upon ultracentrifugation. The first gradient, ranging from 15% iodixanol to 40% iodixanol, was prepared on top of the viral solution in a Beckman Quickseal tube using a Pasteur pipette, as described below.

Layer (from top to bottom)	Component
15 %-iodixanol dilution (7 ml)	1.75 ml OptiPrep
	5.25 ml PBS-buffer 2
25 %- iodixanol dilution (5 ml)	2.08 ml OptiPrep
	2.29 ml PBS-buffer 1
	12.5 µl phenol red (0.5 %)
40 %- iodixanol dilution (4 ml)	2.67 ml OptiPrep
	1.33 ml PBS-buffer 1
60 %- iodixanol dilution (4 ml)	4 ml OptiPrep
	10 µl phenol red (0.5 %)
Virus (18 ml)	

PBS-buffer 1:	1x PBS	PBS-buffer 2:	1x PBS
	1 mM MgCl2		1 mM MgCl2
	2.5 mM KCL		2.5 mM KCL
			1 M NaCl

About 1 ml of space was left above the gradient. Tubes were sealed and centrifuged in a 50.2 Ti rotor at 50,000 g and 10°C for 2 hours. Four gradients were run for each virus (two rounds; harvest and wash). After centrifugation, the 40% iodixanol layer (~3.5 ml) was carefully collected by inserting a 5 ml syringe from underneath. The viral suspension was pooled and stored at -80°C.

2nd Iodixanol gradient
The viral suspension resulting from the first gradient was filled up to 25 ml with lysis buffer. The second gradient was prepared by underlayering, as described below.

Layer (from top to bottom)	Component
25 %- iodixanol dilution (5 ml)	2.08 ml OptiPrep
	2.29 ml PBS-buffer 1
	12.5 µl phenol red (0.5 %)
40 %- iodixanol dilution (4 ml)	2.67 ml OptiPrep
	1.33 ml PBS-buffer 1
60 %- iodixanol dilution (4 ml)	4 ml OptiPrep
	10 µl phenol red (0.5 %)
Virus (25 ml)	

PBS-buffer 1:	1x PBS	**PBS-buffer 2:**	1x PBS
	1 mM MgCl2		1 mM MgCl2
	2.5 mM KCL		2.5 mM KCL
			1 M NaCl

The gradient was then further processed as described for the first gradient.

Virus concentration
The viral solution was concentrated using a VivaSpin concentrator. The solution was consecutively centrifuged at 3,000 rpm and 10°C for 3-6 min until a final volume of about 1 ml.

6.3.8 AAV titration

Viral DNA was isolated by mixing 5 µl of virus suspension with 5 µl H2O and 10 µl 2M NaOH. The mixture was incubated at 56°C for 30 min and the reaction was then neutralized by adding 10 µl 2M HCL. After adding 970 µl H2O, the titer was determined by qPCR using an EGFP standard curve.

6.4 Biochemistry

6.4.1 Preparation of nuclear extracts from liver tissue samples

For extraction of nuclear fractions about 50 mg frozen liver samples was grinded in Dounce homogeniser for 15 strokes with 1 ml of lysis buffer (50 mM Tris pH 7.2, 250 mM Sucrose, 10 mM KCL, 1 mM EDTA, 10 mM NaF, 2 mM Na_3VO_4, 1 mM DTT, 1 x Protease Inhibitor Cocktail (Sigma, Heidelberg, Germany), 1 x Phosphatase Inhibitor II (Sigma, Heidelberg, Germany). Homogenates were rotated end over end at 4°C for 30 min after which they were centrifuged at 4°C for 30 min at 1000g. The pellet was dissolved in 500µl lysis buffer (50 mM Tris pH 7.2, 25% glycerol, 420 mM

NaCl, 1.5 mM MagCl$_2$, 10 mM NaF, 1 mM DTT, 1 x Protease Inhibitor Cocktail, 1 x Phosphatase Inhibitor II, 0.1 % SDS, 1 % NP-40. Pellets were dissolved by grinding with a pestle. Homogenates were rotated end over end at 4°C for 30 after which they were centrifuged at 4°C for 30 min at 9000g.

6.4.2 Determination of Protein Concentration

Protein concentrations were determined using the BCA kit (Pierce) following the manufacturer's instructions. If SDS concentration of the samples was higher than 0.1 %, protein concentration had to be determined using the 2D-Quant kit (Amersham Biosciences) following the manufacturer's instructions. All measurements were performed in duplicates within the linear range of the BSA standard curves (0.1-2 mg/ml).

6.4.3 SDS Polyacrylamide Gel Electrophoresis (SDS-PAGE) and Immunoblotting

Protein samples in SDS sample buffer were loaded onto 6-15 % SDS-polyacrylamide gels and blotted onto nitrocellulose membranes or PVDF membranes using a wet blot system. PVDF membranes were activated with methanol prior to use. Blotting was performed at 70 V for 60 minutes or at 80V for 70min in transfer buffer. Membranes were subsequently blocked by incubation in 5% milk or 5% BSA dissolved in PBS-T or TBS-T for 1 hour. Specific primary antibodies diluted in milk or BSA, according to the manufacturer's recommendations, were incubated with the membranes overnight at 4°C. The membranes were washed with PBS-T or TBS-T the next day and incubated with the secondary antibody conjugated to horse radish peroxidase (HRP) at a dilution of 1:5,000 for 1 hour. To detect specific bands the enhanced chemiluminescence system (ECL) Western Blotting Detection Reagent was applied. The chemiluminescent signal produced by the blots was detected with the ChemiDoc detector (BioRad). Exposure times differed based on the quality of specific antibodies and protein concentrations.

6.4.4 Co-Immunoprecipitation

Hepa 1c1 cells were cotransfected with a HA-TBL1, Myc-TBLR1 or an empty Flag vector in combination with a Flag-TSC22D4 vector. Subsequently, cells were lysed with lysis buffer containing protease and phosphatase inhibitors and centrifuged at 13,000 rpm, 4°C, 15 min. The supernatant was incubated with anti-FLAG M2 Agarose for 2 hours at 4°C and washed vigorously to remove unspecific binding. Precipitated proteins were eluted using excess Flag peptide. The immunoprecipitates were subsequently analyzed by Western blot as described.

6.4.5 GST-pulldown

GST-pulldown experiments were performed to map the interaction of TSC22D1 with TBL1. TBL1 protein was purified from bacteria using a GST-tag and TSC22D1 protein was in vitro transcribed and translated in the presence of radiolabeled methionine. Full length and truncated GST fusion proteins were produced in BL21 cells and affinity purified using glutathione sepharose. In vitro transcription/translation was performed using the TNT T7/T3 quick coupled transcription/translation system according to the manufacturer's instructions. GST and in vitro translated full length and truncated proteins were incubated at 4°C overnight. After extensive washing, GST-precipitated proteins were separated by SDS-PAGE and detected by autoradiography.

6.4.6   Isolation of Hepatic Triglycerides

Lipids were extracted from frozen and pulverized liver tissue using chloroform/methanol (2:1 v/v). About 100 mg (the exact weight was noted) of frozen, pulverized liver were transferred into a 2 ml tube containing 1.5 ml chloroform/methanol and a steel bead. The tissue was homogenized using a tissue lyzer for three times 30 s at a frequency of 30 Hz. For the lipid extraction, samples were incubated on a rotating wheel at room temperature for 20 min. Samples were centrifuged at 13,000 rpm for 30 min at RT and 1m of the supernatants were transferred to fresh tubes. The organic layer was mixed 200μl with 0.9% sodium chloride and the aqueous solution was carefully discarded. The solution was centrifuged for 5 min at 2000 rpm. 750 μl of the lower organic layer were transferred to a fresh tube and stored at -80°C. For lipid resuspension 40 μl of triton-X 100/chloroform (1:1 v/v) was pipetted into fresh tubes and 200μl of the organic lipid sample was added. The reagents were mixed and the solvent was evaporated overnight using a speed vac. The residue containing the hydrophobic contents of the liver was resuspended in 2000 μl water and stored at -20°C until further use.

6.4.7   Determination of Free Fatty Acid Levels

Free Fatty Acids were determined in serum samples using a colorimetric assay from WAKO (NEFA kit) following the manufacturer's instructions. 4 μl of serum samples were measured in duplicates. A standard curve was determined using a dilution series of oleic acid. OD-values were determined at 540 nm.

6.4.8   Determination of Glycerol Levels

Glycerol content of serum was measured using a calorimetric assay. The Free Glycerol component of the serum TG determination kit from Sigma was used for this assay. 4 μl of serum or 20 μl of supernatants were transferred to a 96well plate, 100 μl Free Glycerol Reagent were added and glycerol levels were measured at 540 nm against a glycerol standard.

6.4.9   Determination of Triglyceride Levels

TG levels were determined by separating TGs into one glycerol and three fatty acid molecules and measuring the glycerol using a colorimetric assay. The serum TG determination kit from Sigma was used for this assay. 4 μl of isolated hepatic TG or 4 μl of serum were transferred to a 96well plate. In order to determine a blank value, 100 μl Free Glycerol Reagent were added to each well and the plate was incubated at 37°C for 5 min. Free glycerol levels were measured at 540 nm. In a second reaction (assay), 100 μl TG Reagent were added. This mixture contains the enzyme lipase, which catalyses the release of fatty acids from TGs. Plates were incubated at 37°C for 5 min and measured at 540 nm. TG content (TG-bound glycerol) was determined by subtracting the free glycerol (blank) from the second measurement of total glycerol (assay).

6.4.10 Determination of Cholesterol Levels

Liver or serum cholesterol concentrations were determined using a total cholesterol determination kit (Randox Laboratories) following the manufacturer's instructions. 4 μl of each sample were mixed with 100μl assay reagent and incubated at 37°C for 5 min. The optical density was measured at 492 nm and the sample concentration was determined using a standard curve resulting from a serial dilution of cholesterol (200 mg/dl; provided with the kit).

6.4.11 Serum TGF-beta 1 measurement

Serum TGF-beta 1 level was determined using the Mouse Quantikine ELISA Kit provided by R&D Systems. Activated serum samples were diluted 1:100 the rest of the assay was performed according to manufacturer's instruction. The TGF-beta 1 level was measured at 450 nm and the sample concentration was determined using a standard curve.

6.4.12 Determination of Blood Glucose Levels

Blood glucose levels were determined using a drop of blood obtained from the tail vein and an automatic glucose monitor (One Touch, Lifescan).

6.4.13 Isolation of hepatic glycogen

Liver glycogen was extracted from snap frozen and pulverized liver tissue. About 45-55 mg of tissue (exact values were noted down) were added to a 2 ml Eppendorf tube containing a stainless steel bead and 500 µl 30% Potassium Hydroxide. The tissue was homogenized using a tissue lyzer for three times 30 s at a frequency of 30 Hz. The solution was transferred into new tubes and incubated at 95°C for 1 h. For precipitation of the glycogen 1.4 ml of 95% ethanol was added and the tubes were placed at -20°C for at least 20 min. Following, the samples were centrifuged for 20 min at 3000 g and the remaining glycogen pellet was washed with 1ml 95% ethanol. The glycogen pellets were dissolved in 250 µl H_2O for 30 min at 37°C.

For measuring liver glycogen content the dissolved glycogen was digested with amyloglucosidase. For that purpose 50 µl of the glycogen solution were mixed with of 250 µl of a 10-20 Units/ml amyloglucosidase solution (amyloglucosidase in sodium acetate). The mix was incubated at 37°C overnight with shaking. The sample was neutralized by adding 6 µl of Potassium Hydroxide.

Liver glycogen was measure using the Glucose (HK) assay kit provided by Sigma-Aldrich. The assay was performed with 20 µl of glycogen digest according to the manufacturer's instructions. For fed mice digests were diluted 1:4 prior to assaying. The glucose liver sample concentration was determined using a glucose standard curve.

6.4.14 Fast protein liquid chromatography (FPLC)

FPLC was used to separate serum proteins according to their size. The FPLC set-up consisted of a Superose 6 10/300 GL column (GE Healthcare), a fraction collector and an ÄKTA FPLC System (Amersham). During separation, a liquid phase, containing the mixture to be fractionated was pumped over a stationary resin of cross-linked agarose beads with varying surface structure. Certain proteins subsequently eluted at specific times in specific fractions. A pool of 200 µl serum plus 100 µl PBS, from 4 animals, was injected into the machine, diluted in 25 ml PBS and fractionated into 500 µl fractions. 40 µl of each fraction were subsequently used for cholesterol and TG analysis using the TG Liquicolor (Human GmbH, Germany) and Cholesterol determination kit (Randox, UK) respectively. Distinct VLDL and HDL peaks could be observed in specific fractions.

6.5 Histochemistry

6.5.1 Hemotoxylin and Oil red O

During preparation of liver tissue, slices were embedded Tissue Tek OCT compound and shock frozen in liquid nitrogen. 5 µm cryosections were cut and fixed in Baker's formol. Neutral lipids and TGs were stained with oil red O and nuclei were counterstained with hematoxylin.

6.6 Animal experiments

6.6.1 General procedures

The animals were housed according to international standard conditions with a 12 hrs dark, 12 hrs light cycle and regular unrestricted diet if not stated otherwise. Animal handling and experimentation was performed in accordance with NIH guidelines and approved by local authorities (Regierungspräsidium Karlsruhe). Blood was taken after cervical dislocation. Organs including liver, kidney, fat pads, and gastrocnemius muscles were collected, weighed, snap-frozen in liquid nitrogen and used for further analysis

6.6.2 Obesity models

8-12 week old ob/ob or db/db or mice were obtained from Charles River Laboratories (Brussels, BEL) and maintained on a 12 hrs light-dark cycle with regular unrestricted diet. In high-fat diet experiments, C57Bl6 mice were fed a high-fat diet (45% or 60% energy from fat, New Brunswick, USA) or low-fat control diet (10% energy from fat, New Brunswick, USA) for a period of 12-20 weeks.

6.6.3 Colon26 murine cachexia model

For tumor induction in cachexia models, 1.5x 106 Colon 26 cells in PBS were injected subcutaneously into 10 week old Balb/c mice (Charles River Laboratories, Brussels). Control mice were injected with PBS. Mice were sacrificed approximately 2 weeks after injection.

6.6.4 Methionine/choline deficiency studies

For a methionine/choline deficiency study, mice at the age of 10 weeks were fed the MCD diet for 4 weeks (Research diets) before sacrifice.

6.6.5 Fasting and Refeeding

For an extensive fasting and refeeding study, male C57Bl6 mice at the age of 13 weeks were used. Different groups of mice were fasted for 8 hrs, 24 hrs and 48 hrs, respectively, and subsequently refed for 1 hr, 6 hrs or 24 hrs before the sacrifice.

6.6.6 Adenovirus injections

For studies with knockdown of TSC22D1 by shRNA, 1-2 x10^9 plaque-forming units per recombinant adenovirus were administered via tail vein injection into male C57Bl6 at the age of 9-11 weeks. For studies with over expression of TSC22D1, 1x10^9 plaque-forming units per recombinant virus were administered via tail vein injection into male C57Bl6 at the age of 10 weeks .In each experiment, 5 animals received identical treatments. Fasting was standardly conducted for 24 h and refeeding for 6 h.

6.6.7 AAV injections

For studies with knockdown of TSC22D1 by miRNA, 5 x10^9 virus paricles per recombinant AAV were administered via tail vein injection into male C57Bl6 at the age of 9-11 weeks. In each experiment, 5 animals received identical treatments. Fasting was standardly conducted for 24 h and refeeding for 6 h.

6.6.8   TGF-beta injections

For TGFbeta experiments, C57Bl/6 mice were injected intravenously with either 150 μl PBS or 5 μg human recombinant TGFbeta1 in 150 μl PBS and organs were taken 2, 8 or 24 h after injection.

6.6.9   Blood serum

Blood serum was obtained by incubation of blood samples at room temperature for 30 min and subsequent centrifugation for 1 hr at 3,000 rpm, 4°C. The serum (upper phase) was transferred to a new tube and stored at -80°C.

6.6.10 VLDL clearance

Blood was drawn from a fasted individual and human VLDL was isolated by ultracentrifugation as described (125). 3.5 ml serum were put in a polyallomer tube (SW40Ti) and mixed with 1.39 g KBr, over-layered with 3x2.8 ml of a NaCl/KBr solution (D= 1.063, 1.019 and 1.006 g/ml) and run for 18 hours at 40,000 rpm. 20 μg of human VLDL were injected into each animal and serum samples were taken at 2, 10, 30, 60 and 120 min. Human ApoB-100 levels were measured using a human-specific ApoB ELISA. For the ELISA, a primary coating antibody generated against human ApoB-100 (mAb47, kindly supplied by J. Witztum, University of San Diego, USA), at a concentration of 2 μg/well and a secondary biotinylated polyclonal antibody raised in goat against human ApoB at a concentration of 4 μg/well in 1.5% BSA/TBS/0.1% tween were used. To prevent non-specific binding, plates were blocked with 1.5% BSA/TBS/0.1% tween. Samples were diluted 25-fold. Absorbance was read 30 min after addition of TMB and termination of the reaction with 2 M H_2SO_4 at 450 nm (P.H. Groot, 1991).

6.6.11 VLDL release

VLDL production was determined after tyloxapol injection as described (S. Mandard, 2006). Tyloxapol is a Lipoprotein Lipase (LPL) inhibitor, meaning that, after administration, any secreted VLDL particles could not be cleared from the blood stream. One day before the experiment, tyloxapol was dissolved in saline to obtain a 20% w/v solution. Six C57BL/6J mice per group were fasted overnight for 16 hours. On the following day, before administration, 40μl of blood was drawn from each mouse by cutting the tip of the tail. The tyloxapol (20%) volume (in μl) applied per mouse was approx. 3 times that of the weight of the mouse in grams; i.e. a 25 g mouse received 75 μL of the 20% solution. Specified amounts were administered via the tail vein and 40 μL blood samples were taken every 50 min for 2.5 hours. The mice were sacrificed after 300 min. The serum TG values were determined and plotted against the time.

6.7   Human subjects

Normal liver tissue samples were obtained by open liver biopsy from 30 patients, 15 with and 15 without cachexia, who underwent surgery for pancreatic ductal adenocarcinoma as described previously (M. E. Martignoni, 2009). The study was approved by the local ethics committee of the University of Heidelberg, Germany. All patients gave preoperative written informed consent for the use of their samples.

6.8 Statistical Analysis

For each experiment means ± SEM were determined. Statistical analyses were performed using student's t-test in one-factorial designs. Correlation was determined using Pearson's correlation coefficient; F-test was applied to determine significance. For multifactorial study designs, Two-way ANOVA and TWO-way ANOVA RM were used when appropriate. Holm-Sidak post hoc was applied when significant differences were found with an overall significance level = 0.05.

7 Material

7.1 Solutions and Buffers

All buffers were diluted in H20, unless otherwise stated.

Name	Component
2xBBS	280 mM NaCl 50 mM BES 1.5 mM Na2HPO4 pH 6.95
2x SDS sample buffer	120 mM Tris /HCl pH 6.8 4% SDS 20% glycerol 200 mM DTT 0.01% bromphenol blue
5x SDS sample buffer	250 mM Tris/HCl pH 6.8 0.5 M DTT 10 % SDS 50 % glycerol 0.01% bromphenol blue
Block buffer	1x PBS 0.1% Tween 20 5% milk powder
CoIP Lysis buffer	20 mM HEPES/KOH pH 7.4 125 mM NaCl 0.5 mM EDTA 0.1% NP-40 10% Glycerol
Coomassie stain	4 parts Coomassie Colloidal Blue 1 part Methanol
Destain for Coomassie stained gels	25% Isopropanol 10% Acetic acid
Gly-Gly buffer	25 mM Gly-Gly pH 7.8 15 mM MgSO4 4 mM EGTA
HANKS I buffer	8 g NaCl 0.4 g KCl 3.57 g Hepes 0.06 g KH2PO4

	0.06 g Na2HPO4 x 2 H2O
	add 1L Distilled H2O
	2.5 mM EGTA
	0.1% Glucose
	pH 7.4
HANKS II buffer	8 g NaCl
	0.4 g KCl
	3.57 g Hepes
	0.06 g KH2PO4
	0.06 g Na2HPO4 x 2 H2O
	add 1L Distilled H2O
	3 mg/ml Collagenase CLSII 5 mM CaCl2
	0.1% Glucose
	pH 7.4
LB medium	10 g/l Trypton
	5 g/l Yeast extract
	10 g/l NaCl
	pH 7.0
Oil Red O stock solution	0.7 g Oil Red O
	200 ml Isopropanol
	Stirred overnight, sterile filtrated
Luciferase Harvest Buffer	100% Gly-Gly buffer;
	1% Triton X-100
	1 mM DTT
Luciferase Assay Buffer	20 mM K3PO4 pH 7.8
	80% (v/v) Gly-Gly buffer
	1.6 mM DTT
	2mM ATP
Luciferase Luciferin Buffer	1 mM Luciferin
	10 mM DTT in Gly-Gly buffer
Oil Red O working solution	6 parts Oil Red O stock solution
	4 parts H2O
ONPG buffer	0.1 M NaP pH 7.5
	1 mM MgCl2
	10 mM KCl
	1 mg/ml ONPG
	100 mM ß-mercaptoethanol (added freshly)
Orange G loading dye (6x)	10 mM EDTA
	70% Glycerol
	A pinch Orange G
PBS (10x)	1.4 M NaCl
	27 mM KCl
	100 mM Na2HPO4
	8 mM KH2PO4
	pH 6.8

PBS-T	1x PBS with 0.1 % Tween-20
PBS-TOSH	30.8 mM NaCl 120.7 mM KCl 8.1 mM Na2HPO4 1.46 mM KH2PO4 10 mM MgCl2 pH 7.2, sterile filtrated
Proteinase K lysis buffer	10 mM Tris pH 8.0 100 mM NaCl 15 mM EDTA 1 % SDS
SDS gel fixation buffer	25% Isopropanol 10% Acetic acid
SDS running buffer (10x)	0.25 M Tris 1.92 M Glycin 1% SDS
Supplement buffer	1.5 M NaCl 10 % NP-40
TBE buffer (10x)	100 mM Tris 1 mM EDTA 90 mM Boric acid pH 8.0
TE buffer (10x)	1 mM EDTA 10 mM Tris HCl pH 8.0
Transfer buffer	25 mM Tris 192 mM Glycin 20% Methanol 0.01% SDS

7.2 Oligonucleotides

All oligonucleotides possessed a G/C content between 40% and 60% and were approximately 20-30bp in length.

Restriction sites for specific enzymes were added to the cloning primers in 5'→3' orientation, allowing directed insertion into a specific target vector. Six thymidine residues were added to the 5' ends of the restriction sites in order to facilitate cleavage. The primers were designed to hybridize at temperatures of approximately 60°C.

Oligonucleotide	Sequence 5'→3'
TSC22D1 luc for 3	TTTTGCGGCCGCCACTCGAGCCAGCACCACCG
TSC22D1 luc rev 3	TTTTAAGCTTTGGGGGACATGCGCAGAACG
miTSC22D1 4.2	CTCACACGCTGTTCTCGCTTT
Control miRNA	AAATGTACTGCGCGTGGAGAC
shTSC22D1 395	GCCATTTGATGTATGCGGTGA

Control shRNA   GATCTGATCGACACTGTAATG

7.3   Antibodies

Primary Antibody	Dilution	Isotype	Distributor
Actin	1:1000	Mouse	Santa Cruz #A5441
ApoB	1:1000	Rabbit	Santa Cruz, Sc-11795
Akt	1:1000	Rabbit	Cell Signaling, 9272
phophoAkt	1:1000	Rabbit	Cell Signaling, 9271
Flag M2	1:1000	Mouse	Sigma, #A8592
Foxo	1:1000	Rabbit	Cell Signaling, 9454
phosphoFoxo	1:1000	Rabbit	Cell Signaling, 9465
VCP	1:10000	Mouse	Abcam #ab11433

TSC22D1 antibody was generated from Eurogentec in rabbit and was used as 1:200 dilution from serum.

Secondary Antibody	Dilution	Isotype	Distributor
Anti-mouse IgG-HRP	1:5000	Goat	BioRad, Munich
Anti-rabbit, IgG-HRP	1:5000	Goat	BioRad, Munich
Anti-goat, IgG-HRP	1:10000	Donkey	Sigma, #sc2020

7.4   Kits

Kit	Distributor
BLOCK-iT^{TM} U6 RNAi Entry Vector Kit	Invitrogen, Karlsruhe
BLOCK-iT^{TM} Adenoviral RNAi Expression System	Invitrogen, Karlsruhe
BLOCK-iT^{TM} Pol II miR RNAi Expression Vector Kit	Invitrogen, Karlsruhe
Cholesterol determination Kit	Randox, Crumlin, UK
Enhanced Chemiluminescence (ECL) Kit	Amersham Biosciences, Freiburg
First Strand cDNA Synthesis Kit	Fermentas, St. Leon-Rot
Ketone bodies Determination Kit	Wako, Neuss
NEFA – C Determination Kit	Wako, Neuss
Phusion Polymerase Kit	Finnzymes, Vantaa
Platinum® Quantitative PCR Supermix	Invitrogen, Karlsruhe
PureLink HiPure Plasmid FP Maxiprep Kit	Invitrogen, Karlsruhe
Qiaprep Plasmid Miniprep Kit	Qiagen, Hilden
Qiaquick Gel Extraction Kit	Qiagen, Hilden
QIAGEN Plasmid Mega Kit	Qiagen, Hilden
Qiaquick PCR Purification Kit	Qiagen, Hilden
RNeasy RNA Extraction Kit	Qiagen, Hilden

TGF-beta 1 Quantikine ELISA Kit	R&D Systems
TN T T7/T3 Coupled Reticulocyte Lysate System	Promega, Mannheim
Triglycerides Determination Kit	Sigma-Aldich Chemicals GmbH, Steinheim
Triglycerides Liquicolour	Human GmbH Wiesbaden

7.5 Software

Sofware	Distributor
AxioVS40x64 V4.8.3.0	Carl Zeiss, Göttingen
BLAST	http://www.ncbi.nlm.nih.gov
Cell Profiler	http://www.cellprofiler.org
Endnote	Thomson, Carlsbad, USA
Geneious	Auckland, New Zealand
GraphPad	GraphPad Software Inc., La Jolla, USA
Illustrator	Adobe, San Jose, USA
ImageJ	Wayne Rasband, NIH, USA
Image Lab	Bio-Rad Laboratories
Microsoft Office	Microsoft, Unterschleißheim
Photoshop	Adobe, San Jose, USA
Pubmed	http://www.pubmedcentral.nih.gov
Quantity One	Bio-Rad, Munich
StepOne Plus	Applied Biosystems, Darmstadt System Software

7.6 Consumables

Consumable	Distributor
1-stack cell culture dishes	Sigma, Munich
10-stack cell culture dishes	Sigma, Munich
12-well tissue culture dishes	Corning Inc., NY, USA
6 well tissue culture dishes	Falcon, Gräfeling-Lochham
96 well MicroAmp plates	Applied Biosystems
96-well *Microtiter®* luminescense plates	Nunc, Wiesbaden
Amersham Hybond^{TM}-P	GE Healthcare, Freiburg
Cell scrapers (*Costar*)	Corning Inc., NY, USA
Centrifuge tubes (35 ml)	Beckmann, Munich
Cover slips	Carl Roth GmbH, Karlsruhe
Cryo tubes (2 ml)	Cryo tubes (2 ml)
Dialysis tubing	Carl Roth GmbH, Karlsruhe
Disposable scalpels	Feather, Cuome, JP
DNase / RNase free water	Invitrogen, Karlsruhe
Filters (0.22 µm)	Millipore, Eschborn

Filters (0.45 µm	Millipore, Eschborn
Gel staining boxes (Mini)	Carl Roth GmbH, Karlsruhe
Gloves (*Gentle Skin*)	Meditrade, Kiefersfelden
Gloves (*Safe Skin Purple Nitrile*)	Kimberly Clark, BE
Hyperfilm ECL	Amersham, Freiburg
Immobilized streptavidin beads	Pierce Biotech., Rockford, USA
Micro test tubes (1.5 ml, 2 ml)	Steinbrenner, Wiesenbach
Mouth protection	Meditrade, Kiefersfelden
Nitrocellulose membrane	Schleicher and Schüll, Dassel
Parafilm	Pechinery Inc., Wisconsin, USA
Pasteur pipettes	Brand, Wertheim
PCR tubes (200 µl)	Eppendorf, Hamburg
Petri dishes	Greiner, Kremsmünster, AU
Pipette tips (0.1 – 1000 µl)	Starlab, Helsinki, FI
Pipette tips (0.1 – 1000 µl) (Tip One Filter Tips)	Starlab, Helsinki, FI
Polyallomer tubes (25mm x 89 mm)	Beckmann, Munich
Polyallomer tubes	Beckmann, Munich
Rabbit IgG-agarose	Sigma, Munich
Safelock micro test tubes (1.5 ml and 2 ml)	Eppendorf, Hamburg
Saran cling film	Dow Chem. Co., Schwalbenbach
Serological pipettes (5 ml, 10 ml, 25 ml, 50 ml)	BD Biosciences, San Jose, USA
Syringes (10 ml Luer Lock)	Terumo, Leuven
Syringes (50 ml)	Terumo, Leuven
Test tubes (15 ml and 50 ml)	Falcon, Gräfeling-Lochham
Tissue culture dishes (10 cm and 15 cm)	Falcon, Gräfeling-Lochham
Vivaspin Concentrator	Vivaspin Concentrator
Whatman paper	Whatman Int., UK

7.7 Chemicals and Reagents

Chemical/Reagent	Distributor
Acetic acid (99%)	Sigma, Munich
Acetone	Sigma, Munich
Acrylamide-bisacrylamide Solution (37.5 : 1)	Carl Roth GmbH, Karlsruhe
Adenosine triphosphate (ATP)	Sigma, Munich
Agarose	Sigma, Munich
Ammonium persulfate (APS)	Carl Roth GmbH, Karlsruhe
Antibiotics	Sigma, Munich
Bovine serum albumin (BSA)	Sigma, Munich
Bromophenol blue	Sigma, Munich
Chloroform	DKFZ
Collagenase Type ll	Sigma, Munich

Desoxynucleotides (dATP, dCTP, dGTP, dTTP)	Roche, Mannheim
Dexamethasone	Sigma, Munich
DMSO (Dimethyl sulfoxide)	Sigma, Munich
DOTAP Liposomal Transfection Reagent	Sigma, Munich
DTT (Dithiothreitol)	Sigma, Munich
Dulbecco's modified Eagle's medium (DMEM)	Invitrogen, Karlsruhe
EDTA (Ethylenediaminetetraacetic acid)	Sigma, Munich
EGTA (Ethylenglycoltetraacetic acid)	Sigma, Munich
Ethanol (99%)	DKFZ
Ethidium bromide	Carl Roth GmbH, Karlsruhe
Fetal calf serum (FCS)	Invitrogen, Karlsruhe
Formaldehyde	DKFZ
Forskolin	Sigma, Munich
Gene Ruler 1kb DNA	Fermentas, St. Leon Rot
Glucose	Sigma, Munich
Glutathione sepharose	Amersham, Darmstadt
Glycerol	Baker, Deventer, NL
Gly-Gly	Sigma-Aldrich, Munich
Hepes	Roth, Karlsruhe
Hydrochloric acid (HCl) 37%	Acros Organics, New Jersey, USA
Hyperfilm ECL Western Blotting Detection Reagents	Amersham, Freiburg
Igepal (Nonidet NP40)	Sigma, Munich
IBMX	Sigma, Munich
Insulin human (recombinant yeast)	Sigma, Munich
Isopropyl-β-D-thio-galactopyranoside (IPTG)	Sigma-Aldrich, Munich
Isopropanol	Sigma, Munich
LB-Agar	Carl Roth GmbH, Karlsruhe
LB-Medium	Carl Roth GmbH, Karlsruhe
Lipofectamine2000 Reagent	Invitrogen, Karlsruhe
Loading dye solution (6x)	Fermentas, St. Leon Rot
Luciferin	Sigma, Munich
Magnesium chloride (MgCl2)	Merck, Darmstadt
Magnesium sulfate (MgSO4)	Sigma, Munich
Methanol (100%)	Merck, Darmstadt
Methionine (35S radiolabelled)	Perkin Elmer, Rodgau
Milk powder *Rapilait*	Migros, Lörrach, CH
Non-essential amino acids	Invitrogen, Karlsruhe
Oil Red O	Sigma, Munich
o-Nitrophenyl-β-D-galactopyranosid (ONPG)	Sigma, Munich
optiMEM	Invitrogen, Karlsruhe
Orange G	Sigma, Munich

Page Ruler Prestained Protein Ladder	Fermentas, St. Leon Rot
Penicillin / Streptomycin (P/S)	Invitrogen, Karlsruhe
Phosphatase Inhibitor Cocktail	Sigma, Munich
Platinum qPCR SuperMix	Invitrogen, Karlsruhe
Ponceau-S Solution	Sigma, Munich
Potassium chloride (KCl)	Sigma, Munich
Proteinase inhibitor cocktail	Roche, Penzberg
Qiazol Lysis Reagent	Qiagen, Hilden
RiboLock Ribonuclease Inhibitor	Fermentas, St. Leon Rot
Sodium chloride (NaCl)	Invitrogen, Karlsruhe
Sodium dodecyl sulfate (SDS)	Gerbu, Biotechnik GmbH, Gaiberg
Sodium fluoride (NaF)	Sigma, Munich
Sodium hydroxide (NaOH)	Sigma, Munich
Sodium orthovandate	Sigma, Munich
N,N,N',N'-Tetramethylenediamine (TEMED)	Carl Roth GmbH, Karlsruhe
Tripotassium phosphate (K3PO4)	Merck, Darmstadt
Tris base	Sigma, Munich
Triton X-100	Sigma, Munich
Trypsin-EDTA solution	Invitrogen, Karlsruhe
Tween-20	Sigma, Munich
Urea	Sigma, Munich
β-Mercaptoethanol (98%)	Sigma, Munich
Williams Medium E	Sigma, Munich

7.8 Instruments

Instrument	Distributor
Analytical scales	Satorius, Göttingen
Bacterial shaker	Infors AG, Böttmingen, CH
Centrifuge (2K15)	Sigma, Munich
Centrifuge (Biofuge fresco)	Heraeus, Hanau
Centrifuge (Biofuge pico)	Heraeus, Hanau
Centrifuge (Function Line)	Heraeus, Hanau
Centrifuge (Micro 22R)	Hettich GmbH & Co, Tuttlingen
Centrifuge (Super T21)	Heraeus Sorvall, Langenselbold
ChemiDoc	BioRad, Munich
CO2-incubator	Sanyo, Munich
CO2-incubator (Forma Scientific)	Labotect, Göttingen
CO2-incubator (Forma Scientific)	Labotect, Göttingen
Countess Cell counter	Invitrogen, Karlsruhe
Electrophoresis chamber	Steinbrenner, Wiesenbach

Electrophoresis power supply (Power Pack Basic)	BioRad, Munich
Electrophoresis power supply (Power Pack HC)	BioRad, Munich
Film cassette	Amersham, Freiburg
Film developer	Amersham, Freiburg
Freezer, -20°C	Liebherr, Biberach
Freezer, -80°C (Hera Freeze)	Heraeus, Heilbronn
Fridge, 4°C	Liebherr, Biberach
Gel imager	Intas, Göttingen
Heat block (Thermostat Plus)	Eppendorf, Hamburg
Horizontal shaker (Duomax 1030)	Heidolph, Kehlheim
Hotplate / stirrer	VWR, Darmstadt
Incubator (Function Line)	Heraeus, Hanau
Microscope (Axio Imager M2)	Carl Zeiss, Göttingen
Microwave	Bosch, Stuttgart
Multistep pipette	Eppendorf, Hamburg
Neubauer counting chamber	Carl Roth GmbH, Karlsruhe
Nitrogen tank	Thermo Electron corp., Erlangen
pH-meter	VWR, Darmstadt
Photometer (NanoDrop ND-1000)	Peqlab Biotechnology, Erlangen
Pipettes (2 µl, 10 µl, 20 µl, 100 µl, 200 µl, 1000 µl)	Gilson, Middleton, USA
Pipettes (20 µl, 200 µl, 1000 µl)	Eppendorf, Hamburg
Real time PCR System StepOne Plus	Applied Biosystems, Darmstadt
Rotating wheel	Neolab, Heidelberg
Scale	Kern und Sohn GmbH, Balingen
Scale (BL 1500 S)	Satorius, Göttingen
Scanner	Epson, Meerbusch
SDS electrophoresis chambers	BioRad, Munich
Sonicator BioruptorTM	Diagenode, Liège, Belgium
Stand	Carl Roth GmbH, Karlsruhe
Sterile benches (Class II type A/B3)	Sterilgard, Sanford, USA
Tabletop centrifuges (Mini Spin Plus)	Eppendorf, Hamburg
Thermocycler (PTC-200)	Biozym, Oldendorf
Tissue Lyser	Qiagen, Hilden
Ultracentrifuge (Sorvall WX Ultra 80)	Thermo Scientific, Osterode
Vacuum pump	Neolab, Heidelberg
Vortex mixer (REAX 2000)	Heidolph, Kehlheim
Water bath	Neolab, Heidelberg
Western Blot Chamber	BioRad, Munich

8   Glossary

AAV	Adeno-associated virus
ABC	ATP binding cassette
Abd	Abdominal
ACLY	ATP citrate lyase
ANGPTL	Angiopoietin related
Apo	Apoliporotein
ATP	Adenosine triphosphate
BMI	Body mass index
Bp	Base pairs
C	Celsius
C26	Colon 26
CD	Cluster of Differentiation
CE	Cholester-ester
CETP	Cholesterylester transfer protein
CIDE	cell death–inducing DNA fragmentation factor-α-like effector
CMV	Cytolomegavirus
CNP	C-type natriuretic peptide
CVD	Cardiovascular Disease
Cyp7	Cholesterol 7 alpha-hydroxylase
DBD	DNA binding domain
DGAT	Diglyceride acyltransferase
DMEM	Dulbeccos's modified eagle medium
DNA	Deoxyribonucleic acid
dNTP	deoxyribonucleotide triphosphates
ECL	Enhanced chemiluminescence
EGFP	Enhanced green fluorescent protein
ELISA	Enzyme-linked immunosorbent assay
ER	Estrogen receptor
FA	Fatty acids
FABP	Fatty acid binding protein
FASN	Fatty acid synthase
FCS	Fetal calf serum
Fig	Figure
FoxO1	Forkhead box protein O1

FPLC	Fast protein liquid chromatography
GC	Gastrocnemius muscle
GPS2	G protein pathway suppressor 2
GR	Glucocorticoid
GSEA	Gene set enrichment analysis
GST	Glutathion-S-Transferase
h	Hour
HDAC	Histone Deacetylase
HDL	High density lipoprotein
HFD	High fat diet
HL	Hepatic lipase
HRP	Horseradish peroxidase
IDL	Intermediate density lipoprotein
Ing	Inguinal
LB	Ludmilla Broth
LBD	Ligand binding domain
LCAT	Lecithin cholesterol aclytransferase
LDL	Low density lipoprotein
LDLR	LDL receptor
LFD	Low fat diet
LPIN	Lipin
LPL	Lipoprotein lipase
LRP	LDL receptor related protein
LSR	Lipolysis stimulated lipoprotein receptor
LXR	Liver X receptor
MCD	Methionine choline deficient diet
Min	Minute
miRNA	microRNA
mRNA	Messenger RNA
MTTP	Microsomal transfer protein
NAA	Non-essential amino acids
NC	Negative control
NCoR	Nuclear receptor co-repressor
NEFA	Non-esterified fatty acids
NES	Nuclear export signal

Glossary

NR	Nuclear receptor
OE	Overexpression
ONPG	o-Nitrophenyl-β-D-galactopyranosid
PBS	Phosphate buffered saline
PGC	PPARgamma co-activator
PLIN	Perilipin
PLTP	Phospholipid transfer protein
PPAR	peroxisome proliferator-activated receptors
PVDF	Polyvinylidenfluorid
qPCR	Quantitative polymerase chain reaction
RCT	Reverse cholesterol transport
RIP	Receptor interaction protein
Rpm	Rounds per minute
RT	Room temperature
RXR	Retinoid X receptor
SCD1	Stearoyl-CoA desaturase 1
SDS	Sodium dodecyl sulfate
SEM	Standard error of the mean
shRNA	Short hairpin RNA
SMRT	Silencing mediator of retinoic acid and thyroid hormone receptor
SR-B1	Scavenger receptor B1
STZ	Streptozotocin
TBL1	Transducin beta like 1
TBLR1	Transducin beta like 1 related
TCID	Tissue culture infection dose
TG	Triglyceride
TGF	Transforming growth factor beta
TRIB	Tribbles
TSC22D1	Transforming growth factor beta1-stimulated clone 22 D1
UV	Ultra Violet
VCP	Valosin-containing protein
VLDL	Very low density lipoprotein
WHO	World health organization
wt	Wildtype

9   Figures and Tables

9.1   Figures

9.2   Tables

10 References

S. Acton, A. Rigotti, K.T. Landschulz, S. Xu, H.H. Hobbs, and M. Krieger, Identification of scavenger receptor SR-BI as a high density lipoprotein receptor. Science 271 (1996) 518-20.

K.G. Alberti, R.H. Eckel, S.M. Grundy, P.Z. Zimmet, J.I. Cleeman, K.A. Donato, J.C. Fruchart, W.P. James, C.M. Loria, and S.C. Smith, Jr., Harmonizing the metabolic syndrome: a joint interim statement of the International Diabetes Federation Task Force on Epidemiology and Prevention; National Heart, Lung, and Blood Institute; American Heart Association; World Heart Federation; International Atherosclerosis Society; and International Association for the Study of Obesity. Circulation 120 (2009) 1640-5.

M. Anbalagan, B. Huderson, L. Murphy, and B.G. Rowan, Post-translational modifications of nuclear receptors and human disease. Nucl Recept Signal 10 e001 (2011).

M. Bardou, A.N. Barkun, and M. Martel, Obesity and colorectal cancer. Gut 62 933-47 (2013).

H. Bays, L. Blonde, and R. Rosenson, Adiposopathy: how do diet, exercise and weight loss drug therapies improve metabolic disease in overweight patients? Expert Rev Cardiovasc Ther 4 (2006) 871-95.

H.E. Bays, P.P. Toth, P.M. Kris-Etherton, N. Abate, L.J. Aronne, W.V. Brown, J.M. Gonzalez-Campoy, S.R. Jones, R. Kumar, R. La Forge, and V.T. Samuel, Obesity, adiposity, and dyslipidemia: A consensus statement from the National Lipid Association. J Clin Lipidol 7 304-83 (2013).

M. Berriel Diaz, A. Krones-Herzig, D. Metzger, A. Ziegler, A. Vegiopoulos, M. Klingenspor, K. Muller-Decker, and S. Herzig, Nuclear receptor cofactor receptor interacting protein 140 controls hepatic triglyceride metabolism during wasting in mice. Hepatology 48 (2008) 782-91.

H. Berrougui, and A. Khalil, Age-associated decrease of high-density lipoprotein-mediated reverse cholesterol transport activity. Rejuvenation Res 12 (2009) 117-26.

H. Berrougui, M. Isabelle, M. Cloutier, G. Grenier, and A. Khalil, Age-related impairment of HDL-mediated cholesterol efflux. J Lipid Res 48 (2007)

C. Bing, M. Brown, P. King, P. Collins, M.J. Tisdale, and G. Williams, Increased gene expression of brown fat uncoupling protein (UCP)1 and skeletal muscle UCP2 and UCP3 in MAC16-induced cancer cachexia. Cancer Res 60 (2000) 2405-10.

R. Buettner, J. Scholmerich, and L.C. Bollheimer, High-fat diets: modeling the metabolic disorders of human obesity in rodents. Obesity (Silver Spring) 15 (2007) 798-808

A.C. Calkin, and P. Tontonoz, Transcriptional integration of metabolism by the nuclear sterol-activated receptors LXR and FXR. Nat Rev Mol Cell Biol 13 213-24 (2012).

T.J. Chahil, and H.N. Ginsberg, Diabetic dyslipidemia. Endocrinol Metab Clin North Am 35 (2006) 491-510, vii-viii

J.D. Chen, and R.M. Evans, A transcriptional co-repressor that interacts with nuclear hormone receptors. Nature 377 (1995) 454-7.

N. Chirmule, K. Propert, S. Magosin, Y. Qian, R. Qian, and J. Wilson, Immune responses to adenovirus and adeno-associated virus in humans. Gene Ther 6 (1999) 1574-83.

S.J. Choi, J.H. Moon, Y.W. Ahn, J.H. Ahn, D.U. Kim, and T.H. Han, Tsc-22 enhances TGF-beta signaling by associating with Smad4 and induces erythroid cell differentiation. Mol Cell Biochem 271 (2005) 23-8.

M. Downes, and C. Liddle, Look who's talking: nuclear receptors in the liver and gastrointestinal tract. Cell Metab 7 (2008) 195-9.

E. Eden, S. Edstrom, K. Bennegard, T. Schersten, and K. Lundholm, Glucose flux in relation to energy expenditure in malnourished patients with and without cancer during periods of fasting and feeding. Cancer Res 44 (1984) 1718-24.

P.W. Emery, R.H. Edwards, M.J. Rennie, R.L. Souhami, and D. Halliday, Protein synthesis in muscle measured in vivo in cachectic patients with cancer. Br Med J (Clin Res Ed) 289 (1984) 584-6.

R.B. Ervin, Prevalence of metabolic syndrome among adults 20 years of age and over, by sex, age, race and ethnicity, and body mass index: United States, 2003-2006. Natl Health Stat Report (2009) 1-7.

R.M. Evans, The steroid and thyroid hormone receptor superfamily. Science 240 (1988) 889-95.

J.S. Falconer, K.C. Fearon, C.E. Plester, J.A. Ross, and D.C. Carter, Cytokines, the acute-phase response, and resting energy expenditure in cachectic patients with pancreatic cancer. Ann Surg 219 (1994) 325-31.

K. Fearon, J. Arends, and V. Baracos, Understanding the mechanisms and treatment options in cancer cachexia. Nat Rev Clin Oncol 10 90-9 (2012).

J.N. Feige, and J. Auwerx, Transcriptional coregulators in the control of energy homeostasis. Trends Cell Biol 17 (2007) 292-301.

G.P. Gao, M.R. Alvira, L. Wang, R. Calcedo, J. Johnston, and J.M. Wilson, Novel adeno-associated viruses from rhesus monkeys as vectors for human gene therapy. Proc Natl Acad Sci U S A 99 (2002) 11854-9.

H.N. Ginsberg, Insulin resistance and cardiovascular disease. J Clin Invest 106 (2000) 453-8.

H.N. Ginsberg, Y.L. Zhang, and A. Hernandez-Ono, Regulation of plasma triglycerides in insulin resistance and diabetes. Arch Med Res 36 (2005) 232-40.

S. Gluderer, E. Brunner, M. Germann, V. Jovaisaite, C. Li, C.A. Rentsch, E. Hafen, and H. Stocker, Madm (Mlf1 adapter molecule) cooperates with Bunched A to promote growth in Drosophila. J Biol 9 (2008).

T. Gordon, W.P. Castelli, M.C. Hjortland, W.B. Kannel, and T.R. Dawber, High density lipoprotein as a protective factor against coronary heart disease. The Framingham Study. Am J Med 62 (1977) 707-14.

W. Gu, C. Chen, and K.N. Zhao, Obesity-associated endometrial and cervical cancers. Front Biosci (Elite Ed) 5 109-18 (2013).

M.G. Guenther, W.S. Lane, W. Fischle, E. Verdin, M.A. Lazar, and R. Shiekhattar, A core SMRT corepressor complex containing HDAC3 and TBL1, a WD40-repeat protein linked to deafness. Genes Dev 14 (2000) 1048-57.

D.J. Grainger, P.R. Kemp, J.C. Metcalfe, A.C. Liu, R.M. Lawn, N.R. Williams, A.A. Grace, P.M. Schofield, and A. Chauhan, The serum concentration of active transforming growth factor-beta is severely depressed in advanced atherosclerosis. Nat Med 1 (1995) 74-9

D. Grimm, A. Kern, K. Rittner, and J.A. Kleinschmidt, Novel tools for production and purification of recombinant adenoassociated virus vectors. Hum Gene Ther 9 (1998) 2745-60.

P.H. Groot, W.A. van Stiphout, X.H. Krauss, H. Jansen, A. van Tol, E. van Ramshorst, S. Chin-On, A. Hofman, S.R. Cresswell, and L. Havekes, Postprandial lipoprotein metabolism in normolipidemic men with and without coronary artery disease. Arterioscler Thromb 11 (1991) 653-62.

R.A. Gupta, P. Sarraf, J.A. Brockman, S.B. Shappell, L.A. Raftery, T.M. Willson, and R.N. DuBois, Peroxisome proliferator-activated receptor gamma and transforming growth factor-beta pathways inhibit intestinal epithelial cell growth by regulating levels of TSC-22. J Biol Chem 278 (2003) 7431-8.

Y.C. Ha, and P.J. Barter, Differences in plasma cholesteryl ester transfer activity in sixteen vertebrate species. Comp Biochem Physiol B 71 (1982) 265-9.

S.M. Haffner, Management of dyslipidemia in adults with diabetes. Diabetes Care 26 Suppl 1 (2003) S83-6.

P. Hahn, Cholesterol metabolism in obese mice. Can J Biochem 58 (1980) 1258-60.

S. Hino, H. Kawamata, D. Uchida, F. Omotehara, Y. Miwa, N.M. Begum, H. Yoshida, T. Fujimori, and M. Sato, Nuclear translocation of TSC-22 (TGF-beta-stimulated clone-22) concomitant with apoptosis: TSC-22 as a putative transcriptional regulator. Biochem Biophys Res Commun 278 (2000) 659-64.

J.E. Hinshaw, B.O. Carragher, and R.A. Milligan, Architecture and design of the nuclear pore complex. Cell 69 (1992) 1133-41.

K. Hirai, H.J. Hussey, M.D. Barber, S.A. Price, and M.J. Tisdale, Biological evaluation of a lipid-mobilizing factor isolated from the urine of cancer patients. Cancer Res 58 (1998) 2359-65.

C. Homig-Holzel, R. van Doorn, C. Vogel, M. Germann, M.G. Cecchini, E. Verdegaal, and D.S. Peeper, Antagonistic TSC22D1 variants control BRAF(E600)-induced senescence. EMBO J 30 1753-65.

A.J. Horlein, A.M. Naar, T. Heinzel, J. Torchia, B. Gloss, R. Kurokawa, A. Ryan, Y. Kamei, M. Soderstrom, C.K. Glass, and et al., Ligand-independent repression by the thyroid hormone receptor mediated by a nuclear receptor co-repressor. Nature 377 (1995) 397-404.

R.H. Houtkooper, C. Argmann, S.M. Houten, C. Canto, E.H. Jeninga, P.A. Andreux, C. Thomas, R. Doenlen, K. Schoonjans, and J. Auwerx, The metabolic footprint of aging in mice. Sci Rep 1 134 (2012).

W.P. Hsieh, T.M. Chu, R.D. Wolfinger, and G. Gibson, Mixed-model reanalysis of primate data suggests tissue and species biases in oligonucleotide-based gene expression profiles. Genetics 165 (2003) 747-57.

F. Jacob, and J. Monod, Genetic regulatory mechanisms in the synthesis of proteins. J Mol Biol 3 (1961) 318-56.

B.A. Janowski, P.J. Willy, T.R. Devi, J.R. Falck, and D.J. Mangelsdorf, An oxysterol signalling pathway mediated by the nuclear receptor LXR alpha. Nature 383 (1996) 728-31.

A. Jatoi, B.D. Daly, V.A. Hughes, G.E. Dallal, J. Kehayias, and R. Roubenoff, Do patients with nonmetastatic non-small cell lung cancer demonstrate altered resting energy expenditure? Ann Thorac Surg 72 (2001) 348-51.

J. Jawien, P. Nastalek, and R. Korbut, Mouse models of experimental atherosclerosis. J Physiol Pharmacol 55 (2004) 503-17.

References

P. Jay, J.W. Ji, C. Marsollier, S. Taviaux, J.L. Berge-Lefranc, and P. Berta, Cloning of the human homologue of the TGF beta-stimulated clone 22 gene. Biochem Biophys Res Commun 222 (1996) 821-6.

C.A. Johnson, Chromatin modification and disease. J Med Genet 37 (2000) 905-15.

A. Jones, K. Friedrich, M. Rohm, M. Schafer, C. Algire, P. Kulozik, O. Seibert, K. Muller-Decker, T. Sijmonsma, D. Strzoda, C. Sticht, N. Gretz, G.M. Dallinga-Thie, B. Leuchs, M. Kogl, W. Stremmel, M.B. Diaz, and S. Herzig, TSC22D4 is a molecular output of hepatic wasting metabolism. EMBO Mol Med 5 294-308 (2013).

A. Kamagate, S. Qu, G. Perdomo, D. Su, D.H. Kim, S. Slusher, M. Meseck, and H.H. Dong, FoxO1 mediates insulin-dependent regulation of hepatic VLDL production in mice. J Clin Invest 118 (2008) 2347-64.

M. Kato, L. Wang, S. Putta, M. Wang, H. Yuan, G. Sun, L. Lanting, I. Todorov, J.J. Rossi, and R. Natarajan, Post-transcriptional up-regulation of Tsc-22 by Ybx1, a target of miR-216a, mediates TGF-{beta}-induced collagen expression in kidney cells. J Biol Chem 285 34004-15 (2010).

T. Kawa-Uchi, K. Nose, and M. Noda, Fibroblast growth factor enhances expression of TGFbeta-stimulated-clone-22 gene in osteoblast-like cells. Endocrine 3 (1995) 833-7.

A. Kaibara, A. Moshyedi, T. Auffenberg, A. Abouhamze, E.M. Copeland, 3rd, S. Kalra, and L.L. Moldawer, Leptin produces anorexia and weight loss without inducing an acute phase response or protein wasting. Am J Physiol 274 (1998) R1518-25.

H.A. Kester, C. Blanchetot, J. den Hertog, P.T. van der Saag, and B. van der Burg, Transforming growth factor-beta-stimulated clone-22 is a member of a family of leucine zipper proteins that can homo- and heterodimerize and has transcriptional repressor activity. J Biol Chem 274 (1999) 27439-47.

U. Klingmuller, A. Bauer, S. Bohl, P.J. Nickel, K. Breitkopf, S. Dooley, S. Zellmer, C. Kern, I. Merfort, T. Sparna, J. Donauer, G. Walz, M. Geyer, C. Kreutz, M. Hermes, F. Gotschel, A. Hecht, D. Walter, L. Egger, K. Neubert, C. Borner, M. Brulport, W. Schormann, C. Sauer, F. Baumann, R. Preiss, S. MacNelly, P. Godoy, E. Wiercinska, L. Ciuclan, J. Edelmann, K. Zeilinger, M. Heinrich, U.M. Zanger, R. Gebhardt, T. Maiwald, R. Heinrich, J. Timmer, F. von Weizsacker, and J.G. Hengstler, Primary mouse hepatocytes for systems biology approaches: a standardized in vitro system for modelling of signal transduction pathways. Syst Biol (Stevenage) 153 (2006) 433-47.

B. Klop, J.W. Elte, and M.C. Cabezas, Dyslipidemia in obesity: mechanisms and potential targets. Nutrients 5 1218-40 (2013).

K. Kobayashi, T.M. Forte, S. Taniguchi, B.Y. Ishida, K. Oka, and L. Chan, The db/db mouse, a model for diabetic dyslipidemia: molecular characterization and effects of Western diet feeding. Metabolism 49 (2000) 22-31.

P.G. Kopelman, Obesity as a medical problem. Nature 404 (2000) 635-43.

P. Kulozik, A. Jones, F. Mattijssen, A.J. Rose, A. Reimann, D. Strzoda, S. Kleinsorg, C. Raupp, J. Kleinschmidt, K. Muller-Decker, W. Wahli, C. Sticht, N. Gretz, C. von Loeffelholz, M. Stockmann, A. Pfeiffer, S. Stohr, G.M. Dallinga-Thie, P.P. Nawroth, M. Berriel Diaz, and S. Herzig, Hepatic deficiency in transcriptional cofactor TBL1 promotes liver steatosis and hypertriglyceridemia. Cell Metab 13 389-400 (2011).

H.A. Krebs, The regulation of the release of ketone bodies by the liver. Adv Enzyme Regul 4 (1966) 339-54.

M. Lafontan, and D. Langin, Lipolysis and lipid mobilization in human adipose tissue. Prog Lipid Res 48 (2009) 275-97

J.H. Lee, S.B. Rho, S.Y. Park, and T. Chun, Interaction between fortilin and transforming growth factor-beta stimulated clone-22 (TSC-22) prevents apoptosis via the destabilization of TSC-22. FEBS Lett 582 (2008) 1210-8.

J.Y. Lee, and J.S. Parks, ATP-binding cassette transporter AI and its role in HDL formation. Curr Opin Lipidol 16 (2005) 19-25.

U. Lemke, A. Krones-Herzig, M. Berriel Diaz, P. Narvekar, A. Ziegler, A. Vegiopoulos, A.C. Cato, S. Bohl, U. Klingmuller, R.A. Screaton, K. Muller-Decker, S. Kersten, and S. Herzig, The glucocorticoid receptor controls hepatic dyslipidemia through Hes1. Cell Metab 8 (2008) 212-23.

S. Lewington, G. Whitlock, R. Clarke, P. Sherliker, J. Emberson, J. Halsey, N. Qizilbash, R. Peto, and R. Collins, Blood cholesterol and vascular mortality by age, sex, and blood pressure: a meta-analysis of individual data from 61 prospective studies with 55,000 vascular deaths. Lancet 370 (2007) 1829-39.

G.F. Lewis, and D.J. Rader, New insights into the regulation of HDL metabolism and reverse cholesterol transport. Circ Res 96 (2005) 1221-32.

J. Li, J. Wang, Z. Nawaz, J.M. Liu, J. Qin, and J. Wong, Both corepressor proteins SMRT and N-CoR exist in large protein complexes containing HDAC3. EMBO J 19 (2000) 4342-50 (2011).

P. Lindstrom, The physiology of obese-hyperglycemic mice [ob/ob mice]. ScientificWorldJournal 7 (2007) 666-85.

W. Liu, Y. Hou, H. Chen, H. Wei, W. Lin, J. Li, M. Zhang, F. He, and Y. Jiang, Sample preparation method for isolation of single-cell types from mouse liver for proteomic studies. Proteomics 11 3556-64.

X. Liu, L. Wang, K. Zhao, P.R. Thompson, Y. Hwang, R. Marmorstein, and P.A. Cole, The structural basis of protein acetylation by the p300/CBP transcriptional coactivator. Nature 451 (2008) 846-50.

Y. Lu, J. Kitaura, T. Oki, Y. Komeno, K. Ozaki, M. Kiyono, H. Kumagai, H. Nakajima, T. Nosaka, H. Aburatani, and T. Kitamura, Identification of TSC-22 as a potential tumor suppressor that is upregulated by Flt3-D835V but not Flt3-ITD. Leukemia 21 (2007) 2246-57.

S. Lucia, M. Esposito, F. Rossi Fanelli, and M. Muscaritoli, Cancer cachexia: from molecular mechanisms to patient's care. Crit Rev Oncog 17 315-21 (2012).

S. Malik, Transcriptional regulation of the apolipoprotein AI gene. Front Biosci 8 (2003) d360-8.

S. Mandard, F. Zandbergen, E. van Straten, W. Wahli, F. Kuipers, M. Muller, and S. Kersten, The fasting-induced adipose factor/angiopoietin-like protein 4 is physically associated with lipoproteins and governs plasma lipid levels and adiposity. J Biol Chem 281 (2006) 934-44.

D.J. Mangelsdorf, C. Thummel, M. Beato, P. Herrlich, G. Schutz, K. Umesono, B. Blumberg, P. Kastner, M. Mark, P. Chambon, and R.M. Evans, The nuclear receptor superfamily: the second decade. Cell 83 (1995) 835-9.

T. Manoli, N. Gretz, H.J. Grone, M. Kenzelmann, R. Eils, and B. Brors, Group testing for pathway analysis improves comparability of different microarray datasets. Bioinformatics 22 (2006) 2500-6.

M. Marcil, A. Brooks-Wilson, S.M. Clee, K. Roomp, L.H. Zhang, L. Yu, J.A. Collins, M. van Dam, H.O. Molhuizen, O. Loubster, B.F. Ouellette, C.W. Sensen, K. Fichter, S. Mott, M. Denis, B. Boucher, S. Pimstone, J. Genest, Jr.,

J.J. Kastelein, and M.R. Hayden, Mutations in the ABC1 gene in familial HDL deficiency with defective cholesterol efflux. Lancet 354 (1999) 1341-6.

M.E. Martignoni, C. Dimitriu, J. Bachmann, H. Krakowski-Rosen, K. Ketterer, R. Kinscherf, and H. Friess, Liver macrophages contribute to pancreatic cancer-related cachexia. Oncol Rep 21 (2009) 363-9.

W. Marz, R. Siekmeier, H. Scharnagl, U.B. Seiffert, and W. Gross, Fast lipoprotein chromatography: new method of analysis for plasma lipoproteins. Clin Chem 39 (1993) 2276-81.

C. Mineo, and P.W. Shaul, Regulation of signal transduction by HDL. J Lipid Res 54 2315-24 (2013).

M. Nakamura, J. Kitaura, Y. Enomoto, Y. Lu, K. Nishimura, M. Isobe, K. Ozaki, Y. Komeno, F. Nakahara, T. Oki, H. Kume, Y. Homma, and T. Kitamura, Transforming growth factor-beta-stimulated clone-22 is a negative-feedback regulator of Ras / Raf signaling: Implications for tumorigenesis. Cancer Sci 103 26-33 (2011).

K. Nakashiro, H. Kawamata, S. Hino, D. Uchida, Y. Miwa, H. Hamano, F. Omotehara, H. Yoshida, and M. Sato, Down-regulation of TSC-22 (transforming growth factor beta-stimulated clone 22) markedly enhances the growth of a human salivary gland cancer cell line in vitro and in vivo. Cancer Res 58 (1998) 549-55.

P. Nguyen, V. Leray, M. Diez, S. Serisier, J. Le Bloc'h, B. Siliart, and H. Dumon, Liver lipid metabolism. J Anim Physiol Anim Nutr (Berl) 92 (2008) 272-83.

S. Ohta, Y. Shimekake, and K. Nagata, Molecular cloning and characterization of a transcription factor for the C-type natriuretic peptide gene promoter. Eur J Biochem 242 (1996) 460-6.

S. Ohta, K. Yanagihara, and K. Nagata, Mechanism of apoptotic cell death of human gastric carcinoma cells mediated by transforming growth factor beta. Biochem J 324 (Pt 3) (1997) 777-82.

A. Oliff, D. Defeo-Jones, M. Boyer, D. Martinez, D. Kiefer, G. Vuocolo, A. Wolfe, and S.H. Socher, Tumors secreting human TNF/cachectin induce cachexia in mice. Cell 50 (1987) 555-63.

R.E. Patterson, C.L. Rock, J. Kerr, L. Natarajan, S.J. Marshall, B. Pakiz, and L.A. Cadmus-Bertram, Metabolism and breast cancer risk: frontiers in research and practice. J Acad Nutr Diet 113 288-96 (2013).

V. Perissi, A. Aggarwal, C.K. Glass, D.W. Rose, and M.G. Rosenfeld, A corepressor/coactivator exchange complex required for transcriptional activation by nuclear receptors and other regulated transcription factors. Cell 116 (2004) 511-26.

S.J. Peterson, G. Drummond, D.H. Kim, M. Li, A.L. Kruger, S. Ikehara, and N.G. Abraham, L-4F treatment reduces adiposity, increases adiponectin levels, and improves insulin sensitivity in obese mice. J Lipid Res 49 (2008) 1658-69.

M.R. Plummer, and A.H. Hasty, Atherosclerotic lesion formation and triglyceride storage in obese apolipoprotein AI-deficient mice. J Nutr Biochem 19 (2008) 664-73.

A.S. Plump, N. Azrolan, H. Odaka, L. Wu, X. Jiang, A. Tall, S. Eisenberg, and J.L. Breslow, ApoA-I knockout mice: characterization of HDL metabolism in homozygotes and identification of a post-RNA mechanism of apoA-I up-regulation in heterozygotes. J Lipid Res 38 (1997) 1033-47.

M. Puccio, and L. Nathanson, The cancer cachexia syndrome. Semin Oncol 24 (1997) 277-87.

G.M. Reaven, Banting lecture 1988. Role of insulin resistance in human disease. Diabetes 37 (1988) 1595-607.

J.J. Repa, S.D. Turley, J.A. Lobaccaro, J. Medina, L. Li, K. Lustig, B. Shan, R.A. Heyman, J.M. Dietschy, and D.J. Mangelsdorf, Regulation of absorption and ABC1-mediated efflux of cholesterol by RXR heterodimers. Science 289 (2000) 1524-9.

M.E. Rinella, M.S. Elias, R.R. Smolak, T. Fu, J. Borensztajn, and R.M. Green, Mechanisms of hepatic steatosis in mice fed a lipogenic methionine choline-deficient diet. J Lipid Res 49 (2008) 1068-76.

M. Rohm, A. Sommerfeld, D. Strzoda, A. Jones, T.P. Sijmonsma, G. Rudofsky, C. Wolfrum, C. Sticht, N. Gretz, M. Zeyda, L. Leitner, P.P. Nawroth, T.M. Stulnig, M.B. Diaz, A. Vegiopoulos, and S. Herzig, Transcriptional cofactor TBLR1 controls lipid mobilization in white adipose tissue. Cell Metab 17 575-85 (2013).

N. Rosenthal, and S. Brown, The mouse ascending: perspectives for human-disease models. Nat Cell Biol 9 (2007) 993-9.

R. Ross, and J.A. Glomset, Atherosclerosis and the arterial smooth muscle cell: Proliferation of smooth muscle is a key event in the genesis of the lesions of atherosclerosis. Science 180 (1973) 1332-9.

Roy J (2007) SAS for mixed models. In J Biopharm Stat, Littell RC, Milliken GA, Stroup WW, Wolfinger RD, Schabenberger O (eds), 2nd edn, Vol. 17, pp 363–365 | Article

J.R. Schultz, H. Tu, A. Luk, J.J. Repa, J.C. Medina, L. Li, S. Schwendner, S. Wang, M. Thoolen, D.J. Mangelsdorf, K.D. Lustig, and B. Shan, Role of LXRs in control of lipogenesis. Genes Dev 14 (2000) 2831-8.

Y. Shi, and J. Massague, Mechanisms of TGF-beta signaling from cell membrane to the nucleus. Cell 113 (2003) 685-700.

M. Shibanuma, T. Kuroki, and K. Nose, Isolation of a gene encoding a putative leucine zipper structure that is induced by transforming growth factor beta 1 and other growth factors. J Biol Chem 267 (1992) 10219-24.

K.O. Shostak, V.V. Dmitrenko, O.M. Garifulin, V.D. Rozumenko, O.V. Khomenko, Y.A. Zozulya, G. Zehetner, and V.M. Kavsan, Downregulation of putative tumor suppressor gene TSC-22 in human brain tumors. J Surg Oncol 82 (2003) 57-64.

D.L. Silver, X.C. Jiang, and A.R. Tall, Increased high density lipoprotein (HDL), defective hepatic catabolism of ApoA-I and ApoA-II, and decreased ApoA-I mRNA in ob/ob mice. Possible role of leptin in stimulation of HDL turnover. J Biol Chem 274 (1999)

N.N. Singh, and D.P. Ramji, The role of transforming growth factor-beta in atherosclerosis. Cytokine Growth Factor Rev 17 (2006) 487-99.

H. Soran, S. Hama, R. Yadav, and P.N. Durrington, HDL functionality. Curr Opin Lipidol 23 353-66 (2012).

A. Subramanian, P. Tamayo, V.K. Mootha, S. Mukherjee, B.L. Ebert, M.A. Gillette, A. Paulovich, S.L. Pomeroy, T.R. Golub, E.S. Lander, and J.P. Mesirov, Gene set enrichment analysis: a knowledge-based approach for interpreting genome-wide expression profiles. Proc Na (2005).

E.J. Tarling, T.Q. Vallim, and P.A. Edwards, Role of ABC transporters in lipid transport and human disease. Trends Endocrinol Metab 24 342-50 (2013).

E. Tazi, and H. Errihani, Treatment of cachexia in oncology. Indian J Palliat Care 16 129-37 (2012).

References

Y. Tanaka, H. Eda, T. Tanaka, T. Udagawa, T. Ishikawa, I. Horii, H. Ishitsuka, T. Kataoka, and T. Taguchi, Experimental cancer cachexia induced by transplantable colon 26 adenocarcinoma in mice. Cancer Res 50 (1990) 2290-5.

S. Temparis, M. Asensi, D. Taillandier, E. Aurousseau, D. Larbaud, A. Obled, D. Bechet, M. Ferrara, J.M. Estrela, and D. Attaix, Increased ATP-ubiquitin-dependent proteolysis in skeletal muscles of tumor-bearing rats. Cancer Res 54 (1994) 5568-73.

R.G. Thaman, and G.P. Arora, Metabolic Syndrome: Definition and Pathophysiology-the discussion goes on!. J. Phys. Pharm. Adv 3(3) 48-56 (2013).

M.J. Tisdale, Cachexia in cancer patients. Nat Rev Cancer 2 (2002) 862-71.

S. Tiwari, and S.A. Siddiqi, Intracellular trafficking and secretion of VLDL. Arterioscler Thromb Vasc Biol 32 1079-86 (2012).

V. Tremaroli, and F. Backhed, Functional interactions between the gut microbiota and host metabolism. Nature 489 242-9 (2012).

D. Uchida, F. Omotehara, K. Nakashiro, Y. Tateishi, S. Hino, N.M. Begum, T. Fujimori, and H. Kawamata, Posttranscriptional regulation of TSC-22 (TGF-beta-stimulated clone-22) gene by TGF-beta 1. Biochem Biophys Res Commun 305 (2003) 846-54.

R.K. Vikramadithyan, Y. Hu, H.L. Noh, C.P. Liang, K. Hallam, A.R. Tall, R. Ramasamy, and I.J. Goldberg, Human aldose reductase expression accelerates diabetic atherosclerosis in transgenic mice. J Clin Invest 115 (2005) 2434-43.

R.H. Waterston, K. Lindblad-Toh, E. Birney, J. Rogers, J.F. Abril, P. Agarwal, R. Agarwala, R. Ainscough, M. Alexandersson, P. An, S.E. Antonarakis, J. Attwood, R. Baertsch, J. Bailey, K. Barlow, S. Beck, E. Berry, B. Birren, T. Bloom, P. Bork, M. Botcherby, N. Bray, M.R. Brent, D.G. Brown, S.D. Brown, C. Bult, J. Burton, J. Butler, R.D. Campbell, P. Carninci, S. Cawley, F. Chiaromonte, A.T. Chinwalla, D.M. Church, M. Clamp, C. Clee, F.S. Collins, L.L. Cook, R.R. Copley, A. Coulson, O. Couronne, J. Cuff, V. Curwen, T. Cutts, M. Daly, R. David, J. Davies, K.D. Delehaunty, J. Deri, E.T. Dermitzakis, C. Dewey, N.J. Dickens, M. Diekhans, S. Dodge, I. Dubchak, D.M. Dunn, S.R. Eddy, L. Elnitski, R.D. Emes, P. Eswara, E. Eyras, A. Felsenfeld, G.A. Fewell, P. Flicek, K. Foley, W.N. Frankel, L.A. Fulton, R.S. Fulton, T.S. Furey, D. Gage, R.A. Gibbs, G. Glusman, S. Gnerre, N. Goldman, L. Goodstadt, D. Grafham, T.A. Graves, E.D. Green, S. Gregory, R. Guigo, M. Guyer, R.C. Hardison, D. Haussler, Y. Hayashizaki, L.W. Hillier, A. Hinrichs, W. Hlavina, T. Holzer, F. Hsu, A. Hua, T. Hubbard, A. Hunt, I. Jackson, D.B. Jaffe, L.S. Johnson, M. Jones, T.A. Jones, A. Joy, M. Kamal, E.K. Karlsson, et al., Initial sequencing and comparative analysis of the mouse genome. Nature 420 (2002) 520-62.

H. Wang, and R.H. Eckel, Lipoprotein lipase: from gene to obesity. Am J Physiol Endocrinol Metab 297 (2009) E271-88.

X. Wu, M. Yamada-Mabuchi, E.J. Morris, P.S. Tanwar, L. Dobens, S. Gluderer, S. Khan, J. Cao, H. Stocker, E. Hafen, N.J. Dyson, and L.A. Raftery, The Drosophila homolog of human tumor suppressor TSC-22 promotes cellular growth, proliferation, and survival. Proc Natl Acad Sci U S A 105 (2008) 5414-9.

H. Yadav, C. Quijano, A.K. Kamaraju, O. Gavrilova, R. Malek, W. Chen, P. Zerfas, D. Zhigang, E.C. Wright, C. Stuelten, P. Sun, S. Lonning, M. Skarulis, A.E. Sumner, T. Finkel, and S.G. Rane, Protection from obesity and diabetes by blockade of TGF-beta/Smad3 signaling. Cell Metab 14 67-79 (2011).

C.H. Yoon, S.B. Rho, S.T. Kim, S. Kho, J. Park, I.S. Jang, S. Woo, S.S. Kim, J.H. Lee, and S.H. Lee, Crucial role of TSC-22 in preventing the proteasomal degradation of p53 in cervical cancer. PLoS One 7 e42006 (2012).

L. Yu, R.E. Hammer, J. Li-Hawkins, K. Von Bergmann, D. Lutjohann, J.C. Cohen, and H.H. Hobbs, Disruption of Abcg5 and Abcg8 in mice reveals their crucial role in biliary cholesterol secretion. Proc Natl Acad Sci U S A 99 (2002) 16237-42 (2002).

Y. Zhang, R. Proenca, M. Maffei, M. Barone, L. Leopold, and J.M. Friedman, Positional cloning of the mouse obese gene and its human homologue. Nature 372 (1994) 425-32.

J. Zhang, M. Kalkum, B.T. Chait, and R.G. Roeder, The N-CoR-HDAC3 nuclear receptor corepressor complex inhibits the JNK pathway through the integral subunit GPS2. Mol Cell 9 (2002) 611-23.

10.1 Other references

A. Jones, PhD Thesis The Role of Hepatic Transforming Growth Factor-Beta1 Stimulated Clone-22 D4 (TSC22D4) in Acute Metabolic Dyslipidemia, 2011, submitted to combined faculties for the Natural Sciences and for Mathematics of the Ruperto-Carola Univerity of Heidelberg, Germany, 2012.

M. Rohm, PhD Thesis, Transcriptional co-factor TBLR1 controls lipid mobilization in white adipose tissue submitted to combined faculties for the Natural Sciences and for Mathematics of the Ruperto-Carola Univerity of Heidelberg, Germany, 2011.

J. Huang, Jayme Borensztajn, and Janardan K. Reddy, Molecular Pathology of Liver Diseases DOI 10.1007/978-1-4419-7107-4, Springer New York Dordrecht Heidelberg London, 2010.

WHO fact sheet No 311, 2013

WHO fact sheet No 317, 2013

11 Appendix

## 11.1 The role of HIPK2 in liver metabolism

Initially, the role of the serine/threonine kinase homeodomain-interacting protein kinase 2 (HIPK2) in liver metabolism was investigated for this thesis. In course of the work we unexpectedly, encountered several technical problems which lead to the decision to halt this project. The work was continued with the studies described in the main body of the thesis. In the following the main results obtained from the HIPK2 project will be presented.

11.2 Gene expression analysis for HIPK2

To assess if HIPK2 expression is deregulated in mouse models of metabolic stress and disease conditions, liver samples were taken and analyzed in regard to HIPK2 expression.

11.2.1 HIPK2 expression is not changed in the New Zealand Obese mouse model

The New Zealand Obese (NZO) mouse represents a polygenic model of diabetes. To determine if HIPK2 expression is influenced by the obese phenotype, hepatic RNA was isolated and HIPK2 mRNA expression was analyzed. A difference in HIPK2 expression between NZO and the respective control strain New Zealand Black (NZB) could not be detected (Fig A1).
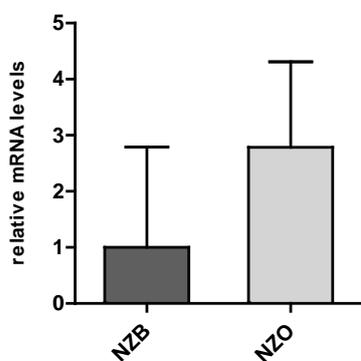
Fig A1: HIPK2 expression is not changed diabetic New Zealand Obese (NZO) mice. Liver mRNA levels of HIPK2 in lean New Zealand Black (NZB) and diabetic New Zealand Obese (NZO) were determined by qPCR. (n=6), (means ± SEM).

### 11.2.2 HIPK2 expression is not changed in mice fed a high fat diet

By feeding mice a high fat diet over the course of several weeks the onset of obesity can be modeled. In this experiment mice were fed either a high fat diet containing 60% energy from fat or a control low fat diet containing 10% energy from fat over a 9 week period. Hepatic HIPK2 expression levels were determined (Fig A2). HIPK2 expression was slightly but not significantly lower in mice fed the high fat diet.
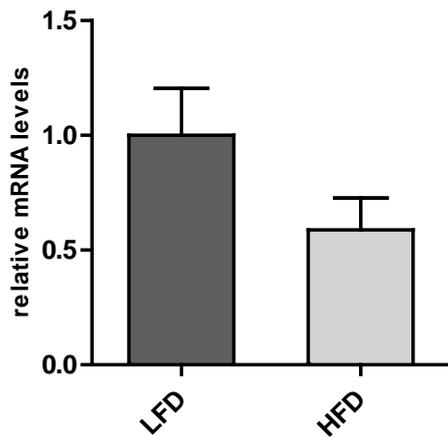
Fig A2: HIPK2 expression is not changed by high fat diet. *Liver mRNA levels of HIPK2 in mice fed either a high fat diet (HFD) or a control low fat diet (LFD) were determined by qPCR. (n=3), (means ± SEM).*

11.2.3 HIPK2 expression is not changed in mice fed a methionine and choline deficient diet

Mice fed with a diet lacking methionine and choline (MCD), encounter dramatic weight loss and develop severe hepatic steatosis and have low serum TG levels. To determine if HIPK2 expression is altered by this conditions hepatic RNA was isolated and HIPK2 mRNA expression was analyzed. A difference in HIPK2 expression between mice fed MCD diet or mice fed a control diet (CD) could not be detected (Fig A3).
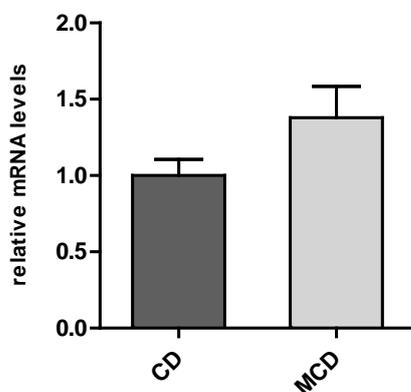

Fig A3: HIPK2 expression is not changed by methionine choline deficient diet. *Liver mRNA levels of HIPK2 in mice fed a methionine choline deficient diet (MCD) or a control diet (CD) were determined by qPCR. (n=3), (means ± SEM).*

11.2.4 HIPK2 expression is reduced upon fasting

To test if HIPK2 expression is regulated in response to nutritional restriction, mice were fasted for 24 hours. After starvation, one group of animals was sacrificed immediately and the other mice were fed for 4 hours, 6 hours or 24 hours. Hepatic HIPK2 mRNA expression was determined by quantitative PCR (Fig A4). HIPK2 levels were significantly reduced (~70%) in livers of mice after 24h

of fasting compared to mice which had been refed for 24 hours. Also 4 hours after refeeding HIPK2 expression was still significantly lower.
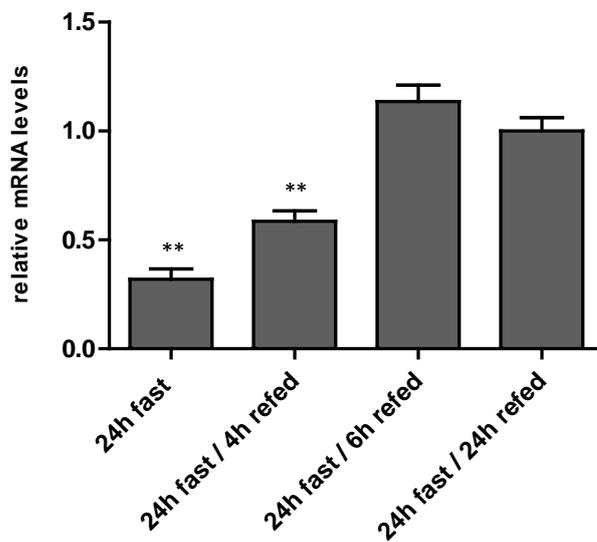
Fig A4: HIPK2 expression is downregulated by fasting. *Liver mRNA levels of HIPK2 in mice fasted for 24 hours and either directly sacrificed or refed for 4 hours, 6 hours or 24 hours were determined by qPCR. (n=5), (means ± SEM). (**) indicates significance p≤0.01*

11.2.5 HIPK2 levels are increased in lipopolysaccharide-induced sepsis

Injection of bacterial lipopolysaccharides (LPS) into mice stimulates an acute septic shock and leads to systemic inflammation and increased lipolysis. Mice were starved over night and subsequently injected intraperitoneally with either LPS at a dose of 20 mg/kg body weight or with PBS as a control. 8 hours after injection, mice were sacrificed. HIPK2 levels were more than 2-fold higher in LPS injected mice, compared to PBS injected mice (Fig A5).
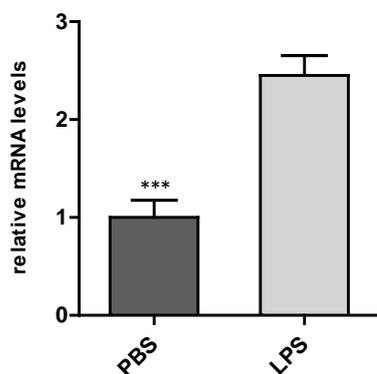

Fig A5: HIPK2 expression is upregulated by LPS treatment. *Liver mRNA levels of HIPK2 in mice injected with LPS or PBS injected control mice were determined by qPCR. (n=6), (means ± SEM). (***) indicates significance p≤0.001*

11.3 Hepatic HIPK2 manipulation *in vivo*

In order to investigate the role of hepatic HIPK2 in an *in vivo* setting an adenovirus expressing a short hairpin RNA (shRNA) against HIPK2 was cloned and produced.

### 11.3.1 Adenovirus expressing HIPK2-specific shRNA reduces HIPK2 mRNA levels in HEPA1c1 cells

Prior to *in vivo* use, the generated adenovirus expressing shRNA specifically targeting HIPK2 was tested in HEPA1c1 cells. For this purpose, cells were infected with different doses (MOI) of either HIPK2-specific or a scrambled shRNA as control. The knockdown efficiency was assessed by qPCR. HIPK2 mRNA levels could be ~80% downregulated with a virus dose of 25 MOI or higher (Fig A6).
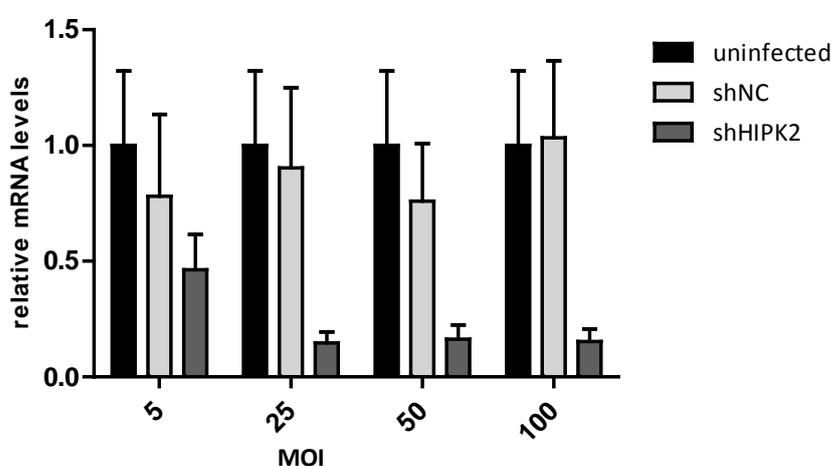
Fig A6: Adenovirus expressing HIPK2-specific shRNA reduces HIPK2 mRNA levels in HEPA1c1 cells. *Hepa1c1 cells were left uninfected or were transduced with control or shHIPK2. Cells were harvested after 24h and HIPK2 mRNA levels determined by qPCR. (n=3), (means ± SEM).*

### 11.3.2 Negative control adenovirus significantly reduces HIPK2 gene expression

In order to investigate the function of hepatic HIPK2 in an *in vivo* setting 10 week old C57BL/6J mice were injected via the tail vein with 1×10^9, 2.5×10^9 or 5×10^9 viral particles expressing either a scrambled shRNA sequence or HIPK2 targeting sequence or phosphate buffered saline (PBS). Mice were given free access to food and considered random fed. Seven days after injection the animals were sacrificed. Liver was collected and shock frozen, additionally, serum was taken for further analysis. HIPK2 knockdown efficiency was assessed at mRNA level by qPCR (Fig A7). HIPK2 specific shRNA reduced HIPK2 expression levels by 60-80% compared to the PBS control in a dose dependent manner. Unexpectedly, HIPK2 gene expression was up to 80% reduced by the negative control virus as well. Thus, the adenovirus system could not be used for HIPK2 *in vivo* studies. The obtained samples were analyzed for changes in serum triglyceride, non-esterified fatty acid or ketone bodies. No differenced were seen between the groups (data not shown).
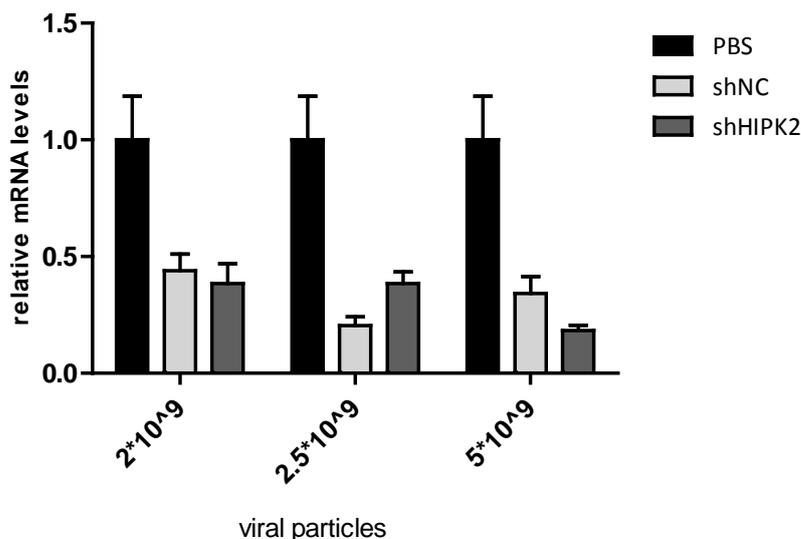
Fig A7: Negative control adenovirus reduces expression of hepatic HIPK2. *C57BL/6J mice were injected via the tail vein with $1x10^9$, $2.5x10^9$ or $5x10^9$ viral particles expressing either a scrambled shRNA sequence or HIPK2 targeting sequence or phosphate buffered saline (PBS). Hepatic HIPK2 mRNA levels were determined by qPCR. (n=3-4), (means ± SEM).*

11.3.3 SiRNA mediated hepatic HIPK2 kockdown

As adenoviral mediated shRNA delivery could not be used as a method for HIPK2 knockdown, we tested the application of siRNAs *in vivo*. For that purpose, 10 week old C57BL/6J mice were injected intravenously with 7 mg/kg body weight siRNA targeting HIPK2, a scrambled control or PBS. Mice were given free access to food and considered random fed. Two, five and seven days after injection a group of animals were sacrificed. Liver was collected and shock frozen, additionally, serum was taken for further analysis. Hepatic HIPK2 mRNA levels were determined by qPCR. SiRNAs targeting HIPK2 could reduce HIPK2 expression by 60-70%, two and five days after transfection (Fig A8). The knockdown was however lost on day 7 as compared to the negative controls. Here, the negative control did not affect HIPK2 expression. The obtained samples were analyzed for changes in serum triglyceride, non-esterified fatty acid or ketone bodies. No differed were seen between the groups (data not shown). Also abdominal adipose tissue, inguinal adipose tissue, kidney and intestine were analyzed for changes in HIPK2 gene expression. No differences were detected (data not shown).
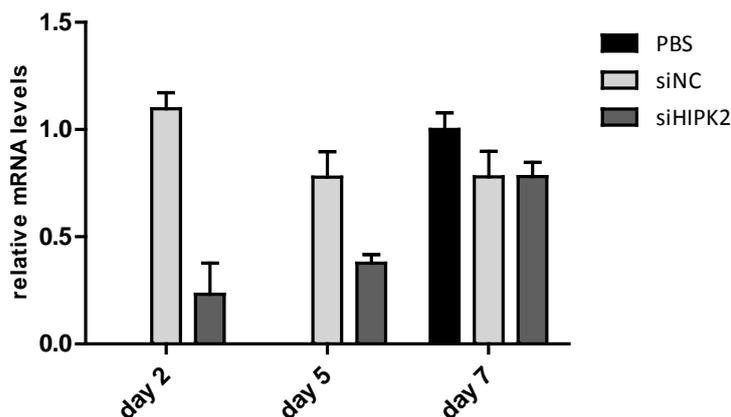
Fig A8: SiRNA mediated hepatic HIPK2 knockdown. *10 week old C57BL/6J mice were injected intravenously with 7 mg/kg body weight siRNA targeting HIPK2, a scrambled control or PBS. Day of sacrifice after injection is indicated. Hepatic HIPK2 mRNA levels were determined by qPCR. (n=3), (means ± SEM).*

11.4 Concluding remarks

Unexpectedly, treatment of C57BL/6 mice with negative control adenovirus resulted downregulation of HIPK2 gene expression that was nearly as strong as seen for the HIPK2 specific shRNA, when compared to PBS injected animals. Application of siRNA could specifically downregulate HIPK2 expression for up to 5 days, but the effect was gone on day 7, which only provides a very limited time frame for *in vivo* experiments. A further problem that occurred was that HIPK2 protein levels could not be detected in the liver with all available antibodies. Even a specifically generated antibody (Vera Greiner, Hoffman Lab), failed to detect endogenous HIPK2. Consequently, we decided to stop the study about HIPK2 function in liver.

11.5 Materials and Methods

In the following only material and methods that are not listed in the main body of the thesis will be named.

11.5.1 Methods

SiRNA injections

For siRNA studies Silencer®siRNA from life technologies was used. SiRNA was mixed with Invivofectamine®2.0 Reagent from life technologies according to the manufactures protocol. Mice were intravenously injected with 7 mg/kg body weight siRNA or PBS. The animals were housed

according to international standard conditions with a 12 hrs dark, 12 hrs light cycle and regular unrestricted diet.

11.5.2 Material

SiRNA

Sequence siHIPK2: 5'→3' GGAAGGGAGUGACAUGUUAUU

As negative control siRNA #1 from life technologies was usedd

shRNA

Sequence shHIPK2: 5'→3' GGACACATAGTTGTAACATCA

Sequence negative control: 5'→3' GATCTGATCGACACTGTAATG